University of Technology Graz

Institute of Molecular Biotechnology

Master Thesis

Construction and characterization of genomically integrated expression systems in *Ralstonia eutropha* H16

JEREMIAS HAGEN

Mag.rer.nat. Dr.rer.nat. Köfinger Petra

Univ.-Prof. Dipl.-Ing. Dr.techn. Helmut Schwab

Graz, Juni 2014

Acknowledgement

First and foremost, I would like to thank my supervisor Prof. Helmut Schwab for his support and for giving me the opportunity to start and successfully complete my master project at the institute of molecular biotechnology. My personal gratitude goes to my research supervisor Dr. Petra Köfinger for her motivating supervision and perpetual assistance in scientific and personal matters.

Moreover, I would like to thank all the members of the first floor with a special thanks to my working group “Team Knallgas” responsible for the great working atmosphere. It was a pleasure to be a part of this amazing team in- and outside the laboratory. Here I also want to express my special thanks to Steffen Gruber for his great support and friendship.

Getting through my dissertation required more than academic support, and there are many, many people to thank for listening and tolerating me during this time. I cannot start to express my gratitude for all the amazing people I met and got friends with during my time in Graz. Furthermore, I want to thank all my childhood friends for always having an open ear and the extraordinary friendship.

Most importantly, none of this could have happened without my family. I want to say thank you to my parents for their unconditional support and always believing in me, to my brother and my sister as well as my grandparents for their interest and support in my work. Thanks for always being there and believing in me...

Statutory declaration

I declare that I have authored this thesis independently, that I have not used other than the declared sources / resources, and that I have explicitly marked all material which has been quoted either literally or by content from the used sources.

....

date (signature)

Abstract

The Gram-negative soil bacterium *Ralstonia eutropha* H16 has attracted significant interest as production organism in recent years due to its capability to grow under lithoautotrophic as well as heterotrophic growth conditions to high cell densities. To date, heterologous gene expression was accomplished by complex inducible expression systems based on P_{phaP} induced by phosphate limitation and P_{araBAD} inducible with L-arabinose (not possible under lithoautotrophic conditions). However, a simple inducible and tightly regulated expression system is yet required for gene expression. Thus, the aim of this work was to create a vector system for genomic integration in *R. eutropha* H16 and thereby, provide the basis for the integration of inducible expression systems into the genome of *R. eutropha* H16.

Therefore, different strategies were developed to integrate into the genome of *R. eutropha* H16. The suicide vector pK470_mobRK2_estA_frt_phaC1 based on the *ColE1* origin of replication, the mobilization region of the RK2 plasmid and the *phaC1* gene as homologous region flanking the fragment to be integrated was constructed establishing an integration system which led to the successful integration of the reporter gene *estA* into the *phaC* locus of *R. eutropha* H16 via homologous recombination. Furthermore, the Flp-frt system was established and proved to work out in *R. eutropha* H16 for the first time. This enables the recycling of selection markers via the site-specific recombinase Flp (flippase) by recognizing the flippase recognition target (frt) sites flanking the selection marker and promoting its excision of the genome.

Moreover, the T7 RNA polymerase as well as the lactose permease were cloned into the suicide vector and successfully integrated into the *R. eutropha* H16 genome to enable inducible high level gene expression.

In this study, a vector system for genomic integration in *R. eutropha* H16 was successfully created, on its basis further gene integrations as well as gene knockouts can be carried out. Additionally, the Flp-frt system was shown to be functional in *R. eutropha* H16 for the first time allowing simple and easy selection marker recycling.

Zusammenfassung

Das gramnegative Bodenbakterium *Ralstonia eutropha* H16 hat in den letzten Jahren aufgrund seiner Fähigkeit unter lithoautotrophen als auch heterotrophen Bedingungen zu hohen Zelldichten wachsen zu können starkes Interesse als Produktionsorganismus geweckt. Die heterologe Genexpression wurde bis jetzt mit komplexen induzierbaren Expressionssystemen basierend auf P_{phaP} induzierbar durch Phosphatlimitierung und P_{araBAD} induzierbar mit L-arabinose (nicht möglich unter lithoautotrophen Bedingungen) durchgeführt. Ein einfaches und streng reguliertes induzierbares Expressionssystem zur Genexpression in *R. eutropha* H16 ist noch immer nicht verfügbar. Das Ziel dieser Arbeit war daher ein induzierbares Expressionssystem zu generieren und dies in das Genom von *R. eutropha* H16 zu integrieren.

Es wurde eine Reihe von unterschiedlichen Strategien entwickelt, um in das Genom von *R. eutropha* H16 zu integrieren. Das Suizidplasmid pK470_mobRK2_estA_frt_phaC1 basierend auf dem Replikationsursprung *ColE1*, der Mobilisationsregion des RK2 Plasmid und dem *phaC1* Gen als homologe Region, welches das zu integrierende Fragment flankierte, wurde konstruiert und somit ein Integrationssystem konstruiert, mit welchem das Reportergen *estA* erfolgreich in den *phaC* Locus von *R. eutropha* H16 mittels homologer Rekombination integriert werden konnte. Weiters wurde das Flp-FRT System etabliert und dessen Funktionalität zum ersten Mal in *R. eutropha* H16 nachgewiesen. Mit Hilfe dieses Systems ist es möglich Selektionsmarker wiederzuverwenden, indem diese durch ortsspezifische Rekombination an den sogenannten *frt sites* wieder aus dem Genom entfernt werden können. Des Weiteren konnten auch noch die T7 Polymerase und die Laktose-Permease unter Verwendung des Suizidplasmides erfolgreich in das *R. eutropha* H16 Genom integriert werden, um die Basis für ein induzierbares Expressionssystem mit hoher Ausbeute zu bilden.

In dieser Arbeit wurde ein Vektorsystem für die genomische Integration in *R. eutropha* H16 erfolgreich erstellt, auf dessen Basis weitere Genintegrationen als auch Gen-Knockouts durchgeführt werden können. Zusätzlich wurde die Funktionalität des Flp-FRT Systems zur einfachen Selektionsmarker Wiederverwertung in *R. eutropha* H16 zum ersten Mal nachgewiesen.

Table of contents

List of abbreviations

Amp	Ampicillin
APS	Ammonium persulfate
ATP	Adenosine triphosphate
bp	Base pairs
ca1	carbonic anhydrase 1
CFU	Colony forming unit
Cm	Chloramphenicol
ddH2O	double-distilled water
dNTP	deoxynucleoside triphosphate
DMSO	Dimethyl sulfoxide
DTT	Dithiothreitol
EDTA	Ethylenediaminetetraacetic acid
EtBr	Ethidiumbromide
flp	Flippase of 2 µm plasmid of *Saccharomyces cerevisiae*
frt site	Flippase recognition target site
FSB	Final sample buffer
Gen	Gentamycin
IPTG	Isopropyl-β-D-thiogalactopyranoside
Kan	Kanamycin
lacI	gene encoding *lac* repressor
lacY	gene encoding lactose permease
LB	Lysogeny broth
mob	mobilization region of pBBR1-MCS5 plasmid
mobRK2	mobilization region of RK2 plasmid
mobRSF1010	mobilization region of pKT231 plasmid of *RSF1010* origin of replication
NaOH	Sodium hydroxide
NB	Nutrient broth
OD_{600}	Optical density at 600 nm
ONC	Overnight culture
oriT	origin of transfer
PCR	Polymerase chain reaction
PEG	Polyethylenglycol
phaC1	gene encoding for PHB synthase
PHB	Polyhydroxybutyrate
rcf	Relative centrifugal force
*Re*H16	*Ralstonia eutropha* H16
RFU	Relative fluorescing unit
rpm	Round per minute
SDS	Sodium dodecyl sulfate
SDS-PAGE	Sodium dodecyl sulfate polyacrylamide gel electrophoresis
TEMED	Tetramethylethylenediamine
TSB	Tryptic soy broth

1. Introduction

1.1. *Ralstonia eutropha* H16

Ralstonia eutropha also known as *Cupriavidus necator*, *Alcaligenes eutropha* and *Wautersia eutropha* is a facultative lithoautotrophic Gram-negative soil bacterium and belongs to the phylogenetic taxonomy of the betaproteobacteria class [1]. It is classified as a metabolically multifarious individual. The *R. eutropha* H16 genome is comprised of three replicons – chromosome 1 (4,052,032 bp), chromosome 2 (2,912,490 bp) and a third replicon, the megaplasmid pHG1 (452,156 bp) encoding for 6626 putative genes [2], [3]. A closer look at the generally high GC ratio of *R. eutropha* H16 shows differences between the GC ratio of the two chromosomes (~66.5 %) and the one of the megaplasmid pHG1 with only 62.3 % [2]. Further analysis revealed that genes responsible for most key functions of DNA replication, transcription and translation are located on chromosome 1 as well as genes encoding for the organic acid metabolism supporting heterotrophic growth. Important enzymes for the degradation of aromatic compounds and the sugar metabolism are located on chromosome 2. Sugars are metabolized via the Entner-Doudoroff (KDPG) pathway; however, the substrate spectrum of sugars is restricted to fructose and N-acetylglucosamine due to the lack of an active transport system for glucose in *R. eutropha* H16 [2], [4]. Two NiFe hydrogenases are encoded on pHG1 as key elements for the H_2-oxidzing system [3].

R. eutropha H16 is also called “knallgas” bacterium due to the fact that it is able to oxidize hydrogen. The ability to switch between heterotrophic and autotrophic growth is an advantage of this versatile organism, thus being able to survive without organic growth substrates only by metabolizing CO_2 and H_2 as its sole carbon and energy source [5]. In the case of no availability of organic substrates, *R. eutropha* H16 can switch to chemoautotrophic growth (tightly regulated) by fixing carbon dioxide via the Calvin-Benson-Bassham (CBB) cycle. The key player of the CBB cycle is the ribulose-1,5-biphosphate carboxylase/oxygenase (RuBisCO) [6]. The energy demand of the organism is provided by the catalytic activity of two [Ni-Fe] hydrogenases – a NAD^+-reducing hydrogenase and a membrane-bound hydrogenase – by the oxidation of available H_2 [7], [8]. Another key advantage of *R. eutropha* H16 is the flexible bioenergetic as it is able to shift between

aerobic and anaerobic respiration depending on the presence or absence of O_2 [2]. Thereby, alternative electron acceptors are used for example NO_3^- and NO_2^- provided by the nitrification pathway [9]. Furthermore, *R. eutropha* H16 possesses a strong metabolic network capable of degrading various toxic chemicals [10], [11]. All this making *R. eutropha* H16 a model organism for the study of CO_2 fixation, hydrogen oxidation and denitrification with concerns of the involved control mechanisms [12].

Additionally, this bacterium has the ability to accumulate organic carbon in form of polyesters (poly[R-(–)-3-hydroxybutyrate], PHB) in intracellular storage granules. *R. eutropha* H16 accumulates these granules during carbon excess but under limitations of oxygen, phosphate or nitrogen [2], [13], [14]. The main enzymes in PHB synthesis are the PHB synthase (*phaC1*), β-ketothiolase (*phaA*) and the acetoacetyl-CoA reductase (*phaB*) which is NADPH dependent. All enzymes are encoded on the phaCAB operon on chromosome 1 [5]. However, sequencing of the *R. eutropha* H16 genome revealed various *phaA* and *phaB* isologs in which their exact role in PHB synthesis still has to be investigated [2]. This potential to accumulate and store large quantities of polyesters drew the interest of the scientific community towards this organism already 50 years ago [2]. The biodegradable thermoplastic Biopol is already commercially available [15].

Although, the organism was widely studied due to the ability of PHB synthesis, in recent years, *R. eutropha* H16 was of particular interest as a new expression host due to its capability to grow under lithoautotrophic as well as heterotrophic growth conditions to cell densities of up to 200 g/L [12]. Moreover, it was shown that the problem of inclusion body formation limiting gene expression in *E. coli* could yet not be observed during *R. eutropha* H16 fermentations [16]. Several studies were performed to express different heterologous genes in *R. eutropha* H16 [16]–[21] using the method of conjugational plasmid transfer [22]. Sichwart et al. [21] described the expression of heterologous genes for glucose uptake (*glf*, glucose-facilitated diffusion transporter of *Zymomonas mobilis*) and utilization (*glk*, glucokinase of *Escherichia coli*) thereby, broadening the sugar substrate range. Voss and Steinbüchel [20] used a PHB negative mutant strain of *R. eutropha* H16 (*R. eutropha* H16-PHB$^-$4) at which the PHB synthesis was disrupted by a precise deletion [23] to be able to lead the nutrient flux towards cyanophycin production. Thereby, two different approaches were demonstrated to enhance the heterologous gene expression in *R. eutropha* H16.

1.2. Conjugative plasmid transfer

Conjugation is a possibility to transfer DNA from a donor to an acceptor cell and is widely spread in nature. In laboratory practise, conjugation is the preferred method to use when transformation or another form of DNA transfer is not possible [24]. Other advantages are that conjugation is much more efficient (up to 100%) in comparison to transformation or electroporation and that DNA enters the acceptor cell as a single strand which favours recombination [25]. The conjugative plasmid transfer was already demonstrated between Gram-negative bacteria [20], [25] as well as from Gram-negative to Gram-positive bacteria [26], [27] and even from bacteria to yeast [28]. Important elements which are essential for conjugation are as follows the transfer-genes (*tra* genes), mobilization site (*mob*) as well as an origin of transfer (*oriT*, transfer starting point) [22], [24]. The latter two regions have to be encoded on the plasmid to be mobilized whereas the *tra*-genes can be encoded either on the plasmid, on a different plasmid (helper plasmid) or in the bacterial genome [29].

The transfer-genes are essential among other things for DNA processing and transfer and the development of sex-pili to enable a direct and stable cell-to-cell contact between donor and recipient strain also known as mating pair formation [30]. Two regions (*tra1* and *tra2*) were identified to encode for the mating pair formation (Mpf) system and the DNA transfer and replication (Dtr) system indispensable for a successful plasmid transfer [31]. *Tra2* genes (*trbB*, *-C*, *-D*, *-E*, *-F*, *-G*, *-H*, *-I*, *-J*, *-K* and *-L*) encode for the Mpf system in combination with the *traF* gene which is located in the *tra1* region responsible for the formation of mating pairs, thereby the donor and recipient cell are brought into close proximity [31], [32]. Following, the two cells fuse forming a transmembrane pore (stabilized by the pili) through which the single-stranded DNA, which is generated by the principle of rolling circle DNA replication, is transferred [33], [34]. The *tra1* genes are essential for DNA processing (nicking of the DNA at *oriT* and unwinding of the DNA) and transfer [35]. The key elements of *tra1* are the relaxase (TraI), origin of transfer binding proteins (TraJ and TraK) and TraG and –F [36]. Moreover, the genes *traM* and *–L* boost the transfer efficiency dramatically but are not absolutely necessary for conjugative plasmid transfer [32], [37]. In the case of the RK2 plasmid of the incompatibility group P (IncP) [38] both the *oriT* as well as the *tra*-genes are encoded directly on the plasmid thus being self-transmissible (Figure 1A). The RSF1010 plasmid (IncQ) on the

other hand is only comprised of the *oriT* and the genes *mobA*, *-B* and *–C* which comply with the *oriT* binding proteins enabling nicking of the DNA (Figure 1B) [39]. Thus, further *tra*-genes encoding for the mating pair formation system are necessary for a successful plasmid transfer to the recipient cell. The plasmid encoded genes *mobA-C* of RSF1010 are essential for nicking the DNA as the genes *traI-K* of the RK2 plasmid would not recognize and nick within the *oriT* of heterologous plasmids [40].

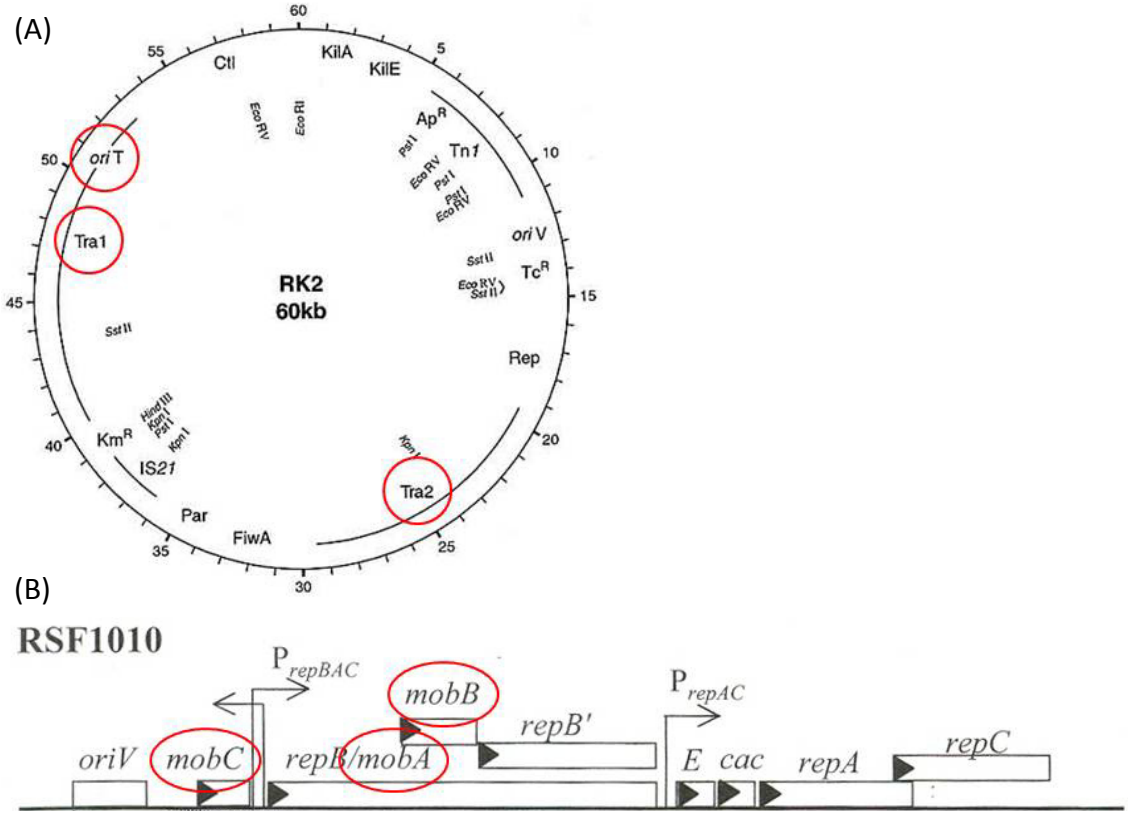

Figure 1. (**A**) Map of the broad-host-range plasmid RK2. The key elements for the conjugative plasmid transfer the transfer starting point *oriT* as well as the regions *tra1* and *tra2* are indicated. *Tra1* genes are essential for DNA processing (unwinding and nicking of the DNA) and transfer and *tra2* encodes for the mating pair formation system [34]. (**B**) Map of the RSF1010 plasmid comprised among others of the genes *mobA*, *mobB* and *mobC* essential for the conjugative plasmid transfer. These genes comply with the *oriT* binding proteins of RK2 encoded by *tra1*. The origin of conjugational plasmid transfer *oriT* is not indicated in the map but is located next to *mob* genes [41], [42].

A DNA-protein complex responsible for nicking the DNA is called relaxosome and consists in the plasmid RK2 of three different proteins namely TraI, TraJ and TraK. These proteins interact with the *oriT* sequence whereas the relaxase (TraI) is responsible for unwinding the supercoiled plasmid DNA and binding at the nicking site (8 bp) of the origin of transfer. Subsequently, TraI cleaves the DNA at the nick site and stays covalently attached to the 5’ end leading the single-stranded DNA to the recipient cell [34], [43], [44]. Further enzymes

like the TraC primase and the single-stranded binding protein (SSBP) are attached to the single-stranded DNA during the transfer through the membrane pore to the recipient cell [43]. It is assumed that recirculation of the transferred strand occurs in the membrane pore by the TraI enzyme indicating the pore is an interactive system [45]. Then, priming of the single-stranded DNA is carried out by the primase TraC and following, the complementary strand synthesized mainly by host encoded enzymes [34]. The transferred plasmid is then either maintained by vegetative replication or by integration into the genome of the new host.

In laboratory practise, the *E. coli* S17-1 strain is used for conjugative plasmid transfer as this strain has already integrated the *tra*-genes of the RK2 plasmid in the genome, thus, reducing the size of plasmids to be transferred [29].

1.3. Integration

1.3.1. Recombination in prokaryotes

Horizontal gene transfer (HGT) mostly followed by a recombination event leading to an integration into the genome was and still is playing a major role in evolution and the diversification of different traits of prokaryotes. The mechanisms of DNA translocation into new hosts can be summarized to transformation, conjugation (see 1.2 Conjugative plasmid transfer) and transduction [46]. These mechanisms will not be discussed in detail any further as in the following the focus will be on the different recombination events including the undergoing cellular mechanisms. DNA can integrate into a organisms chromosome via homologous recombination [46], [47], homology-facilitated illegitimate recombination [48] and illegitimate recombination [49] (Figure 2) as well as site specific recombination. The latter one is carried out by recombinases by cleaving and subsequent religation without the necessity of a long homology between the sequences [50].

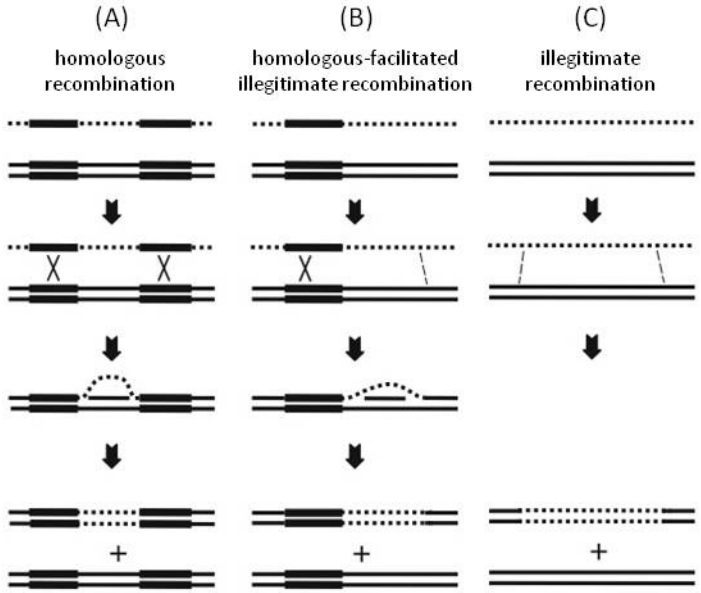

Figure 2. Schematic representation of the principles of DNA integration of (**A**) homologous recombination, (**B**) homologous-facilitated illegitimate recombination, and (**C**) illegitimate recombination. DNA to be integrated is shown as single-strand. Bold line indicates region of homology, dotted line indicates nonhomologous region. Single-stranded DNA represents donor DNA whereas double-stranded DNA is the recipient DNA [46].

Homologous recombination

Homologous recombination (HR) (Figure 2A) is required for essential intracellular processes like the preservation of the genomic integrity and the separation of chromosomes but also for the integration of different genes of interest as well as for gene knock-outs [47]. The DNA sequence of interest can successfully be integrated when flanked by sequences conferring homology to the recipient DNA (Figure 2A). For this HR event to happen numerous enzymes are essential. Different genetic pathways for recombination as RecBCD, RecE and the RecF pathway are known whereupon the RecBCD pathway is the main pathway in prokaryotes. At the beginning, the RecBCD enzymes (helicase and nuclease activity) are responsible for the separation and partial degradation of double-stranded DNA (dsDNA) as for every HR event a single-stranded DNA (ssDNA) is essential [47]. The partial degradation occurs until the RecBCD recognizes the so called Chi (*X*) site. This recombination hotspot suppresses the nuclease activity of RecBCD and thereby generating a ssDNA strand [51]. The ssDNA is then recognized and bound by RecA, RecFOR and single-strand binding (SSB) proteins. The DNA-dependent ATPase RecA has the ability to hold a dsDNA and a ssDNA simultaneously due to two DNA binding sites. Moreover, binding of RecA to ssDNA activates and enables the

protein to cleave off the LexA repressor protein resulting in the expression of several enzymes essential for the homologous recombination pathway. RecA migrates over the DNA searching for homology on the recipient DNA followed by homologous pairing and the exchange of DNA strands generating a plectonemic joint molecule leading to a Holliday junction [47], [52]. In the case of the formation of a paranemic joint, the conversion to a plectonemic joint is carried out by topoisomerase I [53]. Then, the heteroduplex DNA region is extended by RecA whereupon the branch migration is promoted by RuvAB or RecG encoding for DNA helicases specific for Holliday junctions. Finally, the Holliday junction is cleaved by RuvC and the homologous recombination event terminated by religation of DNA ligase [47].

Illegitimate recombination

Microorganisms are able to integrate foreign DNA even if no homology between donor and recipient strain is present. This type of recombination is called illegitimate recombination (IR; Figure 2C). It is exceptionally rare and based on non-homologous sequences with no sequence similarity at all or a few identical nucleotides (microhomology) [54]. According to Hülter and Wackernagel [55] the probability of an integration event to happen in the Gram-negative bacterium *Acinetobacter baylyi* is minimized about 10^{10}-fold with a frequency of 7.3×10^{-13} in the case of integration of non-homologous DNA sequences. The identified double illegitimate recombination (DIR) event was the first to be described probably due to a frequency close to the detection limit. The characterization of the DIR event revealed that the fusion sites did not have any microhomology and were located in close proximity [55]. Thereby, a different intracellular mechanism as the one for homologous recombination is applied showing that a double-strand break is the essential starting point. The enzymes DNA gyrase and topoisomerase I are essential to catalyse an IR event. The mechanism is assumed to happen in broken plasmids and at broken replication forks and involves two double-stranded DNA strands following the break-and-join mechanism [55]–[57].

Homology-facilitated illegitimate recombination

Another type of an illegitimate recombination is the homology-facilitated illegitimate recombination (HFIR; Figure 2B). HFIR was already described in *Pseudomonas stutzeri* [48], *Acinetobacter baylyi* [55], [58] and *Streptococcus pneumoniae* [59]. Thereby, a homologous

segment in the donor strain served as recombinational anchor enhancing the probability of an illegitimate recombination event to happen. HFIR is RecA dependent, bringing the donor and recipient strain in close proximity and in the following leading to an IR event in the heterologous part. It was shown that a recombinational anchor of approximately 1000 bp was highly effective with decreasing effectiveness when reduced in size [48], [58]. HFIR events occurred with a frequency of 6×10^{-6}, thus, less frequent than a homologous recombination event but still with a much higher probability than IR events [55]. Homology-facilitated illegitimate recombination is based on enzymes involved in homologous recombination according to Harms et al. [60] as well as short homologous regions of 3-8 bp. These regions are known as microhomology regions which could be described as hotspots for illegitimate recombination events. Moreover, the microhomology regions showed to have a higher GC content than the overall GC content of donor or recipient assuming to stimulate the IR step. These data suggest that during HFIR the first step in IR is hybridization of the donor and recipient strain (microhomology) followed by strand extension/trimming and finally, the covalent fusion [55].

In general, it can be stated that the integration frequency decreases when the sequence of homology is shorter or the heterologous segments are increasing [55]. Lovett et al. [61] compared different length of homology regions and the following HR frequency. It was shown that with increasing homologous sequence length, the integration frequency increased significantly reaching a plateau with a homologous sequence of around 200 bp or longer in *Escherichia coli* [61]. However, according to Simpson et al. [62] the frequency of an integration event increases by several folds with increasing length of homology whereas the size of the insert to be integrated decreases the integration frequency when increasing in size. For the successful integration of various plasmids in the genome of *R. eutropha* H16 homologous sequences ranging from ~250 to 1100 bp were already described whereupon the homologous sequences were flanking the gene to be integrated in most cases [16], [19], [20], [63].

1.3.2. Selection marker recycling based on the flippase site-specific recombination system

Site-specific recombination is well known in both prokaryotes and eukaryotes [64], [65]. In laboratory practise, site-specific recombination is used to excise unwanted vector backbone

and recycle the selection marker respectively after integration. Several different site-specific recombination systems are known as the Cre-*lox* system [66], the ParA-*res* system [64] as well as the Flp-frt system [67]. In particular, probably the most versatile one is the Flp-frt recombination system of the 2µm plasmid of *Saccharomyces cerevisiae* due to its broad host range ability. Its functionality was already demonstrated among others in different prokaryotes and eukaryotes [67]–[71].

The recombinase of *S. cerevisiae* termed flippase (Flp) recognizes and binds the flippase recognition target (frt) sites promoting the excision of the sequence between the frt sites if placed in the same direction. An orientation in the opposite direction of the frt sites would lead to DNA inversion [65], [72]. The frt sites are comprised of 34 bp whereupon 8 bp can be designated as the core region flanked by two identical 13 bp regions important for the binding of the Flp. In this core region the crossing over event mediated by the Flp takes place [65]. The reaction catalyzed by the flippase can be summarized to the cleavage of four phosphodiester bonds in the frt sites and the subsequent formation of four new phosphodiester bonds [72]. After the phosphodiester bond cleavage and the generation of single-stranded 8 bp long nicks, the Flp stays attached to the free 3' terminus forming a 3'phosphotyrosine linkage [73], [74]. Thus, the Flp recombinase is also classified as topoisomerase as it conserves the energy of the phosphodiester bond in this protein-phosphate linkage using it for the formation of the new phosphodiester bond [74]. Hence, no energy-providing cofactors are necessary for its catalytic activity [72]. Gronostajski et al. [74] proposed that at least two Flp recombinases are essential for a successful recombination event.

In contrast to other site-specific recombinases which prefer supercoiled DNA, the Flp recombinase has a wider substrate spectrum acting efficiently on linear DNA, relaxed circular DNA and supercoiled DNA [75]. Furthermore it could be demonstrated by McLeod et al. [65] that mutations in the core region of the frt site reduce the recombination efficiency severely, however, no single-bp mutation led to the complete loss of Flp recombination. Moreover it was shown, that the recombination efficiency was higher in clones carrying the same point mutation in the core region at both interacting frt sites than only in one [65].

The flippase recombination system is well described and already applied in a variety of Gram-negative organisms for selection marker recycling [67]–[69]. However, up to now the

Flp-frt system was not tested of its functionality in *R. eutropha* H16 even though this recombination system would provide an elegant approach for the recycling of the antibiotic resistance in *R. eutropha* H16.

1.4. Inducible expression systems in *Ralstonia eutropha* H16

Inducible expression systems for heterologous gene expression are essential to be able to suppress the expression during cell growth and enable the precise induction of the gene of interest at a desired fermentation stage. Several different inducible expression systems were successfully identified and characterized whereupon the regulatory mechanism of the lactose metabolism is one of the simplest and best studied ones. The regulatory element of the *lac* operon which can be induced via lactose or IPTG respectively was yet not possible to use in *R. eutropha* H16 due to a lack of the necessary transport system for the inducer [76], [77]. An inducible expression system which was already applied in *R. eutropha* H16 to enable inducible gene expression was based on the BAD promoter inducible with L-arabinose [78], [79]. However, this inducible expression system cannot be used when *R. eutropha* H16 is grown under lithoautotrophic conditions. Furthermore, Srinivasan et al. [16] identified a promoter (P_{phaP}) which was up-regulated during phosphate limitation, thus being able to induce the expression of organophosphohydrolase (OPH) by varying a simple process parameter. However, a simple and tightly regulated inducible expression system for *R. eutropha* H16 was still missing.

1.4.1. Inducible expression system based on the *lac* operon regulatory mechanism

The lactose permease is a gene of the *E. coli lac* operon which is further comprised of the β-galactosidase (LacZ) and the thiogalactoside transacetylase (LacA) of a total of three genes regulating the lactose metabolism. *LacY* encodes for a membrane-bound transport system based on a proton gradient for lactose enabling its uptake into the cell. After the successful transport of lactose, LacZ cleaves it into galactose and glucose whereupon LacA adds an acetyl group to the galactoside. The expression of these genes is tightly regulated by the *lac* repressor gene *lacI* encoded upstream of the *lac* operon. The repressor inhibits transcription by binding to the operator region not allowing the RNA polymerase to bind to the promoter site. On the other hand, present lactose when bound to *lacI* results in a structural change of the repressor not being able to bind to the operator region anymore and thus allowing

transcription. Moreover, the activator protein CAP (catabolite activator protein) induced by cAMP, which arises when glucose levels are low, leading to a conformational change allowing the activator to bind specific DNA sequences. Thereby, the weak interaction of the RNA polymerase and the promoter is stabilized and maximum expression achieved [80], [81].

In numerous studies, the *lac* expression system based on the lac/tac promoter and its repressor was used for inducible heterologous gene expression in various organisms [82]–[85]. However, this inducible expression system could not yet be applied in *R. eutropha* H16 due to its inability to take up lactose or its analogue isopropyl-β-D-thiogalactopyranoside (IPTG) [77]. The establishment of the lactose utilization pathway in *R. eutropha* H16 was already demonstrated to be functional by Pries et al. [86]. Thereby, the *lacZ* and the *lacY* gene were expressed and slow growth of *R. eutropha* H16 on lactose could be observed [86]. Moreover, Bi et al. [87] expressed the *lacY* gene as well in *R. eutropha* H16 allowing IPTG uptake. Subsequently, the IPTG inducible expression of the red fluorescent protein (RFP) under the control of the lac_{UV5} promoter could be confirmed. However, the expression level under the defined conditions of the study was really low after induction with IPTG compared to the gene expression in *E. coli* using the same regulatory mechanism [87]. Nevertheless, the functionality of a simple and tightly regulated inducible expression system based on the *lac* operon in particular the lactose permease in *R. eutropha* H16 was demonstrated.

1.5. T7 expression system

The RNA polymerase of the bacteriophage T7 has several advantages over other prokaryotic RNA polymerases as well as the ability for high-level gene expression. First, the structural simplicity of the T7 RNA polymerase is a main advantage. The polymerase is a monomeric enzyme comprised of 98 kDA without the need of further protein factors to perform the RNA synthesis [88]–[90]. Second, the T7 RNA polymerase is very specific and efficient for its own promoters. The promoter sequence recognized by the T7 RNA polymerase is comprised of 23 highly conserved bp, thus, it is not very likely to find such a sequence in any other organism not related to bacteriophage T7 [90]–[92]. Third, the elongation rate of 100-200 nucleotides per second of the T7 RNA polymerase is significantly faster than other prokaryotic RNA polymerases [89]. Hence, T7 RNA polymerase is very attractive for high-level gene expression in various bacteria like *E. coli* or *R. eutropha* H16 due to its specificity,

activity and capability to synthesize complete mRNA transcripts from any selected DNA [90], [91]. Several different publications show the successful application of the T7 RNA polymerase/promoter system in *E. coli*. Thereby, the T7 RNA polymerase was under the regulation of an inducible promoter like P_{araBAD} [93], P_{lacUV5} [91] or lambda P_L [94] to control the expression of the gene of interest as well as to be able to induce expression of genes toxic to the cell. In addition, any expression e.g. due to an uninduced, leaky promoter of the T7 RNA polymerase can be inhibited by T7 lysozyme [95], [96]. T7 lysozyme inhibits transcription by T7 RNA polymerase by binding the polymerase and forming a complex inhibiting the polymerase to switch (conformational change) to an elongation complex [96], [97]. Moreover, the development of a T7 RNA polymerase based expression system in *R. eutropha* H16 was reported by Barnard et al. [18]. Thereby, the T7 RNA polymerase was integrated into the genome under the control of the inducible, strong phaP promoter and the organophosphohydrolase gene expressed demonstrating the functionality of the T7 RNA polymerase in *R. eutropha* H16 [18].

1.6. Aim of the Project

The main focus of this work was to construct and establish a system for the integration into the genome of *R. eutropha* H16 and in the following to thereby provide the basis for inducible expression systems by integrating the bacteriophage T7 RNA polymerase and the lactose permease respectively to establish the T7 expression system under the regulatory element of the *lac* operon. This would allow the simple induction of gene expression in *R. eutropha* H16 at a certain growth stage with IPTG not having the necessity of a complex induction. Additionally, the Flp-frt system based on the site-specific recombinase Flp was tried to be set up in *R. eutropha* H16 enabling the excision of none favored selection markers after integration into the genome and thereby establishing a marker recycling system.

2. Material and Methods

2.1. Strains and cultivation conditions

The bacteria strains used to conduct this particular project are listed in Table 1. *E. coli* strains were cultivated in lysogeny broth (LB) medium (Carl Roth GmbH CO. KG; Heidelberg, Germany) supplemented with kanamycin [40 µg/mL], ampicillin [100 µg/mL] or chloramphenicol [25 µg/mL]. The *R. eutropha* H16 strain was grown in tryptic soy broth (TSB; BD Diagnostic Systems; Heidelberg, Germany) or nutrient broth (NB) media with a concentration of 20 µg/mL of the antibiotic gentamycin. After conjugation, *R. eutropha* H16 transconjugants were grown on TSB media supplemented with 0.2 % fructose, gentamycin [20 µg/mL] and kanamycin [200 µg/mL] or chloramphenicol [100 µg/mL] (all antibiotics were obtained from Carl Roth GmbH & Co KG, Karlsruhe, Germany). The media composition is listed in Table 2.

Table 1. Strains used in this work.

Strain	Genotype	Source
***R. eutropha* H16**	Wildtype	DSM428
***E. coli* strains**		
Top10	F´(*proAB, lacIq*, *lacZ*ΔM15, Tn10(tet-r)), *mcrA*, Δ(mrr-hsdRMS-mcrBC), Φ80ΔlacZΔM15, Δ*lacX74*, *deoR*, *recA1*, *araD139*(*ara, leu*), 7697, *galU*, *galK*, λ-, *rpsL*(streptomycin-r), *endA1*, *nupG*	Invitrogen
S17-1	*recA pro hsdR* RP4-2-Tc::Mu-Km::Tn7 integrated into the chromosome	#679 IMBT strain collection

Table 2. Composition of growth media.

Media	Composition
LB	Trypton (10 g/L), Yeast extract (5 g/L), Sodium chloride (0.5-10 g/L)
TSB	Bacto Trypton (17 g/L),Bacto Soyton (3 g/L), Dextrose (2.5 g/L), Sodium chloride (5 g/L), Di-potassium hydrogen phosphate (2.5 g/L); pH 7.3 ± 0.2
NB	Peptone (5 g/L), Meat extract (3 g/L)

2.2. Plasmids and primer

All vectors to be used were constructed in *E. coli* Top10 strain and are listed in Table 3 whereupon all used primers are listed in Table 4.

Table 3. Plasmids used in this work.

Plasmid	Description	Source
RK2	Broad-host-range plasmid	#381 IMBT strain collection
pKT231	Kan^r, Sm^r, RSF1010	#320 IMBT strain collection
pJET1.2/blunt cloning vector	Bla (amp^r), P_{lacUV5}, P_{T7}, Rep (pMB1), *eco47IR* Cloning vector	Thermo scientific
pK470_mob_ca1	Kan^r, P_{tac}, ColE1, *mob* (pBBR1), *ca*1 (YP_724689.1) Cloning vector for *E. coli*	#131 plasmid list[1]
pK470_mob_ca1_estA	Kan^r, P_{tac}, ColE1, *mob* (pBBR1), *estA (WP_010593992.1)*, *ca1* Cloning vector for *E. coli* and integration vector for *R. eutropha* H16	#133 plasmid list[1]
pK470_redA9	Kan^r, P_{tac}, ColE1, *redA9*, *lacI* Cloning vector for *E. coli*	#107 plasmid list[1]
pK470_redB2	Kan^r, P_{tac}, ColE1, *redB2*, *lacI* Cloning vector for *E. coli*	#97 plasmid list[1]
pKRtacflp	Kan^r, P_{tac}, Rep, *flp*, *lacI* Cloning vector for *E. coli*	#111 plasmid list[1]
pKRtac_Par_T7Poly_lacI	Kan^r, P_{tac}, Rep, T7 polymerase (M38308.1), *par*, *lacI* Cloning vector for *E. coli*	#74 plasmid list[1]
pCM_PT7_RSF1010_eGFP_Pemlk_lacI	Cm^r, P_{T7}, RSF1010, *egfp*, *Pemlk*, *lacI* Cloning vector for *E. coli*	#235 plasmid list[1]
pKR_Ptac_Par_eGFP_REP_mobRK2	Kan^r, P_{tac}, Rep, *egfp*, *par*, *mobRK2* Cloning vector for *E. coli*	#236 plasmid list[1]
pKR_Ptac_Par_eGFP_mob_pSa	Kan^r, P_{tac}, pSa, *mob* (pBBR1), *egfp*, *par* Cloning and expression vector for *E. coli* and *R. eutropha* H16	#237 plasmid list[1]
pKR_Ptac_Par_eGFP_mobRK2_pSa	Kan^r, P_{tac}, pSa, *mobRK2* (RK2), *egfp*, *par* Cloning and expression vector for *E. coli* and *R. eutropha* H16	This study
pKR_Ptac_Par_eGFP_mobRSF1010_pSa	Kan^r, P_{tac}, pSa, *mobRSF1010* (pKT231), *egfp*, *par* Cloning and expression vector for *E. coli* and *R. eutropha* H16	This study
pCM_mobRK2_redA9	Cm^r, P_{tac}, ColE1, *redA9* (CAJ92536.1), *mobRK2* Cloning vector for *E. coli* and integration vector for *R. eutropha* H16	This study
pCM_mobRK2_redB2	Cm^r, P_{tac}, ColE1, part of *redB2* (CAJ95528.1), *mobRK2* Cloning vector for *E. coli* and integration	This study

	vector for *R. eutropha* H16	
pCM_mobRSF1010_redA9	Cm^r, P_{tac}, ColE1, *redA9*, *mobRSF1010* Cloning vector for *E. coli* and integration vector for *R. eutropha* H16	This study
pCM_mobRSF1010_redB2	Cm^r, P_{tac}, ColE1, part of *redB2*, *mobRSF1010* Cloning vector for *E. coli* and integration vector for *R. eutropha* H16	This study
pK470_mobRK2_estA_frt_phaC1	Kan^r, P_{tac}, ColE1, *estA*, *phaC1* (CAJ92572.1), *mobRK2*, frt Cloning vector for *E. coli* and integration vector for *R. eutropha* H16	This study
pCM_mobRK2_flp	Cm^r, P_{tac}, ColE1, *flp*, *mobRK2* Cloning and expression vector for *E. coli* and *R. eutropha* H16	This study
pK470_mobRK2_T7_frtΔ_phaC1	Kan^r, P_{tac}, ColE1, T7 polymerase (M38308.1), *phaC1*, *mobRK2*, frtΔ Cloning vector for *E. coli* and integration vector for *R. eutropha* H16	This study
pK470_mobRK2_PCIV1bM_lacY_frtΔ_phaC1	Kan^r, P_{CIV1bM}, ColE1, *lacY* (JF300162.1), *phaC1*, *mob*RK2, frtΔ Cloning vector for *E. coli* and integration vector for *R. eutropha* H16	This study
pCM_PT7_RSF1010_eGFP_Pemlk_ΔlacI	Cm^r, P_{T7}, RSF1010, *egfp*, *Pemlk* Cloning and expression vector for *E. coli* and *R. eutropha* H16	This study
pCM_Ptac_Par_eGFP_RSF1010_lacI	Cm^r, P_{tac}, RSF1010, *egfp*, *lacI*, *par* Cloning and expression vector for *E. coli* and *R. eutropha* H16	This study

[1] Number of plasmid refers to internal primer list of the research group of Petra Köfinger.

Table 4. Primers used in this work.

Primer	Number[1]	Sequence[2]	Restriction site
pCM_mobRK2_redA9/redB2; pCM_mobRSF1010_redA9/redB2			
colE1 pK470 Fwd	#429	5'-tcgttccactgagcgtcaga-3'	-
rrnB pK470 Rev	#426	5'-ttcatgagcggatacatatttgaatg-3'	-
Fwd cmR NotI	#337	5'-gcggccgctcatgacgaataaatacctgtgac-3'	*Not*I
Rev cmR SpeI	#338	5'-actagttaactggcctcaggcattt-3'	*Spe*I
RSF1010_mob_fwd	#436	5'-tcagcccggctcatccttctg-3'	-
RSF1010_mob_rev	#437	5'-ctacatgctgaaatctggccc-3'	-
MOB oriT RK2 Fwd	#433	5'-tcgatcttcgccagcagg-3'	-
MOB oriT RK2 Rev	#434	5'-tcgacatccgccctcac-3'	-
3' redA9	#431	5'-cgaagctggtgcaggtctaca-3'	-
rrnB rev	#430	5'-ttgatgcctggcagtttatggc-3'	-
5' redB2 fwd	#432	5'-cgtcgacatgctggtcaacaac-3'	-

pK470_mobRK2_estA_frtΔ_phaC1

pK470 MOB SpeI Fwd	#382	5'-ctagactagtgcatgccaggcagccatcggaa-3'	SpeI
pK470 MOB SpeI Rev	#383	5'-ctagactagtctgcagatggcggcata-3'	SpeI
FRT oben Fwd phaC1	#384	5'-tagagaataggaacttcggcgcgcctttgcgtttctacaaactctttttg-3'	AscI
FRT oben Rev phaC1	#385	5'-gaaagtataggaacttcaaggccatccgtcaggat-3'	-
FRT unten Fwd phaC1	#386	5'-tagagaataggaacttcctcgagcccgtagaaaagatcaaaggatc-3'	XhoI
FRT unten Rev phaC1	#387	5'-gaaagtataggaacttcgtctgacgctcagtggaacg-3'	-
phaC1 Fwd SpeI	#378	5'-ctagactagtatggcgaccggcaaag-3'	SpeI
phaC1 Rev SpeI	#379	5'-ctagactagtagtcgtcccaggtgctgc-3'	SpeI
phaC1 Fwd XhoI	#380	5'-ccgctcgagacatcgagcacgcggc-3'	XhoI
phaC1 Rev XhoI	#381	5'-ccgctcgagtcatgccttggctttgacgtat-3'	XhoI
colE1 Rev	#401	5'-aaaaggccagcaaaaggccag-3'	-
pK470 ColE1 rev	#374	5'-cactgcagcgttcggctgcggc-3'	-
KanR-NotI-fwd	#68	5'-tatgcggccgccaggcagccatcggaagctg-3'	NotI
phaC1 Rev SpeI SphI	#445	5'-ggcatgcactagtagtcgtcccaggtgctg-3'	SpeI, SphI
5' Int phaC1 Fwd	#402	5'-atagcatctccccatgcaaagtgc-3'	-
Int Est Rev	#403	5'-gccgtgcaggtagacgatca-3'	-
Int KanR Fwd	#406	5'-gcagtttcatttgatgctcgatgag-3'	-
3' Int phaC1 Rev	#407	5'-cggatacgatgacaacgtcagtca-3'	-

pK470_mobRK2_estA_frt_phaC1

Fwd Expression cassette NdeI	#440	5'-ggaattccatatggccctcgattccgccacc-3'	*Nde*I
Rev Expression cassette FRT	#441	5'-tattctctagaaagtataggaacttcgtcaaggccatccgtcaggatgg-3'	-
Fwd KanR FRT	#442	5'-cctatactttctagagaataggaacttcatgagccatattcaacgggaaacgtcttg-3'	-
Rev KanR FRT	#443	5'-ctagaaagtataggaacttccttagaaaaactcatcgagcatcaaatg-3'	-
Rev FRT XhoI	#444	5'-ccgctcgaggaagttcctattctctagaaagtataggaacttcctt-3'	*Xho*I
rrnB Fwd	#350	5'-gccataaactgccaggcatcaa-3'	-

pCM_MOB RK2_FLP

FLP Fwd	#363	5'-cgggatccaggagatatacatatgccacaatttgatatattatg-3'	*BamH*I
FLP Rev	#364	5'-catgcatgcttatatgcgtctatttatgtaggat-3'	*Sph*I

pK470_mobRK2_T7_frtΔ_phaC1

seqT7pol_2	#308	5'-gcatttatgcaagttgtcgaggctga-3'	-
seqT7pol_3	#309	5'-ggttgaacattgacacagcgtaaaca-3'	-
seqT7pol_4	#310	5'-atgcttgagcaagccaataagtttgc-3'	-
seqT7pol_5	#311	5'-attcccaaatcagcttagccatgtat-3'	-
fwd gibson T7 BamHI	#453	5'-caatttcacacaggaaacagaattcgagctcggtacccggggatccttaagaaggagaat-3'	BamHI
rev gibson T7 HindIII	#454	5'-gtatcaggctgaaaatcttctctcatccgccaaaacagccaagctttacgcgaacgcga-3'	HindIII

pCM_PT7_RSF1010_eGFP_PemIk_ΔlacI

nT7MCS_PstI_fwd2	#304	5'-aactgcaggtaatacgactcactatagggcgaattggaattgtgagcggataaca-3'	*Pst*I

pK470_mobRK2_PCIV1bM_lacY_frtΔ_phaC1

PCIV1bM SphI Fwd	#446	5'-acatgcatgctcaacagcgacgaatacagcac-3'	*Sph*I

lacY rev	#314	5'-cccaagcttttaagcgacttcattcacctg-3'	*Hind*III
PCIV1bMrev	#500	5’-gattggcttcttcgagagac-3’	-
pCM_Ptac_PAR_eGFP_RSF1010_lacI			
LacI_SpeI_fwd	#419	5´-caactagtgttctttcctgcgttatcccc-3´	*Spe*I
LacI_SpeI_rev	#420	5´-caactagtacgccagaagcattggtg-3´	*Spe*I
P-2-fwd	#29	5'-actcatatggcttcactcgcgcg-3'	*Nde*I
P-2-rev	#30	5'-atcaagctttagtgacggattctcaggac-3'	*Hind*III
MOB fwd	#353	5'-cactgcagtcatcccaggtggcacttttc-3'	*Pst*I
MOB rev	#354	5'-cactgcagatggcggcatacgcgat-3'	*Pst*I
Int CA1 Fwd	#347	5'-agcgattcattcaccgctacagc-3'	-
Int KanR Rev	#348	5'-cgatagattgtcgcacctgattgc-3'	-
CA1 3' downstream rev	#351	5'-tctcttccatgtcgggtctc-3'	-
KanR Int Fwd	#404	5'-gcaatcaggtgcgacaatctatcg-3'	-
KanR Int Rev	#405	5'-ggcaagatcctggtatcggtctg-3'	-

[1] Primer number refers to the internal primer list of the research group of Petra Köfinger.
[2] Restriction sites are underlined.
Fwd, forward primer; Rev, reverse primer.

2.3. General cloning protocols

2.3.1. Preparation of competent *E. coli* cells

For the preparation of competent *E. coli* Top10 or *E. coli* S17-1 cells, first, two overnight-cultures a 15 mL of LB media were inoculated with a single colony and incubated over night at 37 °C and 200 rpm. Then, two main cultures each with a volume of 500 mL of LB media (2 L flasks) were inoculated to an OD_{600} of 0.1 and incubated at 37 °C and 200 rpm. The main cultures were harvested as the OD_{600} reached 0.6-0.7, poured into centrifugation flasks (pre-cooled) and cooled on ice (4 °C) for one hour. Afterwards, the cells were centrifuged for 10 minutes at 3000 rcf and 4 °C (Avanti^{TM} J-20 XP, JA-10 rotor, Beckmann Coulter, Vienna, Austria). Then, the supernatant was removed, the pellet resuspended in ~60 mL H_2O supplemented with 1M HEPES buffer pH7 (1 mL HEPES Buffer/L H_2O) followed by another centrifugation step at 4000 rcf at 4 °C for 10 minutes. After the supernatant was removed, the pellet was resuspended in little volume of H_2O supplemented with 1M HEPES buffer and ice-cold glycerol (10 %) followed by a further centrifugation step at 4500 rcf at 4 °C for 20 minutes. The supernatant was removed and the pellet resuspended in 2 mL of ice-cold glycerol (10 %) per litre of medium. Finally, aliquots of 80 µL of the cell suspension were filled into Eppendorf tubes (pre-cooled), frozen in liquid nitrogen and stored at -80 °C.

2.3.2. DNA manipulation

Restriction digests were performed with restriction enzymes and buffers of Thermo Scientific (Waltham, Massachusetts, USA) and prepared as shown in Table 5.

Table 5. Restriction digest reaction mixture.

x µL	200-800 ng DNA
0.5-1 µL	restriction enzyme
1.5 µL	reaction buffer (10x)
y µL	ddH_2O up to 15 µL total volume
15 µL	

The restriction digest with the conventional enzymes was carried out at 37 °C for at least four hours whereas an incubation time of only 30 minutes to one hour was necessary for the fast digest enzymes. Following, the reaction mixture was inactivated at 65 °C or 80 °C for 20 minutes according to the thermal inactivation temperature of the used restriction enzyme. Subsequently, if necessary the digested vector backbone was dephosphorylated using 1-2 µL of FastAP Thermosensitive Alkaline Phosphatase of Thermo Scientific (Table 6).

Table 6. Dephosphorylation reaction mixture.

x µL	linear DNA
2 µL	10x Thermo Scientific FastDigest Buffer
2 µL	FastAP Thermosensitive Alkaline Phosphatase
y µL	ddH_2O up to 20 µL total volume
20 µL	

After 30 minutes of incubation at 37 °C the FastAP Thermosensitive Alkaline Phosphatase was inactivated at 75 °C for 5 minutes.

To create blunt end DNA fragments for cloning purposes as well as for phosphorylation of DNA ends the Fast DNA End Repair Kit of Thermo Scientific was used. See Table 7 for Fast DNA End Repair reaction mixture.

Table 7. DNA End Repair reaction mixture.

x µL	DNA fragment
5.0 µL	10x End Repair Reaction Mix
2.5 µL	End Repair Enzyme Mix
y µL	ddH_2O up to 50 µL total volume
50 µL	

The reaction mixture was incubated at 20 °C for 15 minutes in a thermal cycler (Eppendorf Thermomixer comfort) and immediately purified with the Wizard® SV Gel and PCR Clean-Up System Kit of Promega (see 2.3.10 Gel purification).

The phosphorylation of PCR products for blunt end cloning was carried out with the T4 Polynucleotide Kinase of Thermo Scientific. A general reaction mixture for phosphorylation is shown in Table 8.

Table 8. Phosphorylation reaction mixture.

x µL	linear DNA fragment
2 µL	Reaction Buffer A
2 µL	ATP 10mM
1 µL	T4 Polynucleotide Kinase
y µL	ddH_2O up to 20 µL total volume
20 µL	

The reaction mixture was incubated at 37 °C for 20 minutes prior heat inactivation at 75 °C for 10 minutes and then purified with the Wizard® SV Gel and PCR Clean-Up System Kit of Promega (see 2.3.10 Gel purification).

2.3.3. Ligation

Ligation was conducted with T4 DNA Ligase as recommended by the manufacturers' protocol (Promega; Mannheim, Germany). Approximately 50 ng of vector backbone were used for a standard ligation reaction and the amount of insert calculated by a vector to insert ratio of 1:3. A general ligation mix is shown in Table 9.

Table 9. Standard ligation reaction mix.

x µL	~ 50 ng vector backbone
y µL	insert DNA (appropriate amount)
1.5 µL	ligation buffer (10x)
1.0 µL	T4 DNA ligase
z µL	ddH_2O up to 15 µL total volume
15 µL	

The ligation mixture was incubated at 16 °C over night or at 22 °C (room temperature) for four hours. Then, thermal inactivation at 70 °C for 10 minutes was carried out. In order to increase the efficiency of the transformation and to avoid any short-circuit the ligation mixture was desalted on water using nitrocellulose filters (MFTM Membrane Filters, 0.025 µm VSWP, Merck Millipore; Billerica, Massachusetts, USA).

2.3.4. Transformation

Transformation was conducted using electro competent cells of *E. coli* Top10 or S17-1. First, the cells were thawed on ice and then, 100-300 ng of DNA were added. After an incubation step of 10 minutes on ice, the cell suspension was pipetted into the cuvette and transformation carried out using the transformation program EC2 (0,2 mm cuvettes, 2,5 kV) of Micro PulserTM (Bio-Rad, Hercules, USA). Then, 1 mL of LB media was added and the cell suspension incubated at 37 °C for 45 minutes at 650 rpm. Following, 100 µL of the cell suspension as well as the resuspended pellet after centrifugation for 2 minutes at 5000 rpm were plated on LB agar supplemented with the appropriate antibiotic.

2.3.5. PCR

PCR reactions were performed with either the Phusion® High-Fidelity DNA Polymerase (Thermo Scientific) or Q5® High-Fidelity DNA Polymerase (New England Biolabs, Ipswich, Massachusetts, USA) as described in the manufacturers' protocol. A standard PCR reaction was carried as shown in Table 10.

Table 10. Standard PCR reaction with (**A**) Q5® High-Fidelity DNA Polymerase and (**B**) Phusion High-Fidelity DNA Polymerase.

(A)	5.0 µL	5x Q5 Reaction buffer	(B)	5 µL	Phusion HF Buffer (5x)
	0.6 µL	10mM dNTPs		0.6 µL	10mM dNTPs
	1.25 µL	Forward primer		1.25 µL	Forward primer
	1.25 µL	Reverse primer		1.25 µL	Reverse primer
	0.25 µL	Q5 High-Fidelity DNA Polymerase		0.3 µL	Phusion DNA Polymerase
	5.0 µL	5x Q5 High GC Enhancer (optional)		0.75 µL	DMSO (optional)
	x µL	Template DNA		x µL	Template DNA
	y µL	ddH_2O up to 25 µL		y µL	ddH_2O up to 25 µL
	25 µL			25 µL	

The PCR reaction was carried out in the GeneAmp® PCR System 2700 thermocycler of Applied Biosciences (Norwalk, Connecticut, USA). The general PCR program is shown below (Figure 3).

Initial denaturation	98 °C	30 sec	
Denaturation	98 °C	10 sec	25-35 cycles
Annealing	X °C	10-30 sec	
Extension	72 °C	Y sec	
Final Extension	72 °C	2 min (Q5)	
Final Extension	72 °C	10 min (Phusion)	

Figure 3. PCR program for Q5 High-Fidelity DNA Polymerase and Phusion High-Fidelity DNA Polymerase.

The initial denaturation and final extension step are provided whereas the denaturation, annealing and extension step can be varied according to the template DNA depending on the annealing temperature of the primer and the PCR product length.

All conducted PCRs during this project are summarized in Table 11 and are classified into a section for the Phusion® High-Fidelity DNA Polymerase and the Q5® High Fidelity DNA Polymerase.

Table 11. Summary of PCR conditions carried out with Phusion® and Q5® High-Fidelity DNA Polymerase respectively.

Phusion® High-Fidelity DNA Polymerase

PCR fragment	Primer pair	Annealingtemp., -time	Extensiontemp., -time	fragment size
pCM_mobRK2_redA9/redB2; pCM_mobRSF1010_redA9/redB2				
pK470_mob_ca1 Bb	colE1 pK470 Fwd rrnB pK470 Rev	65 °C, 30 sec	72 °C, 2 min	3222 bp
cm^r	Fwd cmR NotI Rev cmR SpeI	61 °C, 20 sec	72 °C, 1 min	1105 bp
pK470_mobRK2_estA_frtΔ_phaC1				
Bb-insertion SpeI	pK470 MOB SpeI Fwd pK470 MOB SpeI Rev	60 °C, 15 sec	72 °C, 1 min 30 sec	4134 bp
Bb-insertion frt up	FRT oben Fwd phaC1 FRT oben Rev phaC1	60 °C, 15 sec	72 °C, 1 min 30 sec	4174 bp
Bb-insertion frt down	FRT unten Fwd phaC1 FRT unten Rev phaC1	60 °C, 15 sec	72 °C, 1 min 30 sec	4214 bp
phaC1_1	phaC1 Fwd SpeI phaC1 Rev SpeI	64 °C, 15 sec	72 °C, 40 sec	886 bp
phaC1_2	phaC1 Fwd XhoI phaC1 Rev XhoI	64 °C, 15 sec	72 °C, 40 sec	908 bp
pCM_mobRK2_flp				
flp	FLP Fwd FLP Rev	67 °C, 15 sec	72 °C, 40 sec	1272 bp

Q5® High-Fidelity DNA Polymerase

PCR product	Primer pair	Annealingtemp., -time	Extensiontemp., -time	fragment size
pCM_mobRK2_redA9/redB2; pCM_mobRSF1010_redA9/redB2				
mobRK2	MOB oriT RK2 Fwd MOB oriT RK2 Rev	66 °C, 30 sec	72 °C, 1 min	788 bp
mobRSF1010	RSF1010_mob_fwd RSF1010_mob_rev	66 °C, 30 sec	72 °C, 1 min	2613 bp
pK470_mobRK2_estA_frtΔ_phaC1				
pK470_estA_frtΔ_phaC1 Bb	phaC1 Fwd SpeI pK470 colE1 rev	65 °C, 30 sec	72 °C, 2 min	5266 bp
Bb-insertion SphI	KanR-NotI-fwd phaC1 Rev SpeI SphI	68 °C, 30 sec	72 °C, 2 min	6054 bp
pK470_mobRK2_estA_frt_phaC1				
estA_rrnB_frtΔ	Fwd Expression cassette NdeI Rev Expression cassette FRT	68 °C, 30 sec	72 °C, 1 min	1389 bp
frtΔ_kanR_frtΔ	Fwd KanR FRT Rev KanR FRT	68 °C, 30 sec	72 °C, 1 min	865 bp
estA_rrnB_frt_kanR_frt	Fwd Expression cassette NdeI Rev FRT XhoI	56 °C, 30 sec	72 °C, 1 min 20sec	2254 bp

estA_rrnBΔ	Fwd Expression cassette NdeI rrnB rev	68 °C, 30 sec	72 °C, 40 sec	1327 bp
rrnBΔ_frt_kanR_frt	rrnB Fwd Rev FRT XhoI	68 °C, 30 sec	72 °C, 40 sec	949 bp
estA_rrnB_frt_kanR_frt	Fwd Expression cassette NdeI Rev FRT XhoI	58 °C, 30 sec	72 °C, 1 min 20sec	2254 bp
pK470_mobRK2_T7_frtΔ_phaC1				
T7pol (Gibson cloning)	fwd gibson T7 BamHI rev gibson T7 HindIII	58 °C, 30 sec	72 °C, 1 min 20sec	2764 bp
pK470_mobRK2_PCIV1bM_lacY_frtΔ_phaC1				
PCIV1bM_lacY	PCIV1bM SphI Fwd lacY rev	58 °C, 30 sec	72 °C, 1 min	1439 bp
pCM_Ptac_PAR_eGFP_RSF1010_lacI				
lacI	LacI_SpeI_fwd LacI_SpeI_rev	58 °C, 30 sec	72 °C, 1 min	1504 bp

2.3.5.1. Overlap Extension PCR

An overlap extension PCR was performed to introduce specific base exchanges in a DNA sequence as well as to be able to construct DNA fragments without the need of restriction sites and is based on the principle of the annealing of two complementary sequences.

All overlap extension PCRs were performed with the Q5® High-Fidelity DNA Polymerase. First, two standard PCRs were performed to amplify the desired DNA fragments (see 2.3.5 for a standard PCR reaction mix). The reverse primer of the first DNA fragment and the forward primer of the second DNA fragment introduced the complementary overlap of 20 bp. These amplified fragments served as templates for the overlap extension PCR. First, the PCR reaction was performed without any primers for six cycles to allow the complementary sequences to anneal. Then, the outer primers of the fragment to be amplified were added and the overlap PCR reaction ran for another 25 cycles to amplify the desired fragment.

2.3.6. Colony PCR

Colony PCR was conducted with DreamTaq DNA Polymerase according to the manufacturers' protocol (Thermo Scientific). Therefore, single colonies of *R. eutropha* H16 transconjugants were picked, resuspended in 20 µL ddH_2O and the cells disrupted at 99 °C for 10 minutes. Following, the cell solution was centrifuged at 5000 rpm for 2 minutes and an aliquot used to run the colony PCR reaction. See Table 12 for a general colony PCR reaction mix.

Table 12. Colony PCR reaction mix.

5 µL	Green GoTaq (5x)
0.6 µL	10mM dNTPs
1.25 µL	Forward Primer
1.25 µL	Reverse Primer
0.2 µL	DreamTaq Polymerase
2.0 µL	Template DNA
x µL	ddH_2O up to 25 µL total volume
25 µL	

The exact conditions for all colony PCR reactions carried out during this project are listed in Table 13.

Table 13. Summary of colony PCR conditions.

PCR fragment	Primer pair	Annealingtemp., -time	Extensiontemp., -time	fragment size
pK470_mob_ca1_estA				
megaplasmid	P-2-fwd P-2-rev	62 °C, 30 sec	72 °C, 50sec	423 bp
mob (pBBR1)	MOB fwd MOB rev	55 °C, 30 sec	72 °C, 1 min	1010 bp
5‘ integration (*ca1*)	Int CA1 Fwd Int KanR Rev	55 °C, 30 sec	72 °C, 1 min	999 bp
3‘ integration (*ca1*)	rrnB Fwd CA1 3’downstream rev	58 °C, 30 sec	72 °C, 1 min	790 bp
kan^r	KanR Int Fwd KanR Int Rev	55 °C, 30 sec	72 °C, 1 min	589 bp
pCM_mobRK2_redA9/redB2				
5‘ integration (*redA9*)	3' redA9 rrnB rev	56 °C, 30 sec	72 °C, 1 min	1553 bp
5‘ integration (*redB2*)	5' redB2 fwd rrnB rev	56 °C, 30 sec	72 °C, 1 min	923 bp
cm^r	Fwd cmR NotI Rev cmR SpeI	55 °C, 30 sec	72 °C, 1 min	1100 bp
pK470_mobRK2_estA_frtΔ/frt_phaC1				
phaC1_2 orientation (1)	phaC1 Fwd XhoI colE1 Rev	55 °C, 30 sec	72 °C, 1 min	1573 bp
phaC1_2 orientation (2)	KanR Int Fwd phaC1 Rev XhoI	55 °C, 30 sec	72 °C, 1 min	1658 bp
5‘ integration (*phaC1*)	5' Int phaC1 Fwd Int Est Rev	53 °C, 30 sec	72 °C, 1 min	1499 bp
3‘ integration (*phaC1*)	Int KanR Fwd 3' Int phaC1 Rev	53 °C, 30 sec	72 °C, 1 min	1137 bp

5‘ phaC1 in 3‘ after integration	5' Int phaC1 Fwd 3' Int phaC1 Rev	53 °C, 30 sec	72 °C, 4 min	4685 bp
kan^r in ColE1 (after Flp)	Int KanR Fwd colE1 Rev	53 °C, 30 sec	72 °C, 1 min	-
pK470_mobRK2_T7_frtΔ_phaC1				
part of T7pol1	seqT7pol_2 seqT7pol_3	53 °C, 30 sec	72 °C, 1 min	759 bp
part of T7pol2	seqT7pol_4 seqT7pol_5	53 °C, 30 sec	72 °C, 1 min	849 bp
3‘ integration (T7)	Int KanR Fwd 3' Int phaC1 Rev	53 °C, 30 sec	72 °C, 1 min	1137 bp
PT7_MCS in cm^r	nT7MCS_PstI_fwd2 Rev cmR SpeI	53 °C, 30 sec	72 °C, 1 min	1988 bp
pK470_mobRK2_PCIV1bM_lacY_frtΔ_phaC1				
5‘ integration (*lacY*)	5' Int phaC1 Fwd PCIV1bMrev	53 °C, 30 sec	72 °C, 1 min	1062 bp
3’integration (*lacY*)	Int KanR Fwd 3' Int phaC1 Rev	53 °C, 30 sec	72 °C, 1 min	1137 bp

2.3.7. Gibson cloning

Gibson cloning is another strategy to clone different fragments by the use of overlapping homologies and was performed according to the Gibson Assembly® Protocol (New England Biolabs). See Table 14 for a general Gibson assembly reaction mixture and Table 15 for the preparation of an assembly master mix.

Table 14. Gibson assembly reaction mix.

5.0 µL	DNA fragments
15.0 µL	Gibson Assembly Master Mix 2x
20 µL	

Table 15. Preparation of (**A**) assembly master mix (2x) and (**B**) 5x isothermal (ISO) reaction buffer.

(A)

320.00 µL	5x ISO reaction buffer
0.64 µL	T5 exonuclease (10 U/µL)
20.00 µL	Phusion® DNA Polymerase (2 U/µL)
160.00 µL	Taq DNA ligase (40 U/µL)
699.36 µL	ddH_2O
1200 µL	

(B)

1.5 g	PEG-8000
3000 µL	1 M Tris/Cl, pH 7.5
150 µL	2 M $MgCl_2$
300 µL	1 M DTT
240 µL	100 mM dNTP
300 µL	100 mM NAD^+
x µL	ddH_2O up to 6 mL
6000 µL	

At least 100 ng of each DNA fragment should be used in equimolar amounts for the Gibson assembly. The reaction mixture was then incubated at 50 °C for 60 minutes. Following, the mixture was centrifuged briefly, desalted and 5 µL electroporated into *E. coli* competent cells.

2.3.8. Gel electrophoresis

Gel electrophoresis was applied to separate DNA fragments of different size. For the separation a 1 % agarose gel was used. Therefor, 2 g of agarose (Biozyme, Vienna, Austria) were mixed with 200 mL TAE buffer (4,84 g/L Tris, 0,29 g/L EDTA, 1,14 g/L acetic acid). Then, the agarose was microwaved till it was dissolved (~ 3 min) and after rinsing the flask with water to cool down the solution 5 µL of ethidium bromide (EtBr) were added and the solution poured into a gel tray. After polymerization was complete the gel was loaded with the samples (prior mixed with loading dye) and a preparative gel ran at 90 V for 1 h 30 min and at 120 V for 45 min for a control gel. The used DNA ladder is shown in the appendix (Figure 50).

2.3.9. Plasmid isolation

The GeneJET Plasmid Miniprep Kit of Thermo Scientific was used for plasmid isolation. The isolation was carried out according to the manufacturers' protocol. Changes to the manufacturers' protocol are marked in bold letters.

1. Resuspension of cells, lysis and neutralization

Added to the pelleted cells:

◦ 250 µL of resuspension solution and vortexed.

◦ 250 µL of lysis solution and inverted tube 4 – 6 times.

◦ 350 µL of neutralization solution and inverted tube 4 – 6 times.

Mixture was centrifuged at full speed for 10 min.

2. Binding of DNA

Supernatant was loaded to GeneJET™ spin column and centrifuged at full speed for 1 min.

3. Wash the column

500 µL of wash solution was added and centrifuged at full speed for 1 min. } Repeat twice

Flow-through was discharged.

Empty column was centrifuge at full speed for 1 min.

4. Elute purified DNA

The column was transferred into a new tube.

50 µL of bidest.H_2O were added to the column and incubated for 2 min.

The column was centrifuged at full speed for 2 min and the flow-through collected.

2.3.10. Gel purification

The Wizard® SV Gel and PCR Clean-Up System Kit (Promega, Mannheim, Germany) was used to dissolve an agarose gel slice or to clean up a PCR product or a restriction digest. The kit was used as recommended by the manufacturer. Changes to the manufacturers' protocol are marked in bold letters.

A. Dissolving the gel slice

1. 10 µL of membrane binding solution per 10 mg of gel slice were added.

The sample was vortexed and incubated at 65 °C until the gel slice was completely dissolved.

B. Processing PCR reactions

1. An equal volume of membrane binding solution was added to the PCR reaction.

C. Binding of DNA

1. SV minicolumn was inserted into the collection tube.

2. The dissolved gel mixture or the prepared PCR reaction was transferred into the minicolumn assembly and incubated at room temperature for 1 min.

3. The minicolumn was centrifuged at 16,000 x *g* for 1 minute. The flow-through was discarded and the minicolumn reinserted into the collection tube.

D. Washing

1. 700 µL membrane wash solution was added, centrifuged at 16,000 x g for 1 min. The flow-through was discarded and the minicolumn reinserted into the collection tube.

2. Step D.1 was repeated with 500 µl of membrane wash solution, centrifuged at 16,000 x g for 5 min.

3. The minicolumn was centrifuged again at 16,000 x g for 1 minute.

E. Elution

1. The minicolumn was transferred into a clean 1.5 mL microcentrifuge tube.

2. 30 µL of bidest.H2O was added, incubated at room temperature for 5 min and centrifuged at 16,000 x g for 1 min.

2.3.11. CloneJET PCR Cloning Kit

The CloneJET PCR Cloning Kit of Thermo Scientific was used according to the manufacturers' protocol to clone amplified PCR products directly into the linearized cloning vector pJET1.2. The big advantage of this method is that no phosphorylation step is necessary prior cloning. A standard ligation mixture is shown in Table 16.

Table 16. Standard ligation mixture of pJET1.2.

10 µL	2x Reaction buffer
x µL	purified PCR product
1 µL	pJET1.2/blunt Cloning Vector
1 µL	T4 DNA Ligase
x µL	ddH_2O up to 20 µL total volume
20 µL	

The optimal PCR product quantity for a ligation reaction increases with the length of the fragment. The ligation mixture was incubated at room temperature (22 °C) for 20 minutes. Then, the ligation mixture was inactivated at 65 °C for 10 minutes and desalted or directly used for transformation.

2.3.12. Sequencing

Sequencing was conducted to determine the correct sequence of the amplified DNA fragments. For that reason, 10 µL of the DNA fragment to be sequenced supplemented with 4 µL (5 µM) of the appropriate primer were sent for sequencing. Sequencing was performed by LGC Genomics GmbH (Berlin, Germany).

2.4. SDS-PAGE

The SDS-PAGE (sodium dodecyl sulfate polyacrylamide gel electrophoresis) was carried out with electrophoresis tools of Hoefer, Inc. (SE 250 Mighty Small II, Hoefer, Inc., Holliston, USA). At the beginning, the resolving gel was poured and after polymerization, butanol which was added to cover the gel surface and avoid the formation of air bubbles during polymerization was removed, the stacking gel was poured. See Table 17 for the composition of the resolving and stacking gel (volumes are given for one gel).

Table 17. Composition of resolving gel and stacking gel.

	Resolving gel (12 %)	**Stacking gel (4 %)**
Acrylamid	0.75 mL	3.2 mL
Resolving gel buffer[a]	2 mL	-
Stacking gel buffer[b]	-	1.25 mL
APS (10 %)	10 µL	25 µL
TEMED	7.5 µL	10 µL
Bromphenol Blue	5 µL	-
H_2O	3 mL	2.8 mL

[a] resolving gel buffer, 0.5 M Tris, 0.4 % SDS, pH 8.8

[b] stacking gel buffer, 0,5 M Tris, 0.4 % SDS, pH 6.8

An overnight culture (ONC) of the samples to be loaded was inoculated with a single colony of either *E. coli* or *R. eutropha* H16. Then, the OD_{600} of each sample was determined and 1 mL of the ONC was taken and centrifuged. The supernatant was discarded and the cell pellet resuspended in potassium phosphate buffer (pH 7.4, 0.1 M). The necessary volume of potassium phosphate buffer was calculated by multiplying the OD_{600} value with 33.3. 5 µL of the *R. eutropha* H16 and 3 µL of the *E. coli* cell suspension were used for further sample preparation. The reaction mixture to disrupt the cells prior loading on the gel is shown in Table 18.

Table 18. Sample preparation for SDS-gel.

	***R. eutropha* H16**	***E. coli***
Resuspended cells	5 µL	3 µL
FSB Buffer 5x	2.4 µL	2.4 µL
NaOH (0.1 M)	1 µL	1 µL
SDS (20 %)	1 µL	1 µL
β-Mercaptoethanol	0.6 µL	0.6 µL
Potassium phosphate buffer (pH 7.4, 0.1 M)	2 µL	4 µL
	12 µL	12 µL

After the reaction mixture was mixed up, it was heated at 99 °C for 10 minutes in a thermocycler, centrifuged briefly and the lysate loaded on the gel. The used protein ladder is shown in the appendix (Figure 51). Then, the gel was covered with running buffer (25 mM

Tris, 192 mM glycine, 0.1 % SDS) and run at 200 V for 10 minutes followed by 110 V approximately for 60 minutes.

After that the gel was unhinged of the fixture and stained with Coomassie Brilliant Blue (Brilliant Blue G 250, Carl Roth GmbH & Co. KG, Heidelberg, Germany) for 20 minutes followed by discolouration with acetic acid (10 %) overnight.

2.5. Esterase activity stain

The unstained SDS-PAGE gel was used to perform an activity stain to be able to detect esterase activity. After the samples were run, the gel was put into renaturation buffer (6.99 g/L $NaH_2PO_4*2H_2O$, 2.64 g/L citric acid monohydrate, to pH 6.3 with NaOH) and 30 % Isopropanol (Carl Roth GmbH & Co KG, Karlsruhe, Germany) for 45 minutes. Following, the gel was put in pure renaturation buffer twice for 20 minutes. Then, the staining solution comprised of 10 mL Tris/HCl 0.1 M pH 7, 750 µL a-naphthylacetate (12 mg/mL acetone; Carl Roth GmbH & Co KG, Karlsruhe, Germany) and 250 µL FastBlueB (20 mg/mL; Sigma-Aldrich Chemie GmbH, Steinheim, Germany) was added and the gel stained for 10 minutes. The esterase band should appear violet after 4-5 minutes. Following the gel was stained with Coomassie Brilliant Blue as described in 2.4 SDS-PAGE.

2.6. Conjugation

Single colonies of *E. coli* S17-1 (donor) and *R. eutropha* H16 (acceptor) were picked to inoculate overnight cultures (ONCs). *R. eutropha* H16 was grown in 10 mL TSB media supplemented with gentamycin [20 µg/mL] at 28 °C for 48 h and the *E. coli* S17-1 strain in 10 mL LB media supplemented with the appropriate antibiotic at 37 °C for approximately 24 h. Afterwards, the cells were harvested by centrifugation (3500 rpm, 20 minutes at 4 °C; Eppendorf centrifuge 5810 R) and the cell pellet resuspended in 0.5 mL NaCl (0,9 %). Subsequent, 200 µL of both the donor and acceptor suspension were trickled on NB media and incubated at 28 °C for 20 hours. Additionally, control plates with either 200 µL donor or acceptor suspension were carried along. Then, the cells were resuspended with 3 mL NaCl (0,9 %) and 100 µL plated on TSB media (0.2 % fructose, gentamycin [20 µg/mL] and kanamycin [200 µg/mL] or chloramphenicol [100 µg/mL]). If a recombination event was the desired result the cell suspension was plated undiluted or as a 1:10 dilution on the selection plate, whereas if a plasmid with an origin of replication which is stable in *R. eutropha* H16

was used, a serial dilution (10^0-10^{-5}) was performed. The TSB plates were incubated at 28 °C till cell growth was visible (approximately 48 h). Following, single colonies were re-streaked for purification purposes prior colony PCR.

2.7. Esterase filter activity assay

The esterase filter activity assay was conducted to test transconjugants for esterase activity. Single colonies of *R. eutropha* H16 transconjugants were transferred on a Whatmann-filter and dried (37 °C, 10 minutes). Then, 1 mL staining solution (5 mL Tris/HCl 0,1M pH7), 375 µL α-naphthyl acetate (12 mg/mL in acetone) and 125 µL FastBlueB (20 mg/mL)) were spilled over the filter and the esterase activity determined by a discolouration to violet [98].

2.8. Mobilization efficiency

Three different mobilization regions of the plasmid pBBR1-MCS5 (*mob*), the RK2 plasmid (*mobRK2*) and the pKT231 (*mobRSF1010*) were compared in their mobilization efficiency according to R. Meyer [99]. Therefore, the plasmids pKR_Ptac_Par_eGFP_mob_pSA, pKR_Ptac_Par_eGFP_mobRK2_pSA and pKR_Ptac_Par_eGFP_mobRSF1010_pSA were constructed (2.11 Construction of pKR_Ptac_Par_eGFP_mobRK2_pSa and pKR_Ptac_Par_eGFP_mobRSF1010_pSa). After the successful construction, the plasmids were transformed into *E. coli* S17-1 and then transferred into *R. eutropha* H16 via conjugation. Prior conjugation, an aliquot of the overnight culture was taken and dilutions were prepared (to 10^{-6}). These dilutions were plated on LB media supplemented with 40 µg/mL kanamycin and the colony forming units (CFUs)/mL determined. After conjugation, the CFUs/mL of *R. eutropha* H16 transconjugants growing on the selective media (TSB supplemented with gentamycin [20 µg/mL], kanamycin [200 µg/mL] and 0.2 % fructose) were determined. Then, the mobilization efficiency was determined by relating the CFU/mL of *R. eutropha* H16 transconjugants to the one of *E. coli* S-17-1 transformants as shown below.

$$\textbf{mobilization efficiency} = \frac{\textit{R. eutropha}\ \text{H16 transconjugant CFU/mL}}{\textit{E. coli}\ \text{S17-1 CFU/mL}}$$

2.9. Fluorescence unit measurement

A single colony of *R. eutropha* H16 transconjugant was used to inoculate a pre-culture in liquid TSB media supplemented with gentamycin [20 µg/ml], kanamycin [200 µg/ml] and chloramphenicol [100 µg/ml]. Following an aliquot of the ONC was used to inoculate TSB media to an OD_{600} of 0.2 and grown at 28 °C for 8 hours and the OD_{600} determined once more. Then, 200 µL of this culture were used for fluorescing unit (FU) measurement. The FUs were determined with FLUOstar Omega (BMG Labtech, Ortenberg, Germany) at an excitation wavelength of 480 nm and an emission wavelength of 510 nm and related to the OD_{600} value. Thereby, the relative fluorescing units (RFUs) could be calculated. The RFU value of *R. eutropha* H16 (pKRSF1010Δegfp) serving as negative control was subtracted of the RFU values.

2.10. Construction of pCM_mobRK2_redA9/redB2 and pCM_mobRSF1010_redA9/redB2

The plasmid pK470_mob_ca1 was chosen as starting vector for the construction of pCM_mobRK2_redA9/redB2 and pCM_mobRSF1010_redA9/redB2 (Figure 4).

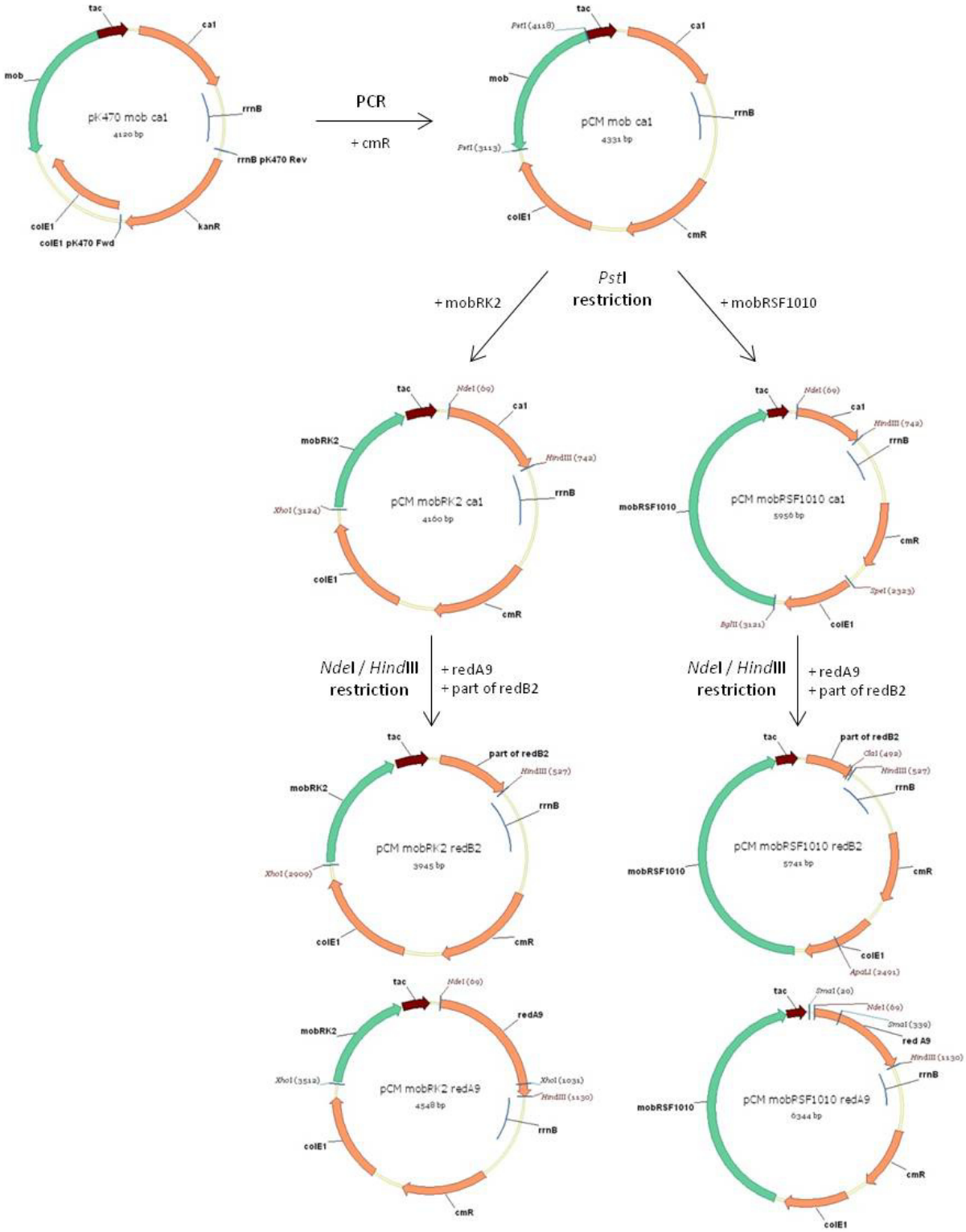

Figure 4. Construction of pCM_mobRK2_redA9/redB2 and pCM_mobRSF1010_redA9/redB2.
The plasmid pK470_mob_ca1 was used as a starting vector. After PCR amplification of the plasmid backbone with colE1 pK470 Fwd and rrnB pK470 Rev, kan^r was replaced by cm^r amplified with Fwd cmR NotI and Rev cmR SpeI. Following a *Pst*I restriction digest the mobilization sequence of the pBBR1-MCS5 plasmid was replaced by the mobilization sequence of RK2 and RSF1010 plasmid respectively. Finally, the homologous sequence *ca1* was replaced by *redA9* and a part of *redB2* after a *Nde*I and *Hind*III restriction digest to generate pCM_mobRK2_redA9/redB2 and pCM_mobRSF1010_redA9/redB2 respectively.

First, the vector pK470_mob_ca1 without the kanamycin resistance was amplified with colE1 pK470 Fwd and rrnB pK470 Rev to replace it with the chloramphenicol resistance. C*m*^{r} was amplified of pJET_cmR (originally amplified of plasmid pSC101) with the primers Fwd cmR NotI and Rev cmR SpeI. Then, the amplified fragments were purified, *cm*^{r} phosphorylated, the DNA concentration determined and a ligation reaction conducted prior transformation. Subsequently, the plasmid pCM_mob_ca1 was isolated and digested with *Pst*I prior blunting and dephosphorylation to replace the *mob* region of the pBBR1-MCS5 plasmid with the *mob* region of the RK2 plasmid (*mobRK2*) and the *mob* region of the pKT231 plasmid (*mobRSF1010*). The *mob* region of the RK2 plasmid was directly amplified from RK2 with the primers MOB oriT RK2 Fwd and MOB oriT RK2 Rev whereas *mobRSF1010* was amplified of pKT231 with RSF1010_mob_fwd and RSF1010_mob_rev. Subsequently, the amplified fragments were purified and cloned into pJET1.2 cloning vector generating pJET_mobRK2 and pJET_mobRSF1010. After the correct sequence was determined via sequencing, the plasmids were digested with *Bgl*II, purified and blunted. Then, ligation reactions with pCM_ca1 backbone and *mobRK2* and *mobRSF1010* were carried out. After transformation, the successful construction of pCM_mobRK2_ca1 and pCM_mobRSF1010_ca1 respectively was determined via restriction digest.

Then, the homologous region *ca1* was replaced by the homologous regions of the reductase A9 (*redA9*) and a part of the reductase B2 (*redB2*). The plasmid pK470_redA9 was double digested with *Nde*I and *Hind*III as well as the plasmids pCM_mobRK2_ca1 and pCM_mobRSF1010_ca1 prior dephosphorylation. The vector pK470_redB2 was first digested with the restriction enzyme *Pst*I and then, blunted prior the *Hind*III restriction digest. The vector backbones were first digested with the restriction enzyme *Nde*I and after the blunting of the fragment as well digested with *Hind*III followed by dephosphorylation. Afterwards, the restriction digests were loaded onto an agarose gel, the appropriate bands excised and purified prior ligation. Transformants were streaked out for plasmid isolation after transformation to check for successful cloning. Finally, the constructed plasmids pCM_mobRK2_redA9/redB2 and pCM_mobRSF1010_redA9/redB2 were transformed into *E. coli* S17-1 cells.

2.11. Construction of pKR_Ptac_Par_eGFP_mobRK2_pSa and pKR_Ptac_Par_eGFP_mobRSF1010_pSa

Three different mobilization regions were compared in their mobilization efficiency as described in 2.8 Mobilization efficiency. The plasmid pKR_Ptac_Par_eGFP_mobRK2_pSa and pKR_Ptac_Par_eGFP_mobRSF1010_pSa had to be constructed whereas the plasmid pKR_Ptac_Par_eGFP_mob_pSa was already constructed by Steffen Gruber. Thereby, the mobilization region of the RK2 plasmid (*mobRK2*) and pKT231 (*mobRSF1010*) were cloned into the plasmid pKR_Ptac_Par_eGFP_mob_pSa replacing the *mob* sequence of pBBR1-MCS5 (Figure 5).

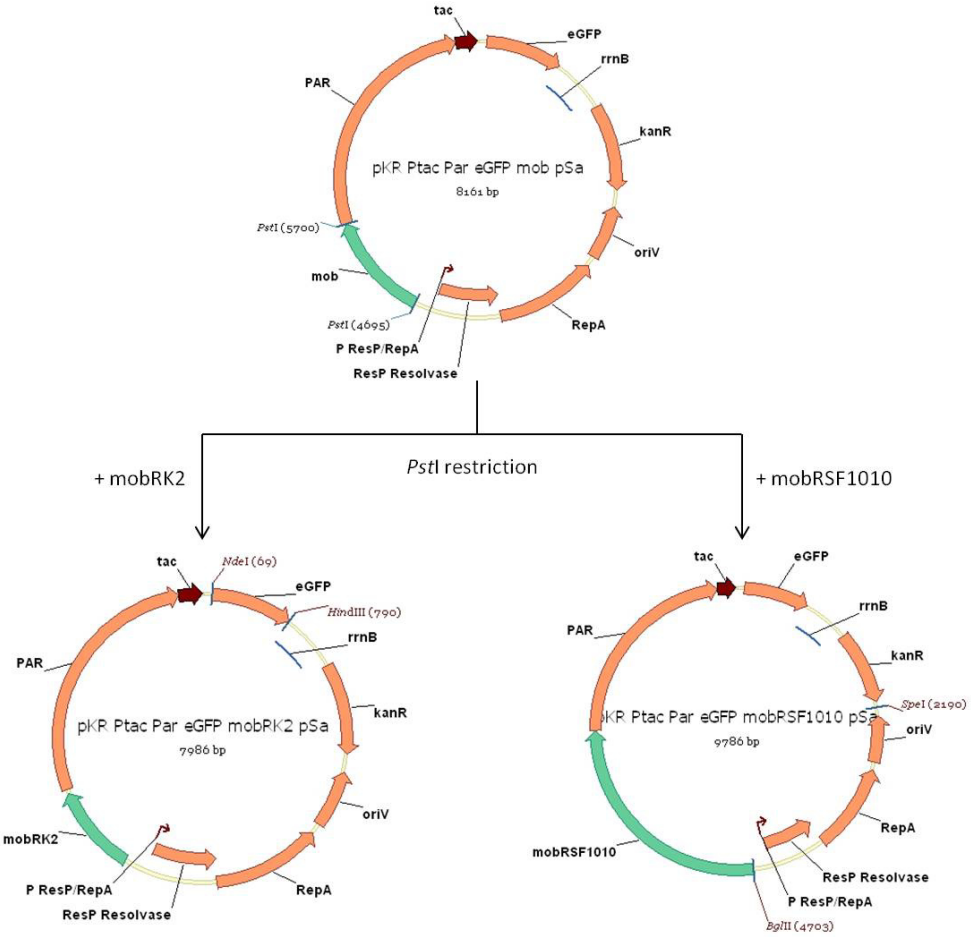

Figure 5. Construction of pKR_Ptac_Par_eGFP_mobRK2_pSa and pKR_Ptac_Par_eGFP_mobRSF1010_pSa. The plasmid pKR_Ptac_Par_eGFP_mob_pSa was used as a starting vector and digested with the restriction enzyme *Pst*I prior blunting. Subsequently, the plasmids pJET_mobRK2 and pJET_mobRSF1010 were restriction digested with *Bgl*II to gain *mobRK2* and *mobRSF1010*, blunted and cloned into the vector backbone to generate pKR_Ptac_Par_eGFP_mobRK2_pSa and pKR_Ptac_Par_eGFP_mobRSF1010_pSa.

The plasmid pKR_Ptac_Par_eGFP_mob_pSA was digested with *Pst*I, blunted and dephosphorylated. To gain the mobilization regions *mobRK2* and *mobRSF1010* the plasmids

pJET_mobRK2 and pJET_mobRSF1010 were digested with *Bgl*II and blunted prior cloning into the vector backbone. Then, the successful construction of the plasmids pKR_Ptac_Par_eGFP_mobRK2_pSa and pKR_Ptac_Par_eGFP_mobRSF1010_pSa was determined via restriction digest. Subsequently, all three plasmids were transformed into *E. coli* S17-1 cells.

2.12. Construction of pK470_mobRK2_estA_frt_phaC1

2.12.1. Construction of pK470_mobRK2_estA_frtΔ_phaC1

The plasmid pK470_mob_ca1 was the starting vector for the construction of pK470_mobRK2_estA_frtΔ_phaC1. The vector construction is illustrated in Figure 6.

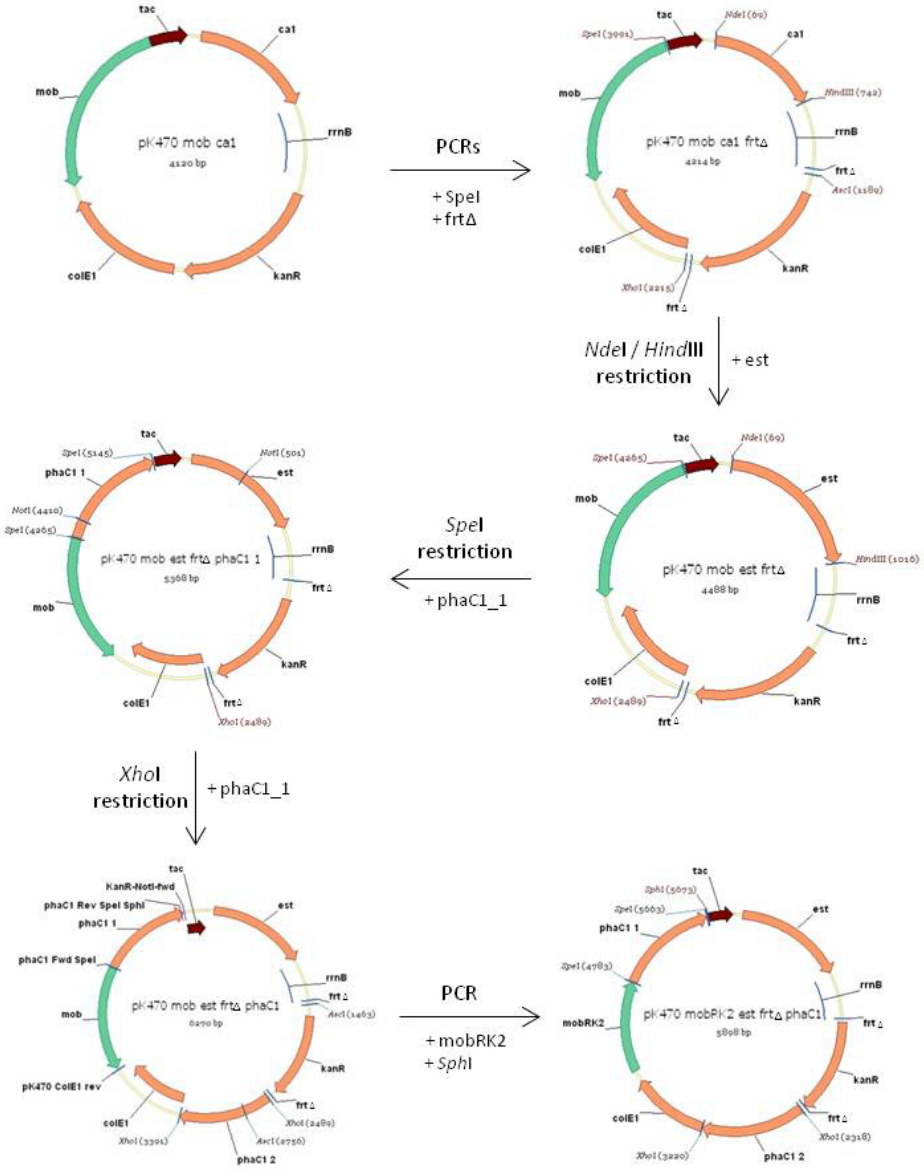

Figure 6. Flowchart of the construction of pK470_mobRK2_estA_frtΔ_phaC1.
The plasmid pK470_mob_ca1 was PCR amplified to introduce a *Spe*I restriction site (pK470 MOB SpeI Fwd and pK470 MOB SpeI Rev) as well as the frt site up including an *Asc*I restriction site (FRT oben Fwd phaC1 and FRT oben Rev phaC1) and the frt site down including an *Xho*I restriction site (FRT unten Fwd phaC1 and FRT unten Rev phaC1). Following the *Nde*I and *Hind*III restriction digest, the reporter gene *estA* was cloned into the vector backbone. Subsequently, the homologous regions *phaC1_1* and *phaC1_2* were cloned into the *Spe*I and *Xho*I restriction site respectively. Then, a further PCR was carried out with the primers phaC1 Fwd SpeI and pK470 ColE1 rev amplifying the vector backbone to replace the *mob* region of pBBR1-MCS5 with the one of the RK2 plasmid. In addition, a further PCR was conducted to introduce a *Sph*I restriction site upstream of the promoter region (KanR-NotI-fwd and phaC1 Rev SpeI SphI). Primers are indicated in the vector map.

At the beginning, the plasmid was amplified with the primers pK470 MOB SpeI Fwd and pK470 MOB SpeI Rev to introduce a *Spe*I restriction site. Then, after purification, a ligation reaction followed by a transformation was carried out. After a control cut to assure the correct introduction of the *Spe*I restriction site, a PCR was conducted to introduce the frt sites up including an *Asc*I restriction site (FRT oben Fwd phaC1, FRT oben Rev phaC1). Again, the amplified fragment was purified and a ligation reaction conducted. Single colonies were analysed for the correct incorporation of the frt site up via restriction digest. Subsequently, the frt site down including a *Xho*I restriction site was introduced via PCR with the primers FRT unten Fwd phaC1 and FRT unten Rev phaC1. After ligation and transformation of the amplified fragment, the correct size and incorporation of the frt site down was verified via restriction digest.

Simultaneously, the homologous regions *phaC1_1* with a *Spe*I restriction site (*phaC1 Fwd SpeI*, *phaC1 Rev SpeI*) and *phaC1_2* flanked by a *Xho*I restriction site (*phaC1 Fwd XhoI*, *phaC1 Rev XhoI*) were amplified of the genome of *R. eutropha* H16 and cloned into the pJET1.2 cloning vector after purification. The correct sequence was verified via sequencing.

After the incorporation of all necessary restriction sites as well as the frt sites, the plasmid pK470_mob_ca1_frtΔ was digested with *Nde*I and *Hind*III to replace the *ca*1 gene with the esterase A of *Rhodococcus ruber* of the plasmid pK470_mob_ca1_estA also digested with the same restriction enzymes. Then, after dephosphorylation of the vector backbone followed by purification, the ligation reaction and transformation were performed followed by a new plasmid isolation. The plasmid pK470_mob_estA_frtΔ was then cut at the previously introduced *Spe*I restriction site and dephosphorylated. Concurrently the plasmid pJET_phaC1_1 was digested with the *Spe*I restriction enzyme as well and the first homologous region *phaC1_1* cloned into the vector backbone. The incorporation of the homologous region in the correct orientation was determined via restriction digest with the restriction enzyme *Not*I. Afterwards, the plasmid pJET_phaC1_2 was digested with *Xho*I and the second homologous region *phaC1_2* cloned into pK470_mob_estA_frtΔ_phaC1_1 backbone previously cut at the *Xho*I restriction site followed by dephosphorylation. To be able to determine the incorporation of the second homologous region *phaC1_2* in the correct orientation after ligation and transformation a colony PCR was conducted with the primers phaC1 Fwd XhoI and colE1 Rev. Finally, after a positive clone was identified, the

plasmid pK470_mob_estA_frtΔ_phaC1 was isolated and used as template to amplify the plasmid backbone and thus being able to replace the *mob* region of pBBR1-MCS5 with the *mob* region of the RK2 plasmid [38]. The PCR was conducted with the primers phaC1 Fwd SpeI and pK470 ColE1 rev whereas the *mob* region of the RK2 plasmid was amplified with the primers MOB oriT RK2 Fwd and MOB oriT RK2 Rev and phosphorylated prior ligation. After transformation, single colonies were streaked out for plasmid isolation and a restriction digest with *Pst*I was carried out to determine the successful construction of pK470_mobRK2_estA_frtΔ_phaC1.

However, the sequencing results of the plasmid pK470_mobRK2_estA_frtΔ_phaC1 showed incomplete frt sites. Before the frt sites were repaired another PCR was performed to introduce a *Sph*I restriction site into pK470_mobRK2_estA_frtΔ_phaC1 upstream of the promoter to be able to replace the expression cassette. The PCR was performed with the primers KanR-NotI-fwd and phaC1 Rev SpeI SphI and the amplified fragment was religated after purification and phosphorylation.

2.12.2. Correction of frt sites and construction of pK470_mobRK2_estA_frt_phaC1

The previously constructed plasmid pK470_mobRK2_estA_frtΔ_phaC1 showed to have incomplete frt sites after sequencing. Thus a new fragment consisting of a *Nde*I restriction site upstream of the fragment, the esterase, terminator sequence, kanamycin resistance flanked by the frt sites and a *Xho*I restriction site downstream of the fragment was constructed.

At the beginning, a PCR reaction on the template pK470_mob_ca1_estA was performed to amplify the two fragments needed to perform the overlap extension PCR (Figure 7).

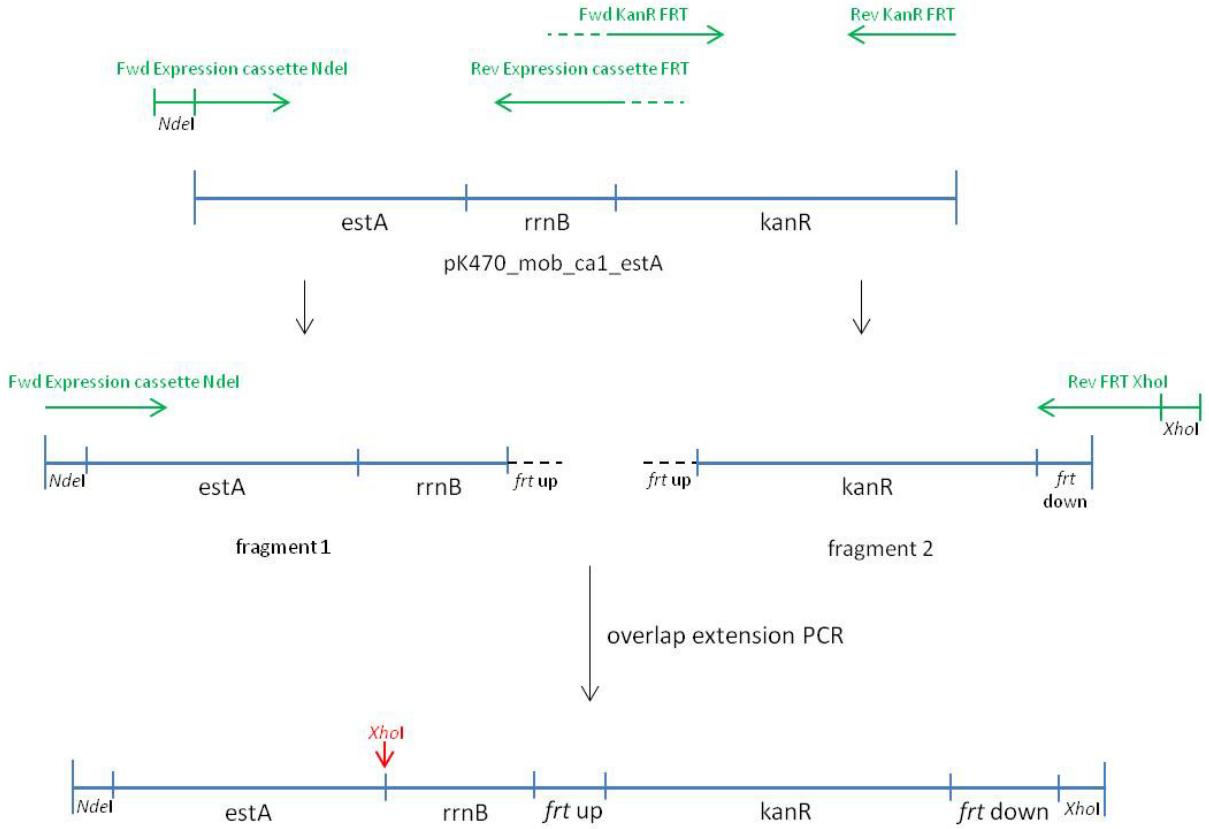

Figure 7. Scheme of the construction of the fragment estA_rrnB_frt_kanR_frt via overlap extension PCR. The plasmid pK470_mob_ca1 was used as template to generate the overlap fragments for a subsequent overlap extension PCR. Fragment 1 was amplified with Fwd Expression cassette NdeI and Rev Expression cassette FRT whereas fragment 2 was amplified with Fwd KanR FRT and Rev KanR FRT using the frt site up as complementary sequence. Following, an overlap extension PCR was performed with the outer primers Fwd Expression cassette NdeI and Rev FRT XhoI to complete the frt site down and introduce the *Xho*I restriction site. The dashed lines are indicating the complementary sequence.

The first fragment ranging from the *Nde*I restriction site in front of the esterase over the terminator region into the frt site up was amplified with the primers Fwd Expression cassette NdeI and Rev Expression cassette FRT whereas the second fragment from the frt site up over the kanamycin resistance into the frt site down was amplified with the primers Fwd KanR FRT and Rev KanR FRT. After the purification of these fragments, an overlap extension PCR with the two fragments as templates with a part of the frt site up as complementary sequence was performed with the outer primers Fwd Expression cassette NdeI and Rev FRT XhoI (Figure 7). The primer Rev FRT XhoI was necessary to complete the frt site down as well as to introduce the *Xho*I restriction site. The fragment generated with the overlap extension PCR was then purified and cloned into the pJET1.2 cloning vector. The following sequencing

revealed that the frt sites were incorporated correctly. However, a further *Xho*I restriction site was revealed between the esterase and terminator sequence as can be seen in Figure 7. Thus, another overlap extension PCR had to get rid of this *Xho*I restriction site using a region of the terminator as complementary sequence (Figure 8).

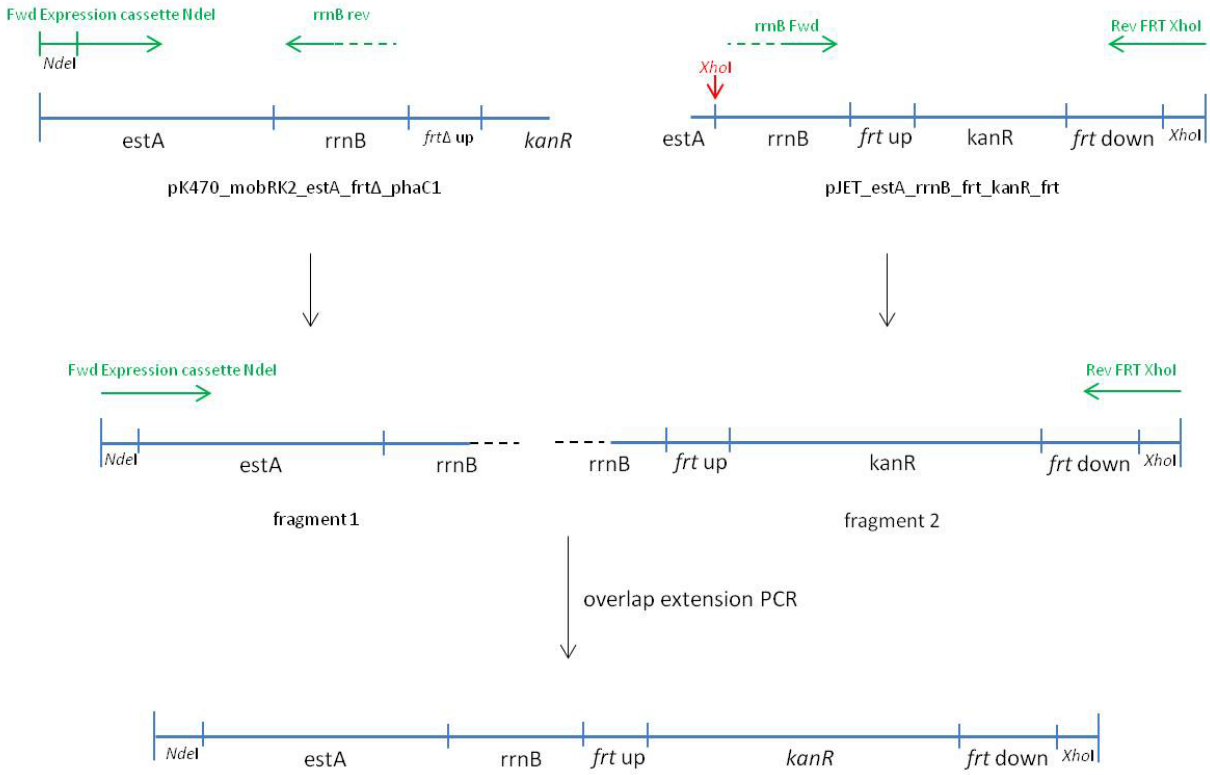

Figure 8. Scheme of the deletion of the *Xho*I restriction site while constructing estA_rrnB_frt_kanR_frt via overlap extension PCR.
Fragment 1 was amplified of pK470_mobRK2_estA_frtΔ_phaC1 with Fwd Expression cassette NdeI and rrnB rev whereas fragment 2 was amplified of pJET_estA_rrnB_frt_kanR_frt with rrnB Fwd and Rev FRT XhoI. Following, an overlap extension PCR with Fwd Expression cassette NdeI and Rev FRT XhoI of these two fragments with a region of rrnB as complementary sequence was performed. The dashed lines are indicating the complementary region.

The first fragment ranging from the *Nde*I restriction site into the terminator region was amplified with Fwd Expression cassette NdeI and rrnB rev with pK470_mobRK2_estA_frtΔ_phaC1 serving as template. The second fragment starting in the terminator region and including the frt site up, the kanamycin resistance and the frt site down with the *Xho*I restriction site was amplified of the pJET_estA_XhoI_frt_kanR_frt vector with the previously cloned overlap fragment with the *primers* rrnB Fwd and Rev FRT XhoI (Figure 8). After purification, an overlap extension PCR of these two fragments was performed with the outer primers Fwd Expression cassette NdeI and Rev FRT XhoI. Again,

the overlap fragment was purified and cloned into the pJET1.2 cloning vector and sent for sequencing.

After the correct sequence was confirmed, the plasmid pJET_estA_frt_kanR_frt was double digested at the previously introduced *Nde*I and *Xho*I restriction sites as well as the plasmid pK470_mobRK2_estA_frtΔ_phaC1. The vector backbone was dephosphorylated and the fragment with the correct frt sites cloned into its backbone (Figure 9).

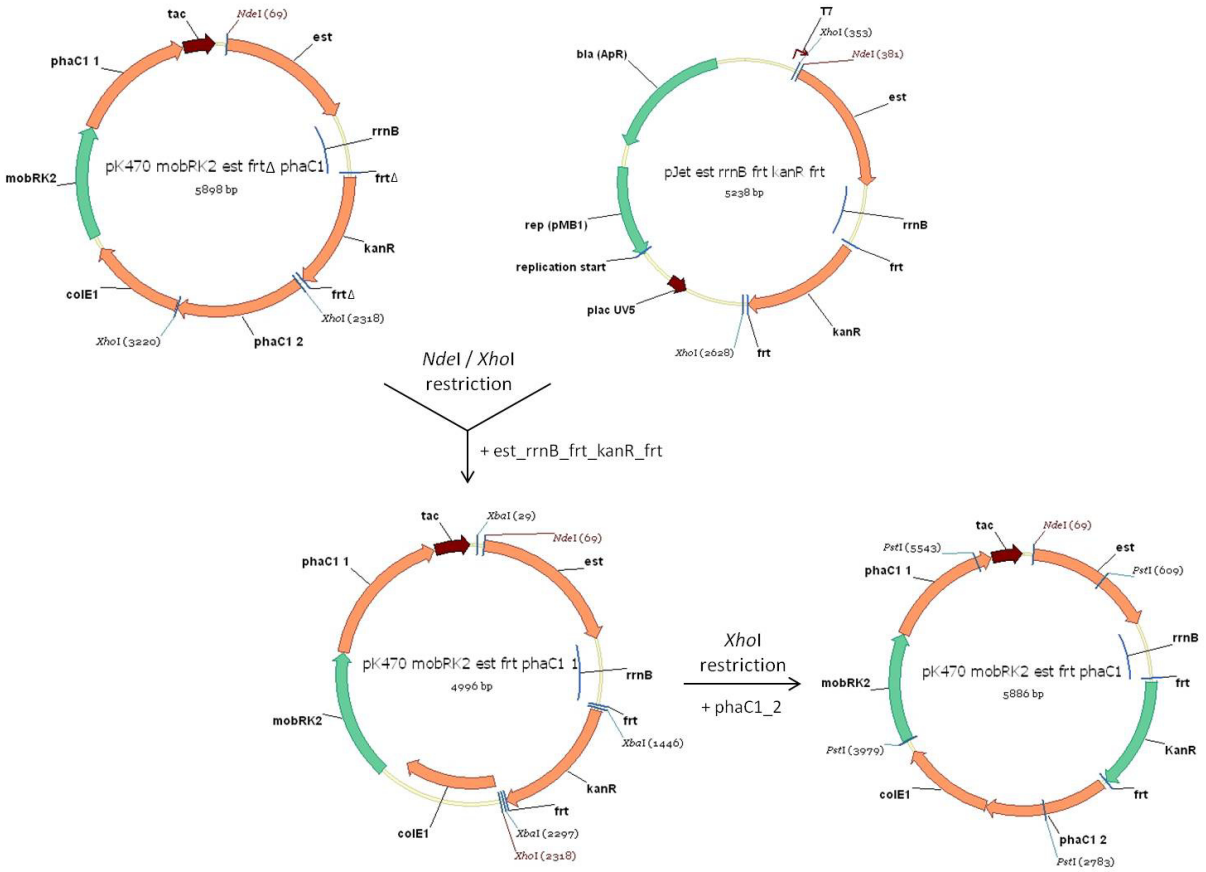

Figure 9. Construction of pK470_mobRK2_estA_frt_phaC1.
The plasmids pJET_estA_frt_kanR_frt and pK470_mobRK2_estA_frtΔ_phaC1 were digested with the restriction enzymes *Nde*I and *Xho*I and the fragment estA_frt_kanR_frt cloned into the vector backbone. Subsequently, the second homologous region *phaC1_2* was PCR amplified with phaC1 Fwd XhoI and phaC1 Rev XhoI and cloned into the *Xho*I restriction site of pK470_mobRK2_estA_frt_phaC1_1 to generate pK470_mobRK2_estA_frt_phaC1.

Single colonies of pK470_mobRK2_estA_frt_phaC1_1 were analysed for correct cloning via restriction digest after ligation and transformation. However, the second homologous region *phaC1_2* was excised of the vector backbone by the *Xho*I digest. Thus, *phaC1_2* was amplified of the plasmid pK470_mobRK2_estA_frtΔ_phaC1 with the primers phaC1 Fwd XhoI and phaC1 Rev XhoI and after purification digested at the *Xho*I restriction site. The plasmid

pK470_mobRK2_estA_frt_phaC1_1 was digested with *Xho*I as well and dephosphorylated prior ligation and transformation. Due to problems cloning the second homologous region, the fragments were blunted prior ligation and transformation. The incorporation of the second homologous region *phaC1_2* in the desired orientation was confirmed via colony PCR with the primers KanR Int Fwd and phaC1 Rev XhoI. Then, the successful construction of the plasmid pK470_mobRK2_estA_frt_phaC1 was confirmed via restriction digest and the plasmid was transformed into *E. coli* S17-1 cells.

2.13. Construction of pK470_mobRK2_T7_frtΔ_phaC1

After the successful construction of pK470_mobRK2_estA_frtΔ_phaC1, this vector was taken as a starting point to construct pK470_mobRK2_T7_frtΔ_phaC1 by replacing the esterase with the T7 RNA polymerase (Figure 10).

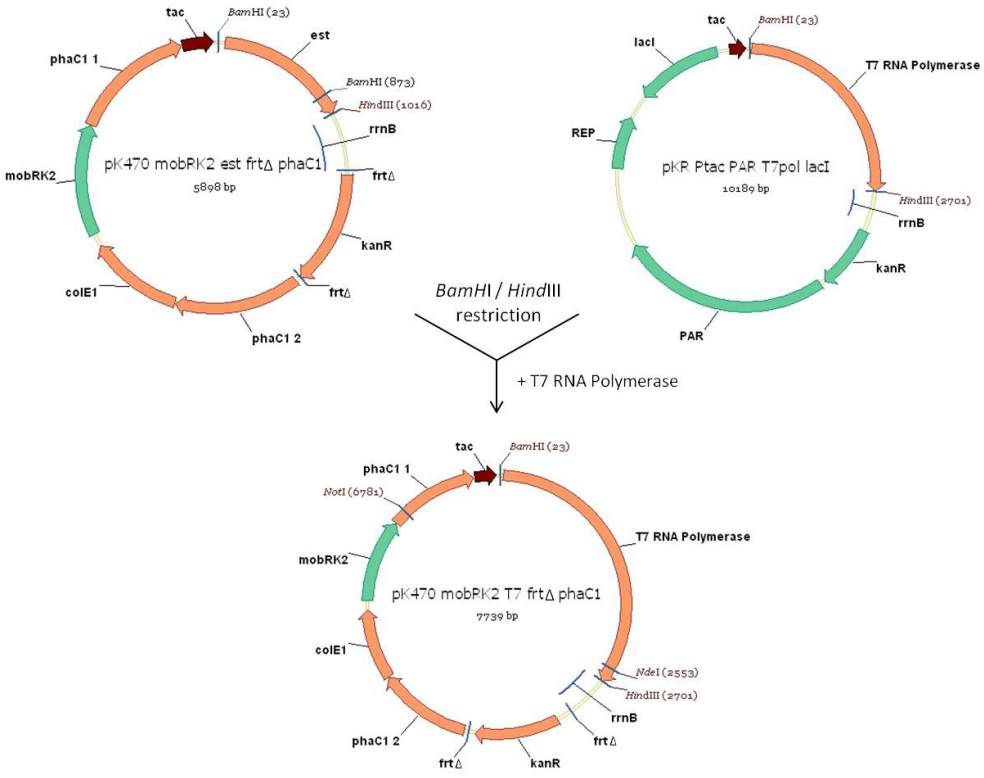

Figure 10. Construction of pK470_mobRK2_T7_frtΔ_phaC1.
The plasmid pKRtac_Par_T7pol_lacI was digested with *BamH*I and *Hind*III to gain the T7 RNA polymerase. Subsequently, the T7 RNA polymerase was cloned into the plasmid backbone of pK470_mobRK2_estA_frtΔ_phaC1, prior digested with the same restriction enzymes, to generate pK470_mobRK2_T7_frtΔ_phaC1.

The T7 RNA polymerase was obtained of the vector pKRtac_Par_T7pol_lacI by a double digest with *BamH*I and *Hind*III. The plasmid pK470_mobRK2_estA_frtΔ_phaC1 was as well

double digested with the same enzymes and dephosphorylated. Then, the restriction digests were loaded onto an agarose gel and the appropriate bands excised and purified. Subsequently, ligation and transformation were conducted. Afterwards, transformants were selected and checked for correct ligation of the T7 RNA polymerase by colony PCR with the primers seqT7pol_2 and seqT7pol_3 as well as seqT7pol_4 and seqT7pol_5 followed by plasmid isolation and a restriction digest. Finally, the plasmid pK470_mobRK2_T7_frtΔ_phaC1 was transformed into *E. coli* S17-1 cells.

A further attempt to construct pK470_mobRK2_T7_frtΔ_phaC1 was to cut out the T7 RNA polymerase of the plasmid pKRtac_Par_T7Poly_lacI with the restriction enzymes *EcoR*I and *Cla*I as well as to digest the plasmid pK470_mobRK2_estA_frtΔ_phaC1 with the same enzymes due to problems cloning the T7 RNA polymerase.

Another strategy to construct the plasmid pK470_mobRK2_T7_frtΔ_phaC1 was via Gibson cloning. The plasmid pK470_mobRK2_estA_frtΔ_phaC1 was digested with the restriction enzymes *BamH*I and *Hind*III to obtain the appropriate vector backbone. Following, the T7 RNA polymerase was amplified with the primers fwd gibson T7 BamHI and rev gibson T7 HindIII thereby creating an overlap complementary with the vector backbone. Then, Gibson cloning with these two DNA fragments was carried out. For the exact procedure see 2.3.7 Gibson cloning. Subsequently, the transformants were analyzed via colony PCR using the primers seqT7pol_4 and seqT7pol_5 and via restriction digest.

2.14. Construction of pK470_mobRK2_PCIV1bM_lacY_frtΔ_phaC1

The plasmid pK470_mobRK2_estA_frtΔ_phaC1 was as well taken as starting point to construct pK470_mobRK2_PCIV1bM_lacY_frtΔ_phaC1 (Figure 11). Thereby, *lacY* under the regulation of the weak CIV1bM promoter was amplified of pJET_PCIV1bM_lacY with the primers PCIV1bM SphI Fwd and lacY rev to introduce the restriction sites *Sph*I and *Hind*III respectively. Then, the PCR mix was loaded onto a preparative agarose gel and the amplified fragment excised and purified. Subsequently, the fragment PCIV1bM_lacY was cloned into the pJET1.2 cloning vector and sent for sequencing.

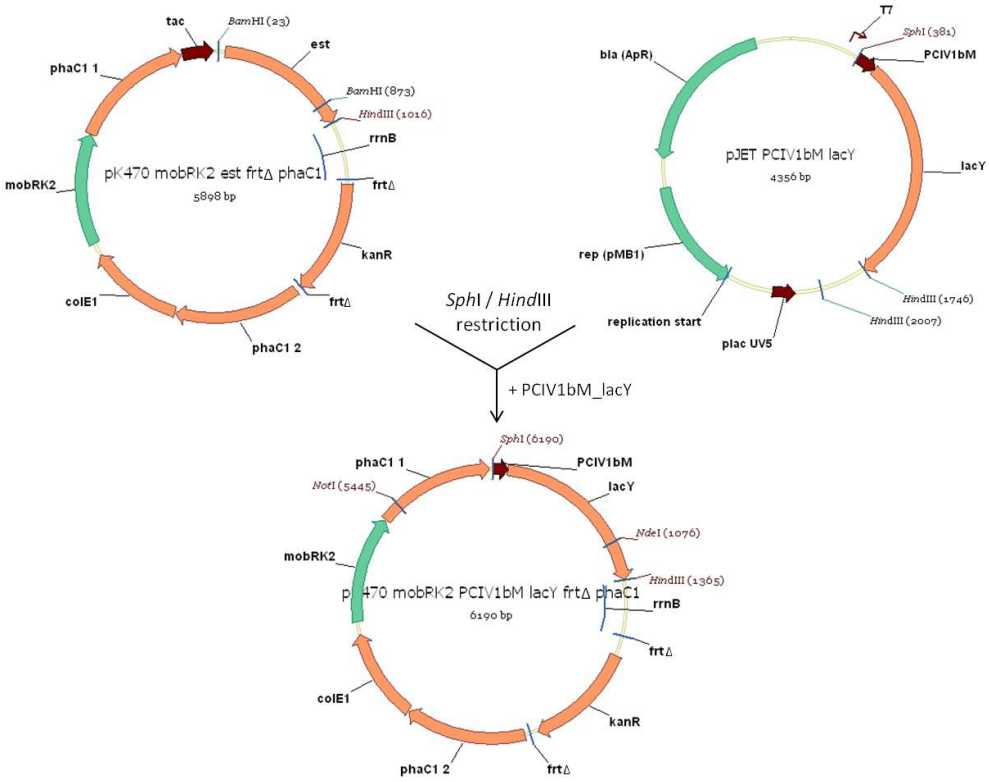

Figure 11. Construction of pK470_mobRK2_PCIV1bM_lacY_frtΔ_phaC1.
After the construction of pJET_PCIV1bM_lacY, the plasmid was restriction digested with *Sph*I and *Hind*III. Following, the fragment PCIV1bM_lacY was cloned into the plasmid backbone of pK470_mobRK2_estA_frtΔ_phaC1 digested as well with *Sph*I and *Hind*III to generate pK470_mobRK2_PCIV1bM_lacY_frtΔ_phaC1.

Afterwards, both pJET_PCIV1bM_lacY and pK470_mobRK2_estA_frtΔ_phaC1 were double digested with *Sph*I and *Hind*III. The fragments were loaded onto an agarose gel, the appropriate bands excised and purified prior ligation and transformation. Then, transformants were selected and checked for the successful construction of pK470_mobRK2_PCIV1bM_lacY_frtΔ_phaC1 via restriction digest. Subsequently, the plasmid was transformed into *E. coli* S17-1 cells.

2.15. Construction of pCM_mobRK2_flp

The plasmid pCM_mobRK2_redA9 was taken as a starting vector to construct pCM_mobRK2_flp (Figure 12). Thereby, the *flp* was amplified of the plasmid pKRtacflp with the primers FLP Fwd and FLP Rev to introduce a *BamH*I and *Sph*I restriction site. The PCR mix was loaded onto an agarose gel and the appropriate band excised and purified. Following, the *flp* was cloned into the pJET1.2 cloning vector to generate pJET_flp.

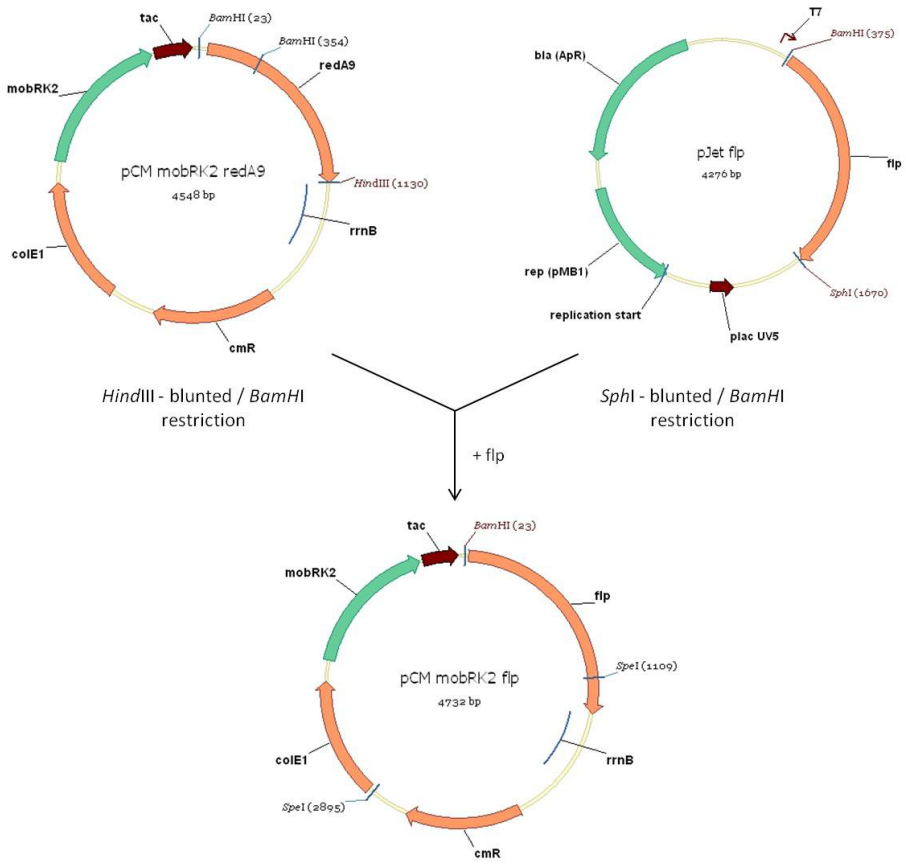

Figure 12. Construction of pCM_mobRK2_flp.
After the construction of pJET_flp, the plasmid was restriction digested with *Sph*I and blunted followed by a *BamH*I restriction digest. On the other hand, the plasmid pCM_mobRK2_redA9 was digested with *Hind*III prior blunting and then digested as well at the *BamH*I restriction site. Subsequently the flippase was cloned into the vector backbone replacing *redA9* to generate pCM_mobRK2_flp.

After the correct sequence was confirmed by sequencing, the plasmid pJET_flp was digested with *Sph*I and the vector pCM_mobRK2_redA9 digested at the *Hind*III restriction site. In the following, both restriction digests were purified, blunted and digested with the *BamH*I restriction enzyme. The restriction digests were loaded onto an agarose gel and the appropriate bands excised, purified and ligation and transformation carried out. Transformants were streaked out for plasmid isolation and a control cut was conducted. Finally, the successful constructed plasmid pCM_mobRK2_flp was transformed into *E. coli* S17-1 cells.

2.16. Construction of pCM_Ptac_Par_eGFP_RSF1010_lacI

The plasmid pCM_Ptac_Par_RSF1010_eGFP_lacI was constructed to verify the functionality of *lacY* in *R. eutropha* H16 as well as its correct incorporation into the membrane. Thereby, the plasmid pKR_Ptac_Par_eGFP_REP_mobRK2 was taken as a starting point (Figure 13).

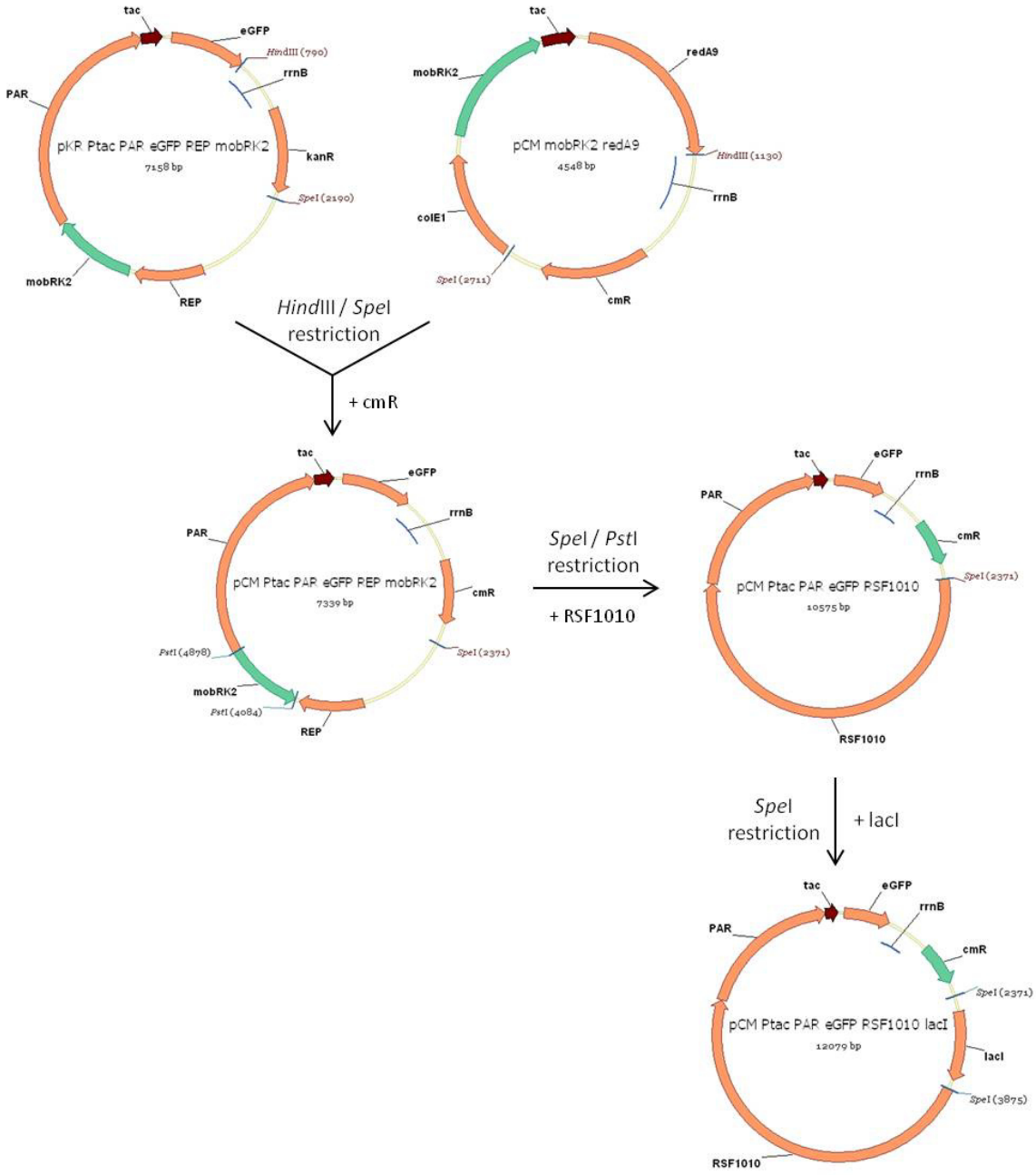

Figure 13. Construction of pCM_Ptac_Par_eGFP_RSF1010_lacI.
The plasmid pKR_Ptac_Par_eGFP_REP_mobRK2 was used as a starting point and kan^r replaced by cm^r of pCM_mobRK2_redA9 after a *Spe*I and *Hind*III restriction digest. Following, the plasmid pCM_Ptac_Par_eGFP_REP_mobRK2 was digested with the restriction enzymes *Spe*I and *Pst*I to excise the *Rep* origin of replication and *mobRK2* of the vector backbone and replace it with the *RSF1010* origin of replication of pKT231. A further *Spe*I restriction digest allowed the cloning of *lacI* into the vector backbone to generate pCM_Ptac_Par_eGFP_RSF1010_lacI.

At the beginning the plasmids pKR_Ptac_Par_eGFP_REP_mobRK2 and pCM_mobRK2_redA9 were double digested with *Hind*III and *Spe*I to generate pCM_Ptac_Par_eGFP_REP_mobRK2 by exchanging kan^r to cm^r. The double digest was loaded onto an agarose gel, the appropriate bands purified and ligation and transformation were carried out. After transformants were streaked out for plasmid isolation, the constructed plasmid pCM_Ptac_Par_eGFP_REP_mobRK2 was digested with the restriction enzymes *Spe*I and *Pst*I thereby cutting out the *Rep* origin of replication and the *mob* region of the RK2 plasmid and replacing it with the *RSF1010* origin of replication of *Salmonella enterica* of the plasmid pKT231. Transformants were analyzed for successful cloning of pCM_Ptac_Par_eGFP_RSF1010 via restriction digest after purification of the fragments and the successive ligation and transformation. Then, another *Spe*I digest of the plasmid pCM_Ptac_Par_eGFP_RSF1010 was conducted. Simultaneously, the *lacI* was amplified of the plasmid pCM_PT7_RSF1010_eGFP_Pemlk_lacI with the primers LacI_SpeI_fwd and LacI_SpeI_rev and after excision of the agarose gel and purification, digested at the previously introduced *Spe*I restriction site. The vector backbone as well as the *lacI* was gel purified and a ligation and transformation carried out. The transformants were streaked out for plasmid isolation and a control cut wit *Not*I was conducted to determine the successful construction of pCM_Ptac_Par_eGFP_RSF1010_lacI. Finally, the plasmid pCM_Ptac_Par_eGFP_RSF1010_lacI was transformed into *E. coli* S17-1 cells.

2.17. Construction of pCM_PT7_RSF1010_eGFP_Pemlk_ΔlacI

The plasmid pCM_PT7_RSF1010_eGFP_Pemlk_lacI was obtained as a starting vector. In the following, *lacI* was deleted to be able to use this vector to prove the functionality of the T7 RNA polymerase in *R. eutropha* H16 (Figure 14).

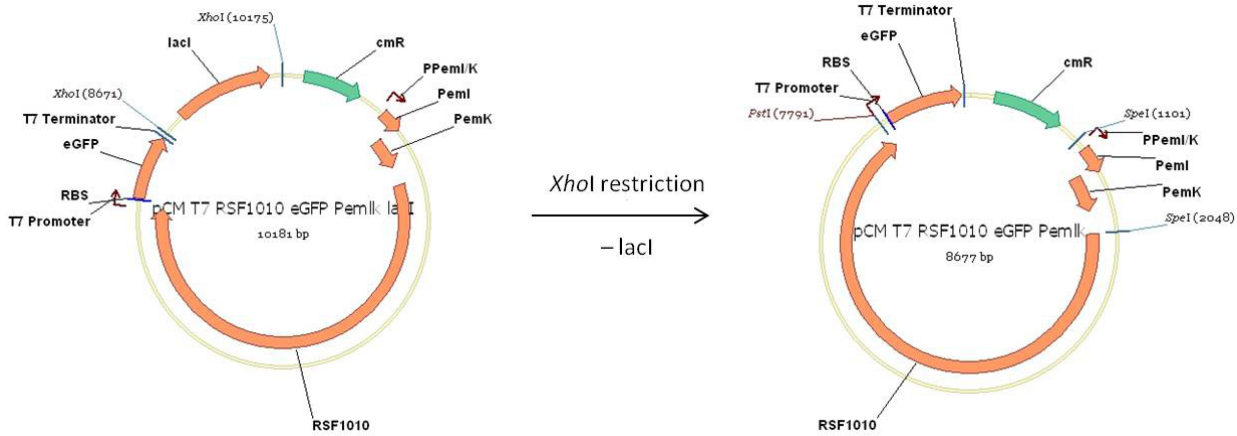

Figure 14. Construction of pCM_PT7_RSF1010_eGFP_Pemlk_ΔlacI.
The plasmid pCM_PT7_RSF1010_eGFP_Pemlk_lacI was restriction digested with *Xho*I and thereby excising *lacI* of the vector backbone to generate pCM_PT7_RSF1010_eGFP_Pemlk_ΔlacI.

The plasmid pCM_PT7_RSF1010_eGFP_Pemlk_lacI was digested with *Xho*I to excise *lacI* (Figure 14) and the sample loaded onto an agarose gel. Then, the appropriate plasmid fragment was excised of the gel, purified and directly used for re-ligation. The successful construction of pCM_PT7_RSF1010_eGFP_Pemlk_ΔlacI was determined via colony PCR (nT7MCS_PstI_fwd2, Rev cmR SpeI) and restriction digest (*Pst*I, *Spe*I). Finally, the plasmid pCM_PT7_RSF1010_eGFP_Pemlk_ΔlacI was transformed into *E. coli* S17-1 cells.

3. Results

3.1. Construction of a vector for genomic integration in *R. eutropha* H16

3.1.1. Integration of pK470_mob_ca1_estA

At the beginning, the plasmid pK470_mob_ca1_estA, which was constructed during the project lab, was transferred into *R. eutropha* H16 via conjugation from *E. coli* S17-1. The plasmid pK470_mob_ca1_estA was comprised of the carbonic anhydrase 1 (*ca*1) as homologous region of 672 bp, the mob region of the plasmid pBBR1-MCS5 and the esterase A of *Rhodococcus ruber* as a reporter gene (Figure 15).

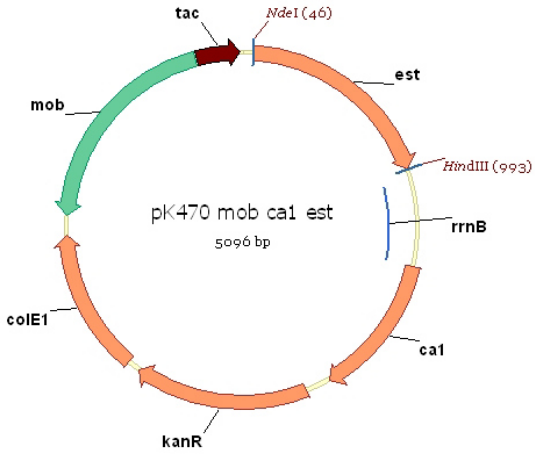

Figure 15. Vector map of the suicide plasmid pK470_mob_ca1_estA containing, the *ColE1* origin of replication, the mobilization region of the pBBR1-MCS5 plasmid, the homologous sequence *ca1*, the tac promoter and *estA* as reporter gene.

After conjugation was carried out, the *R. eutropha* H16 transconjugants were incubated for 4-5 days until cell growth was visible. Then, single colonies were re-streaked twice on TSB media supplemented with gentamycin [20 µg/mL] and kanamycin [200 µg/mL] prior a possible recombination event was determined via colony PCR (Figure 16). Due to the results it can be stated that all the selected transconjugants carried the megaplasmid as a fragment of 423 bp could be amplified (Figure 16A) and thus can be considered as *R. eutropha* H16 cells. This PCR was conducted to assure that the selected cells were *R. eutropha* H16 cells and not any *E. coli* S17-1 contamination. The second PCR was carried out to determine a possible recombination event (Figure 16B). However, an integration event could not be determined in any of the analysed transconjugants. The expected fragment would have been 999 bp. A further PCR on the *mob* region was conducted as well (Figure 16C) but only slight

unspecific bands were amplified of the transconjugants. The amplification of the *mob* sequence (1010 bp) would have shown that the plasmid would have been still present in the *R. eutropha* H16 transconjugant. The location of the primer binding site is shown in Figure **16**D and E.

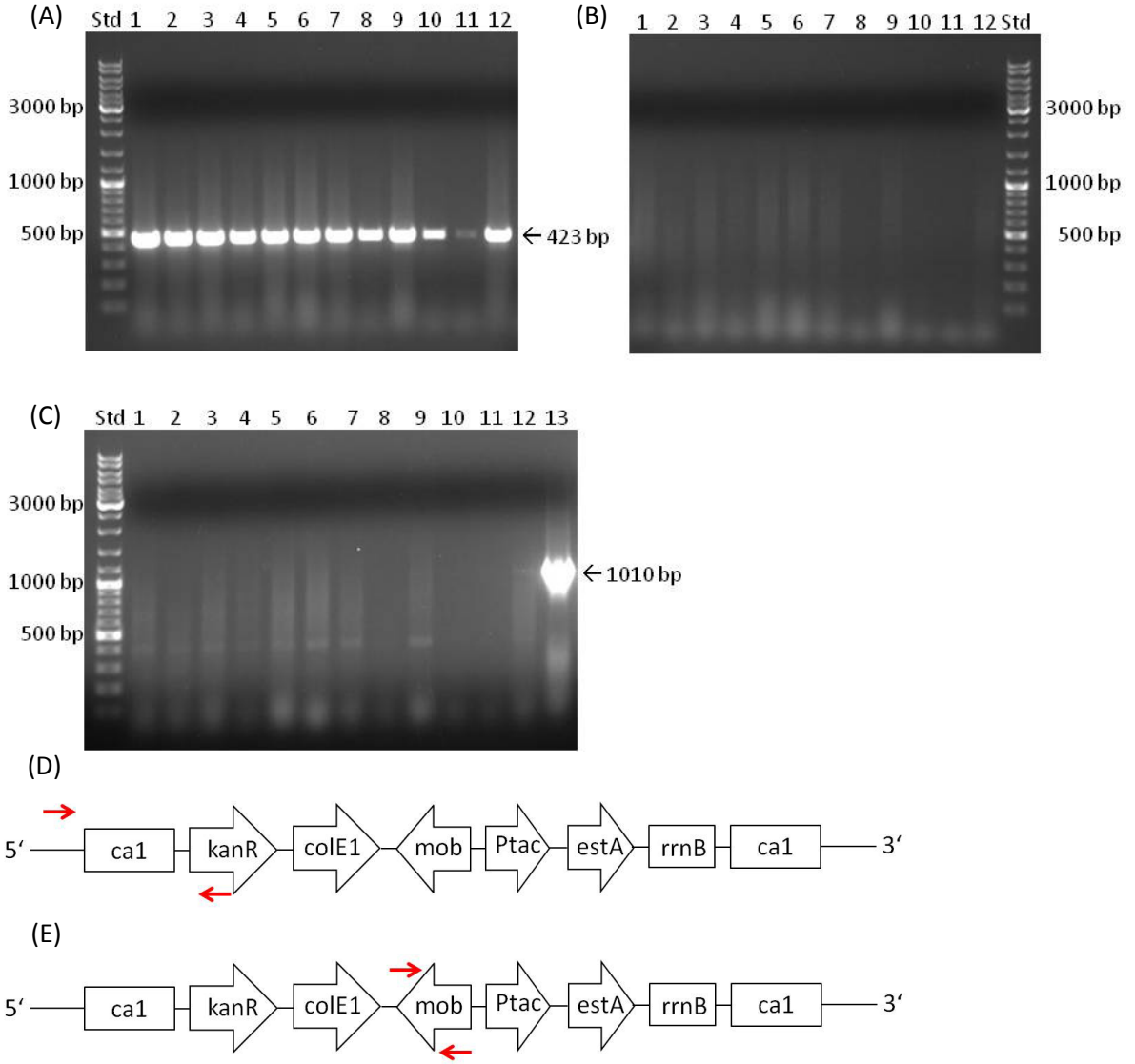

Figure 16. Agarose gel of colony PCR of *R. eutropha* H16 transconjugants on (A) the megaplasmid, (B) integration and (C) *mob* region after conjugation with *E. coli* S17-1 [pK470_mob_ca1_estA]; (D,E) Location of primer binding site.
Std.: Gene Ruler^{TM} DNA Ladder Mix (500 ng); (1-11) *R. eutropha* H16 transconjugants pK470_mob_ca1_estA, (12) *R. eutropha* H16 wildtype, (13) *E. coli* S17-1 [pK470_mob_ca1_estA]; (**A**) amplification of a fragment of the megaplasmid to verify the genus *R. eutropha* H16 (P-2-fwd, P-2-rev; 423 bp); (**B**) amplification of a fragment ranging from the 5' genomic region into the kanamycin resistance to check for integration (Int CA1 Fwd, Int KanR Rev; 999 bp); (**C**) amplification of the mob region (MOB fwd, MOB rev; 1010 bp).
(**D**) Location of the primer binding site to verify an integration event in the 5' genomic region of *R. eutropha* H16 transconjugant (Int CA1 Fwd, Int KanR Rev), (**E**) Primer binding site of MOB fwd and MOB rev to amplify the mob region.

Due to the results of the colony PCR it can be stated that none of the analysed transconjugants showed to have integrated the plasmid pK470_mob_ca1_estA although the *R. eutropha* H16 transconjugants were able to grow on TSB media supplemented with kanamycin. Thus, the transconjugants were re-streaked again and another PCR performed on the still growing transconjugants to amplify a part of kan^r (Figure 17). This PCR was performed to verify whether *R. eutropha* H16 transconjugants had only integrated the resistance gene and degraded the rest of the plasmid and thus being able to grow on TSB media supplemented with kanamycin.

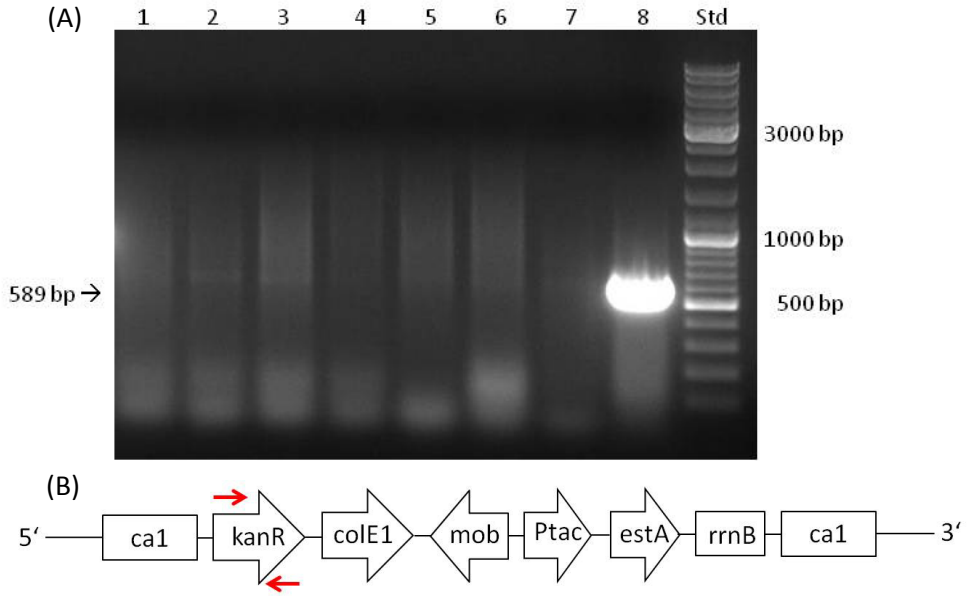

Figure 17. (A) Agarose gel of colony PCR on kan^r of *R. eutropha* H16 transconjugants after conjugation with *E. coli* S17-1 [pK470_mob_ca1_estA]; (B) Location of primer binding site.
(**A**) Std.: Gene Ruler^{TM} DNA Ladder Mix (500 ng); amplification of a part of the kanamycin resistance gene (KanR Int Fwd, KanR Int Rev; 589 bp); (1-6) *R. eutropha* H16 transconjugants pK470_mob_ca1_estA, (7) *R. eutropha* H16 wildtype, (8) *E. coli* S17-1 [pK470_mob_ca1_estA].
(**B**) Location of the primer binding site of KanR Int Fwd and KanR Int Rev to amplify a fragment of kan^r.

Surprisingly, none of the analysed *R. eutropha* H16 transconjugants carried the kanamycin resistance as no fragment of kan^r of 589 bp as shown in the positive control could be amplified (Figure 17) even though it was able to grow on kanamycin plates. However, the growth of *R. eutropha* H16 cells after conjugation was also observed on the control plates. Thereby, *R. eutropha* H16 was handled exactly the same way just with the exception that it was in no contact with *E. coli* S17-1 cells. Thus it was speculated that *R. eutropha* H16 may be able to adapt to its environment and thus being able to grow on media supplemented with kanamycin.

3.1.2. Construction of pCM_mob_ca1

No recombination event could be determined using the plasmid pK470_mob_ca1_estA. Hence, in the following the plasmid pK470_mob_ca1 was taken as a starting point with the *ca1* as homologous region and the *mob* region of the plasmid pBBR1-MCS5 to carry out various modifications on the plasmid to be able to verify the reason for the non occurring integration event. Thereby, different fragments on the plasmid were exchanged like the selection marker, the homologous region and the *mob* region.

First the selection marker kan^r was replaced by cm^r. The plasmid pK470_mob_ca1 (3222 bp) was amplified as well as cm^r (1105 bp) as described in the material and method section 2.10. In so doing, both fragments were purified and a control gel run (Figure 18A) to determine the accurate size of the fragments and to determine its DNA concentration prior blunt end ligation. After the transformation, single colonies were streaked out for plasmid isolation and a restriction digest with *Pst*I was carried out. Due to the results of the restriction digest (Figure 18B), the cloning of cm^r into the vector backbone was successful as two fragments with a size of 3326 bp and 1005 bp were visible. The slight fragment at ~2000 bp was uncut plasmid.

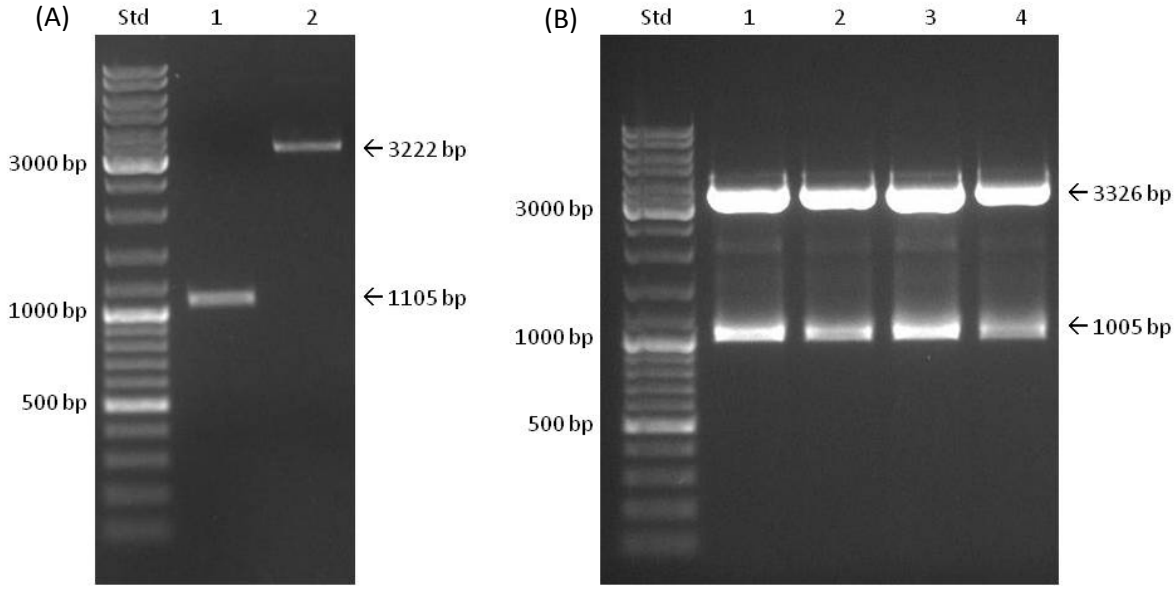

Figure 18. Agarose gel of (A) PCR amplified fragments cm^r and pK470_mob_ca1 backbone without kan^r after purification and (B) restriction digest of pCM_mob_ca1 with *Pst*I.
Std.: Gene Ruler^{TM} DNA Ladder Mix (500 ng); (**A**) (1) purified cm^r (1105bp), (2) purified pK470_mob_ca1 without kan^r (3222bp); (**B**) (1-4) pCM_mob_ca1 digested with *Pst*I (3326bp and 1005bp).

3.1.3. Integration of pCM_mob_ca1

After the construction of pCM_mob_ca1, the plasmid was transformed into *E. coli* S17-1 cells and transferred into *R. eutropha* H16 via conjugation. Prior the conjugation of pCM_mob_ca1, a conjugation with another plasmid carrying the *RSF1010* origin of replication which is stable in *R. eutropha* H16 was carried out to verify which chloramphenicol concentration is optimal to just allow growth of *R. eutropha* H16 transconjugants. Chloramphenicol concentrations of 25 µg/mL, 50 µg/mL, 100 µg/mL and 200 µg/mL were compared. TSB media supplemented with gentamycin [20 µg/mL] and chloramphenicol [100 µg/mL] was considered to be optimal for the selection of transconjugants carrying the chloramphenicol resistance.

Several conjugations of pCM_mob_ca1 were conducted resulting in weak cell growth of *R. eutropha* H16 transconjugants after 5-6 days of incubation at 28 °C or no transconjugants at all were obtained on the selective media. However, if transconjugant colonies grew on the selective media, almost the same amount of cells was obtained on the control plate. The *R. eutropha* H16 transconjugants which grew after 5-6 days could be reasoned by an antibiotic concentration which was already too little to inhibit growth due to the low stability of chloramphenicol [100] or again to the adaptation behaviour of *R. eutropha* H16 as already mentioned above. The performed colony PCRs on a possible integration event in the up- and downstream region of *ca1* respectively as well as on the *mob* region and cm^r did not show any positive result (data not shown). However, all in all it can be stated that the number of false-positive transconjugants could be decreased dramatically by the exchange of the selection marker from kanamycin to chloramphenicol.

3.1.4. Construction of pCM_mobRK2_redA9/redB2 and pCM_mobRSF1010_redA9/redB2

Thus, in the following the *mob* region of pBBR1-MCS5 of the plasmid pCM_mob_ca1 was replaced by the *mob* regions of the RK2 plasmid (*mobRK2*) and pKT231 (*mobRSF1010*). The *mobRK2* fragment (788 bp) was amplified of the plasmid RK2 and *mobRSF1010* (2613 bp) amplified of pKT231. Additionally, the mobilization frequency of mobRK2, mobRSF1010 and the original used mobilization region of the plasmid pBBR1-MCS5 were compared (see therefore 3.2 .Mobilization efficiency). The correct sequence of both fragments was confirmed by sequencing after cloning into the pJET1.2 vector. Then, pJET_mobRK2 and

pJET_mobRSF1010 were restriction digested with *Bgl*II, blunted prior purification and loaded onto a control gel to determine the accurate size and the DNA concentration (Figure 19A+B). Simultaneously, the plasmid pCM_mob_ca1 was digested with the restriction enzyme *Pst*I, blunted and dephosphorylated prior the determination of the DNA concentration. The fragment pCM_ca1 backbone had a size of 3326 bp as shown in Figure 19A.

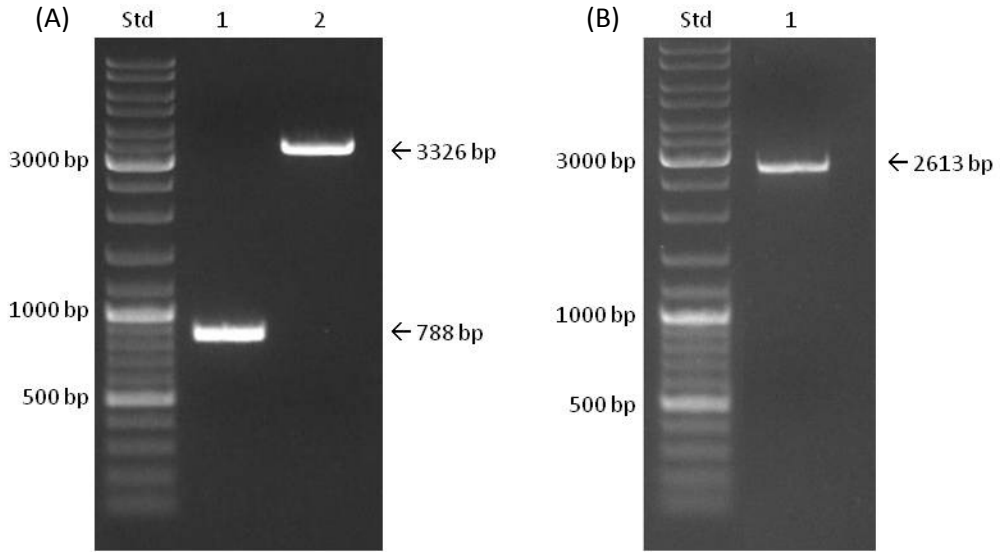

Figure 19. Agarose gel of the blunted fragments of (A) *mobRK2* and pCM_ca1 backbone and (B) *mobRSF1010*.
Std.: Gene Ruler^{TM} DNA Ladder Mix (500 ng); (**A**) (1) *mobRK2* (788 bp), (2) pCM_ca1 Bb (3326 bp), (**B**) (1) *mobRSF1010* (2613 bp).

After the blunt-end ligation and transformation, single colonies of pCM_mobRK2_ca1 and pCM_mobRSF1010_ca1 were streaked out for plasmid isolation. Then, restriction digests were carried out to assure the successful cloning of the *mob* regions. The plasmid pCM_mobRK2_ca1 was restriction digested with *Xho*I and *Hind*III whereas the plasmid pCM_mobRSF1010_ca1 was digested with the enzymes *Spe*I and *Bgl*II. The isolated plasmids in lane 2 and 3 of pCM_mobRK2_ca1 showed to have the correct fragments of 2382 bp and 1778 bp after the restriction digest (Figure 20A). All digested pCM_mobRSF1010_ca1 plasmids had incorporated the *mobRSF1010* fragment successfully. However, the sample in lane 4 (5158 bp and 798 bp) was cloned in the different orientation than the others which showed fragments of 3413 bp and 2543 bp after the restriction digest (Figure 20B). The fragment of ~2000 bp resulted of the *RSF1010* origin of replication and is most likely due to its conformational behaviour. This fragment can be assumed as special conformation of the

plasmid which is not possible to be digested, at least not with a standard restriction digest, and thus correlates to uncut plasmid as can be seen in Figure 20B.

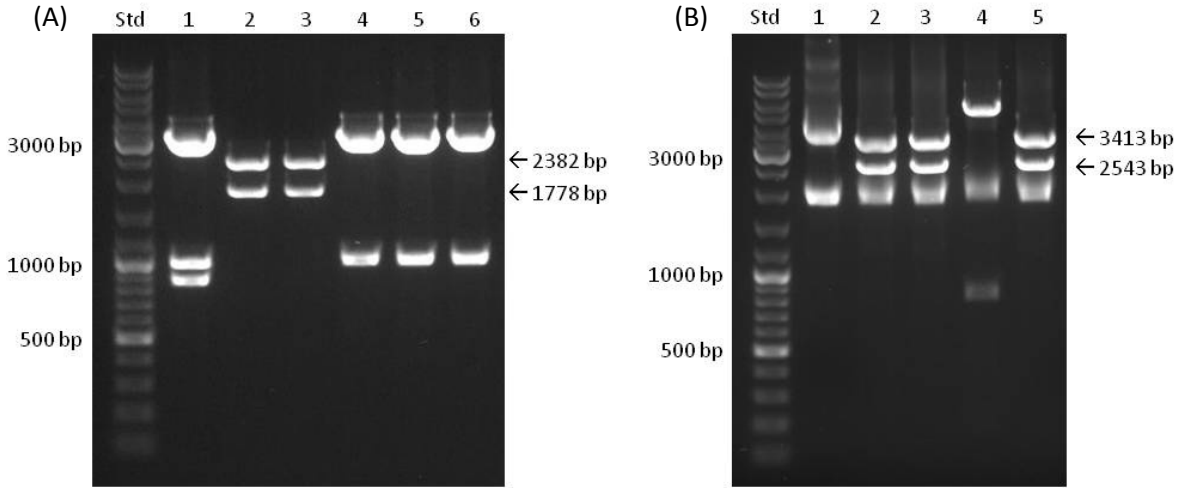

Figure 20. Agarose gel of restriction digest of (A) pCM_mobRK2_ca1 with *Xho*I and *Hind*III and (B) pCM_mobRSF1010_ca1 with *Spe*I and *Bgl*II.
Std.: Gene Ruler^{TM} DNA Ladder Mix (500 ng); (**A**) (1-6) pCM_mobRK2_ca1 digested with *Xho*I and *Hind*III (2382 bp and 1778 bp); (**B**) (1) pCM_mobRSF1010_ca1 uncut, (2-5) pCM_mobRSF1010_ca1 digested with *Spe*I and *Bgl*II (3413 bp and 2543 bp).

Moreover, the homologous region *ca1* of both plasmids pCM_mobRK2_ca1 and pCM_mobRSF010_ca1 was replaced by the reductase A9 (*redA9*, 1061 bp) and a part of the reductase B2 (*redB2*, 458 bp). These two fragments were selected because the size of ~ 1000 bp and of almost 500 bp was considered to be optimal to verify whether the length of the homologous sequence is essential for a recombination event. The plasmids pCM_mobRK2_ca1 and pCM_mobRSF1010_ca1 were both restriction digested with *Nde*I and *Hind*III as well as in a separate digest with *Nde*I, blunted and digested with *Hind*III and dephosphorylated as described in the material and method section 2.10. Additionally, the *redA9* fragment was gained by cutting the plasmid pK470_redA9 at the *Nde*I and *Hind*III restriction site whereas pK470_redB2 was restriction digested with *Pst*I prior blunting and then digested with the restriction enzyme *Hind*III to gain a part of *redB2*. Then, after purification, the samples were loaded onto a control gel and the DNA concentration was determined. The fragment *redA9* had a size of 1061 bp (Figure 21B) and *redB2* of 458 bp (Figure 21A) whereas the plasmid backbone of pCM_mobRK2 had a size of 3487 bp (Figure 21C) and the one of pCM_mobRSF1010 of 5283 bp (Figure 21D).

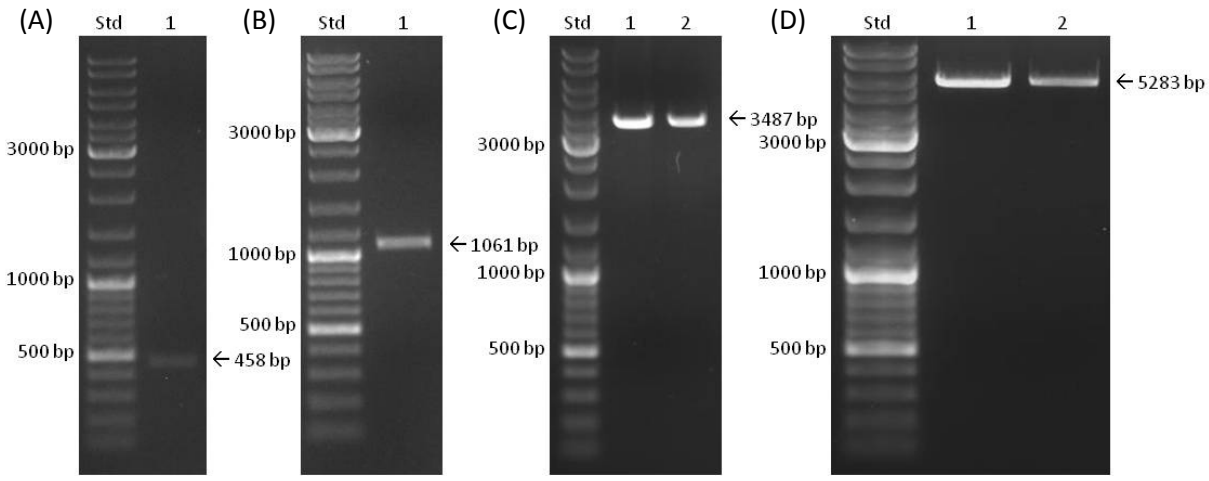

Figure 21. Agarose gel of (A) part of *redB2*, (B) *redA9*, (C) pCM_mobRK2 backbone and (D) pCM_mobRSF1010 backbone.
Std.: Gene Ruler^{TM} DNA Ladder Mix (500 ng); (**A**) (1) purified *redB2* digested with *Pst*I prior blunting of the sticky ends and *Hind*III restriction digest (458 bp); (**B**) (1) purified *redA9* restriction digested with *Nde*I and *Hind*III (1061 bp); (**C**) purified pCM_mobRK2 backbone after (1) *Nde*I and *Hind*III restriction digest (3487 bp) and (2) *Nde*I restriction digest, blunting of the sticky ends and *Hind*III digest (3487 bp); (**D**) purified pCM_mobRSF1010 backbone after (1) *Nde*I and *Hind*III restriction digest (5283 bp) and (2) *Nde*I restriction digest, blunting of the sticky ends and *Hind*III digest (5283 bp).

After ligation and transformation, single colonies were streaked out for plasmid isolation and restriction digested to determine the successful construction of the different plasmids. The isolated pCM_mobRK2_redB2 plasmid was digested with *Xho*I and *Hind*III and showed the correct restriction pattern with 2382 bp and 1563 bp (Figure 22A). The plasmid in slot three was fully digested whereas a slight band was visible in the samples one and two corresponding to uncut plasmid. The plasmid pCM_mobRK2_redA9 was as well digested with *Xho*I and *Hind*III resulting in fragments of 2382 bp, 2067 bp and 99 bp (Figure 22B). After the isolation of the plasmid pCM_mobRSF1010_redB2, it was restriction digested with *Cla*I and *ApaL*I. All plasmids had incorporated the part of *redB2* resulting in 3742 bp and 1999 bp fragments (Figure 22C). The plasmid pCM_mobRSF1010_redA9 was digested with the restriction enzyme *Sma*I and showed the correct plasmid fragments of 6025 bp and 319 bp (Figure 22D). An additional band of ~ 2000 bp which is clearly visible in the samples of pCM_mobRSF1010_redA9 and slightly visible as a smear in the sample of pCM_mobRSF1010_redB2 is the result of the conformational behaviour of the *mobRSF1010* fragment as already discussed earlier.

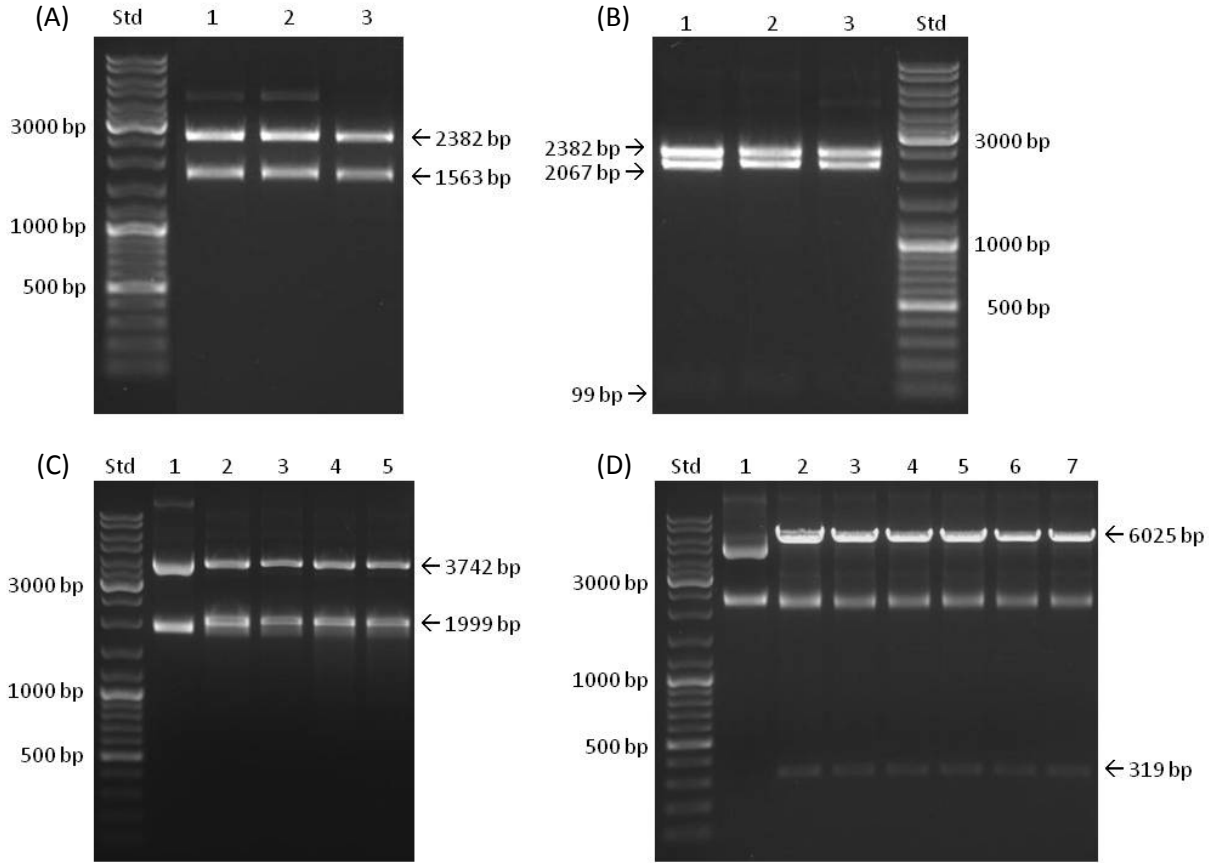

Figure 22. Agarose gel of restriction digest of (A) pCM_mobRK2_redB2 with *Hind*III and *Xho*I, (B) pCM_mobRK2_redA9 with *Hind*III and *Xho*I, (C) pCM_mobRSF1010_redB2 with *Cla*I and *ApaL*I and (D) pCM_mobRSF1010_redA9 with *Sma*I.
Std.: Gene Ruler^{TM} DNA Ladder Mix (500 ng); (**A**) (1-3) pCM_mobRK2_redB2 digested with *Hind*III and *Xho*I (2382 bp and 1563 bp); (**B**) (1-3) pCM_mobRK2_redA9 digested with *Hind*III and *Xho*I (2382 bp, 2067 bp and 99 bp); (**C**) (1) pCM_mobRSF1010_redB2 uncut, (2-4) pCM_mobRSF1010_redB2 digested with *Cla*I and *ApaL*I (3742 bp and 1999 bp); (**D**) (1) pCM_mobRSF1010_redA9 uncut (2-7) pCM_mobRSF1010_redA9 digested with *Sma*I (6025 bp and 319 bp).

3.1.5. Integration of pCM_mobRK2_redA9/redB2

Even though, all four plasmids (pCM_mobRK2_redA9, pCM_mobRK2_redB2, pCM_mobRSF1010_redA9 and pCM_mobRSF1010_redB2) were successfully constructed, only the plasmids including the *mob* region of the RK2 plasmid (pCM_mobRK2_redA9 and pCM_mobRK2_redB2) were transformed into *E. coli* S17-1 cells und transferred in *R. eutropha* H16 via conjugation to determine whether the length of the homologous region has an influence of the probability of a recombination event. These plasmids were selected due to the results of the comparison of the mobilization efficiencies (see 3.2. Mobilization efficiency).

After conjugation was carried out, the selective plates (TSB media supplemented with 0.2 % fructose, gentamycin [20 µg/mL] and chloramphenicol [100 µg/mL]) had to be incubated for

4-5 days until cell growth was visible. Then, single colonies were streaked out twice prior a colony PCR was conducted. The colony PCR was performed with primers binding on the genome of *R. eutropha* H16 upstream of *redA9* and *redB2* respectively and the reverse primer in the terminator region of the plasmid to determine a possible integration event (Figure 23). However, none of the analysed transconjugants showed to have integrated the plasmid neither with the long homologous region of 1061 bp (Figure 23A) nor with the shorter homologous sequence of 458 bp (Figure 23B). A possible integration with *redA9* should have revealed a fragment of 1153 bp whereas a fragment of 923 bp would have been expected after an integration of the plasmid with *redB2*.

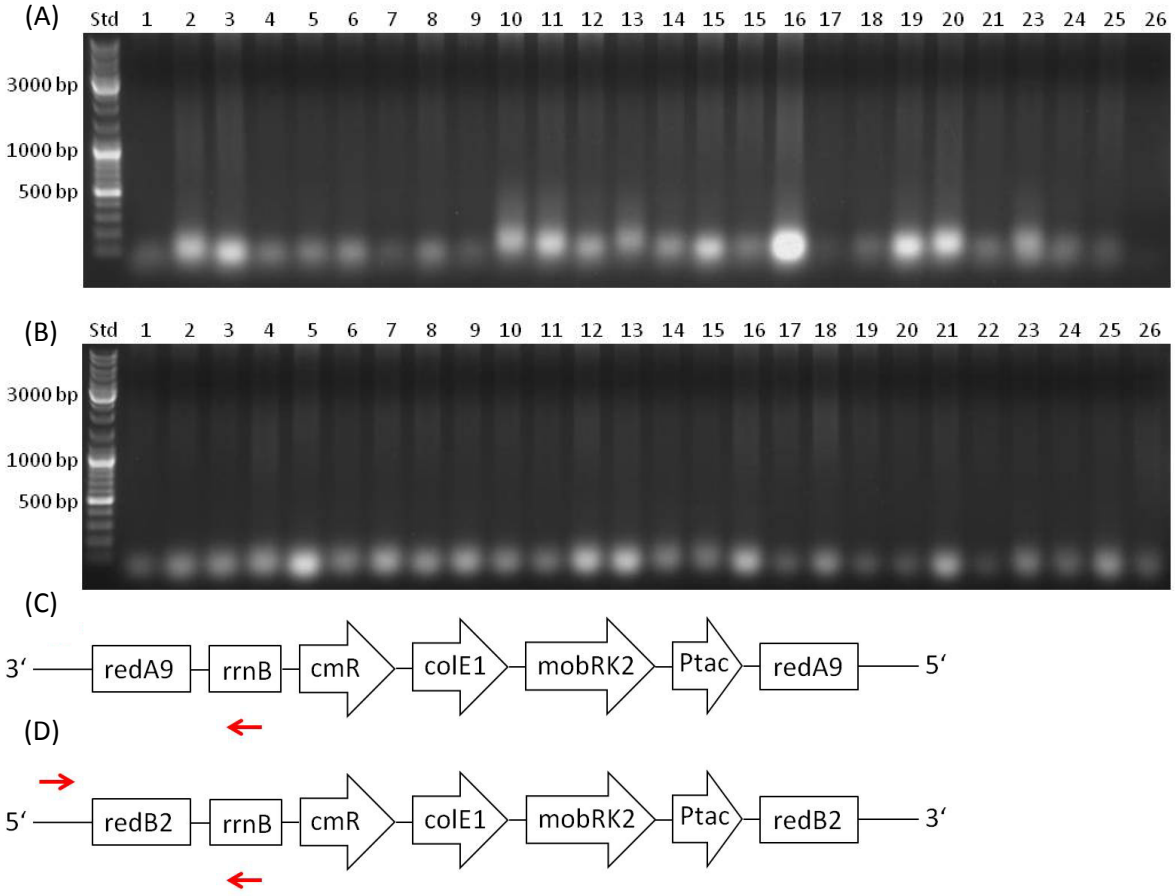

Figure 23. Agarose gel of colony PCR of (A) pCM_mobRK2_redA9 integration and (B) pCM_mobRK2_redB2 integration; (C, D) Location of primer binding site.
Std.: Gene Ruler^{TM} DNA Ladder Mix (500 ng); (**A**) amplification of a fragment from the genomic region in front of *redA9* of *R. eutropha* H16 into the terminator region (3’ redA9, rrnB rev), (1-24) *R. eutropha* H16 transconjugant pCM_mobRK2_redA9, (25) *R. eutropha* H16 wildtype, (26) Mastermix; (**B**) amplification of a fragment from the 5’ genomic region in front of *redB2* of *R. eutropha* H16 into the terminator region (5’ redB2 fwd, rrnB rev), (1-25) *R. eutropha* H16 transconjugant pCM_mobRK2_redB2, (26) *R. eutropha* H16 wildtype. (**C**) Primer binding site of 3’ redA9 and rrnB rev to verify an integration event. (**D**) Location of primer binding site to verify an integration event in the 5’ genomic region of *R. eutropha* H16 transconjugant (5’ redB2 fwd, rrnB rev).

Although, the PCR of an integration event showed a negative result, another colony PCR on the chloramphenicol resistance of the same transconjugants was carried out. Thereby, cm^r should be amplified to verify the integration of the chloramphenicol resistance into the genome of *R. eutropha* H16. A positive PCR result of cm^r was expected as the transconjugants were able to grow on chloramphenicol. However, none of the analysed transconjugants showed to have the chloramphenicol resistance gene (Figure 24). The amplified fragment should have had a size of 1105 bp as can be seen in the positive control (Figure 24B).

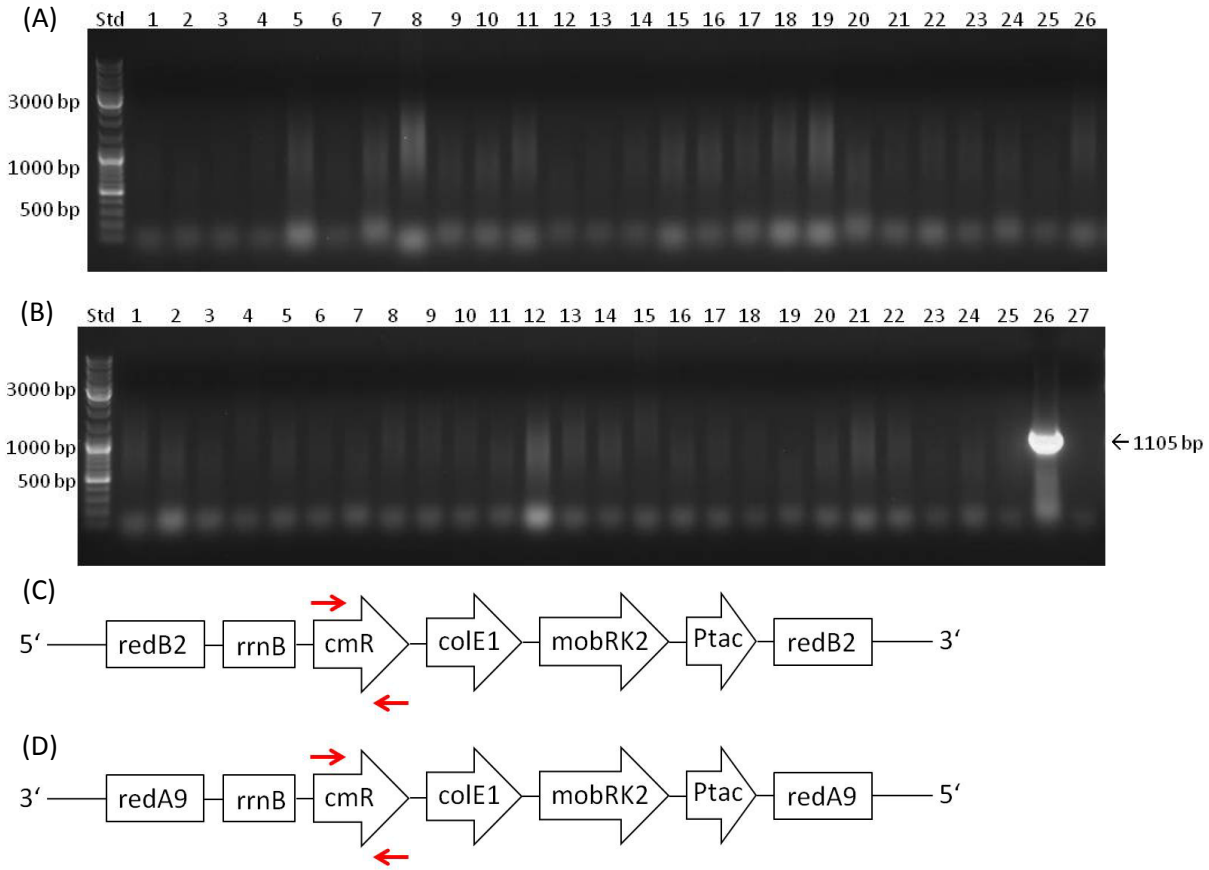

Figure 24. (A, B) Agarose gel of the colony PCR of cm^r of *R. eutropha* H16 transconjugants; (C, D) Location of primer binding site.
Std.: Gene Ruler™ DNA Ladder Mix (500 ng); (**A**) amplification of cm^r of *R. eutropha* H16 transconjugants pCM_mobRK2_redB2 (Fwd cmR NotI, Rev cmR SpeI; 1105 bp), (1-25) *R. eutropha* H16 transconjugant pCM_mobRK2_redB2, (26) *R. eutropha H16* wildtype; (**B**) amplification of cm^r of *R. eutropha* H16 transconjugants pCM_mobRK2_redA9 (Fwd cmR NotI, Rev cmR SpeI; 1105 bp), (1-24) *R. eutropha* H16 transconjugant pCM_mobRK2_redA9, (25) *R. eutropha* H16 wildtype, (26) *E. coli* S17-1 [pCM_mobRK2_redA9], (27) Mastermix. (**C**, **D**) Primer binding site of Fwd cmR NotI and Rev cmR SpeI to amplify the chloramphenicol resistance fragment.

Even though the number of false-positive clones could be reduced severely by changing to the antibiotic chloramphenicol, still some false-positive clones were obtained as the latest

results showed. The best explanation for the growth of these transconjugants is again adaptation. However, it was assumed that *R. eutropha* H16 cells after a homologous recombination event should grow within one or two days by conferring the appropriate resistance. Thus, it was supposed that transconjugants of which cell growth was visible after 4-5 days can be considered as false-positive ones. Hence, no cell growth was visible after 1-2 days, a new approach was developed using a suicide vector with two homologous regions flanking the expression cassette (3.3 . Establishment of the *flippase* system in *Ralstonia eutropha* H16). Thereby, not only the probability of an integration event should be increased but it is also possible to carry out gene knock-outs, which is not achievable using only one homologous region.

3.2. Mobilization efficiency

The plasmid pKR_Ptac_Par_eGFP_mob_pSa was used to compare the original mobilization region of the plasmid pBBR1-MCS5 with the *mob* regions of the RK2 plasmid (*mobRK2*) and pKT231 (*mobRSF1010*) in their mobilization efficiency. The origin of replication *pSa118* was of particular importance, as an origin of replication had to be used which was stable in both *E. coli* and *R. eutropha* H16 to be able to determine the mobilization efficiency. Thereby, the plasmids pKR_Ptac_Par_eGFP_mobRK2_pSa and pKR_Ptac_Par_eGFP_mobRSF1010_pSa were constructed by replacing *mob* (pBBR1-MCS5) of pKR_Ptac_Par_eGFP_mob_pSa with *mobRK2* and *mobRSF1010* as described in the material and method section (2.11). After the successful construction of these fragments, the correct sequence was confirmed by sequencing.

Following, overnight cultures of *R. eutropha* H16 and *E. coli* S17-1 [pKR_Ptac_Par_eGFP_mob_pSa], *E. coli* S17-1 [pKR_Ptac_Par_eGFP_mobRK2_pSa] and *E. coli* S17-1 [pKR_Ptac_Par_eGFP_mobRSF1010_pSa] were inoculated with a single colony. Then, 1 mL of each *E. coli* S17-1 ONC was taken and a 10^{-6} dilution prepared and plated on LB agar plates. The growing colonies were counted and the colony forming units/mL (CFU/mL) were calculated (Table 19). Thereby, the dilution factor as well as the volume which was plated on the LB media (0.1 mL) had to be taken into account. The dilutions were carried out in triplicate and the mean value calculated. The calculated CFUs/mL were all in the same range (Table 19).

Table 19. Calculation of CFU/mL of *E. coli* S17-1.

Plasmid	**Colonies** (10^{-6})	**Colonies** (10^{0})	**CFU / mL**
pKR_Ptac_Par_eGFP_mob_pSa	218[1]	2,18 x 10^{8}	2,18 x 10^{9}
pKR_Ptac_Par_eGFP_mobRK2_pSa	197[1]	1,97 x 10^{8}	1,97 x 10^{9}
pKR_Ptac_Par_eGFP_mobRSF1010_pSa	172[1]	1,72 x 10^{8}	1,72 x 10^{9}

[1] mean value

Then, the remaining *E. coli* S17-1 ONCs as well as the *R. eutropha* H16 ONC were pelleted and conjugation carried out according to the material & method section 2.6. A 10^{-3} dilution was prepared of the *R. eutropha* H16 transconjugants carrying the plasmid with the *mobRK2* or *mobRSF1010* region whereas the transconjugant carrying the plasmid pKR_Ptac_Par_eGFP_mob_pSa was plated undiluted on the selective media (TSB media supplemented with 0.2 % fructose, gentamycin [20 µg/mL] and chloramphenicol [100 µg/mL]) and the growing colonies were counted. The dilutions were again conducted in triplicate and the mean value was calculated.

Additionally, the *R. eutropha* H16 wildtype strain was handled the same way as the transconjugants and plated on the selective media with the exception that it was in no contact with one of the *E. coli* S17-1 strains. Thus, the *R. eutropha* H16 wildtype should not be able to grow on TSB plates supplemented with kanamycin [200 µg/mL]. However, as reported earlier, some *R. eutropha* H16 cells were growing anyway. Hence, the *R. eutropha* H16 colonies growing on the selective media were counted and subtracted from the calculated number of colonies of the transconjugants to deduct the false-positive ones. Moreover, to calculate the *R. eutropha* H16 CFU/mL the dilution as well as the volume which was plated on the selective media (0.1 mL) had to be considered (Table 20). The number of transconjugants with either the *mob* region of the RK2 or pKT231 plasmid could be increased drastically as shown in Table 20.

Table 20. Calculation of CFU/mL of *R. eutropha* H16 transconjugants.

***R. eutropha* H16 transconjugant**	**Colonies** (10^{-3})	**Colonies** (10^{0})	**Colonies** (absolut)	**CFU/mL**
R. eutropha H16	-	12		
ReH16 pKR_Ptac_Par_eGFP_mob_pSa	-	15	3	3,00 x 10^{1}
ReH16 pKR_Ptac_Par_eGFP_mobRK2_pSa	147[1]	147000	146988	1,47 x 10^{6}
ReH16 pKR_Ptac_Par_eGFP_mobRSF1010_pSa	14[1]	14000	13988	1,40 x 10^{5}

[1] mean value

After the CFU/mL of the *E. coli* S17-1 cells used for conjugation and the CFU/mL of the *R. eutropha* H16 transconjugants were calculated, the mobilization efficiency of the three different mobilization regions was determined (Table 21). Thereby, the CFU/mL of the *R. eutropha* H16 transconjugants was divided by the CFU/mL of the corresponding *E. coli* cells. Thereby, a strong increase in the mobilization efficiency of *mobRK2* and *mobRSF1010* could be determined. The mobilization region *mobRSF1010* was ~$5.9*10^3$ times more efficient than the one of the pBBR1-MCS5 plasmid whereas the *mob* region of the RK2 plasmid was even ~$5.5*10^4$ times more efficient, demonstrating that *mobRK2* mobilizes and transfers approximately 55.000 plasmids as the mobilization region of the pBBR1-MCS5 plasmid mobilizes and transfers only one (published in [101]).

Table 21. Calculation of the mobilization efficiency of the mobilization regions of the plasmids pBBR1-MCS5, RK2 and pKT231.

mobilization region	**CFU/mL *E. coli* S17-1**	**CFU/mL *Re*H16 transconjugant**	**mobilization efficiency**
mob (pBRR1-MCS5)	$2{,}18 \times 10^9$	$3{,}00 \times 10^1$	$1{,}38 \times 10^{-8}$
mobRK2 (RK2)	$1{,}97 \times 10^9$	$1{,}47 \times 10^6$	$7{,}46 \times 10^{-4}$
mobRSF1010 (pKT231)	$1{,}72 \times 10^9$	$1{,}40 \times 10^5$	$8{,}13 \times 10^{-5}$

3.3. Establishment of the *flippase* system in *Ralstonia eutropha* H16

The reason that until now no integration event could be determined was most likely due to the usage of a *mob* region (of pBBR1-MCS5) with a really low mobilization efficiency (see 3.2) as well as due to the used homologous region. Even though homologous regions with different length ranging from 458 bp (*redB2*), 672 bp (*ca1*) to 1061 bp (*redA9*) were used no integration event was detected. In literature, various publications indicate that the probability of an integration event to happen is much higher using a suicide vector with two homologous regions flanking the fragment to be integrated [16]–[18], [20]. Another advantage of two homologous regions is that it is possible to knock-out genes whereas with one homologous region only gene insertions can be conducted.

In the following the plasmid pK470_mobRK2_estA_frt_phaC1 was constructed with two homologous regions. The *phaC1* gene of *R. eutropha* H16 encoding for the polyhydroxybutyrate (PHB) synthase was chosen as homologous region. Both fragments were comprised of ~ 900 bp each and surrounded the expression cassette with the reporter gene *estA* of *Rhodococcus ruber*. The *mob* region of the RK2 plasmid was used to construct this plasmid due to its best results regarding the mobilization efficiency. Moreover, kan^r was flanked by flippase recognition target (frt) sites and thus it was possible to excise the selection marker after successful integration by the flippase.

3.3.1. Construction of pK470_mobRK2_estA_frtΔ_phaC1

In order to construct a suicide vector with two homologous regions for integration as well as with frt sites flanking the selection marker, the plasmid pK470_mob_ca1 was used as a starting vector. At the beginning, a PCR was performed to introduce a *Spe*I restriction site upstream of the promoter (see Table 11 for exact PCR conditions). Moreover, the frt sites were introduced as well via PCR (see Table 11). The frt site up was placed upstream of the kanamycin resistance whereas the frt site down was introduced directly after kan^r including a *Xho*I restriction site. See also material & method section 2.12.1.

After the incorporation of the restriction sites *Spe*I and *Xho*I as well as the frt sites, the plasmid pK470_mob_ca1_frtΔ was digested with the restriction enzymes *Nde*I and *Hind*III to replace *ca1* with *estA* of *R. ruber* of the plasmid pK470_mob_ca1_estA digested at the same restriction sites. After purification, determination of the DNA concentration, ligation and

transformation, single colonies were streaked out for plasmid isolation. The isolated plasmids were digested with the restriction enzymes *Hind*III and *Not*I. The restriction pattern of 3973 bp and 515 bp confirmed the successful cloning of the esterase (Figure 25).

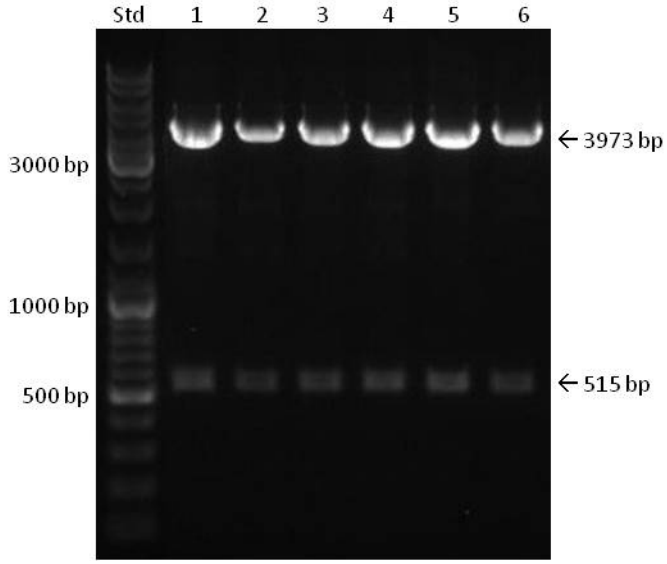

Figure 25. Agarose gel of restriction digest with *Hind*III and *Not*I of pK470_mob_estA_frtΔ.
Std.: Gene Ruler^{TM} DNA Ladder Mix (500 ng); (1-6) pK470_mob_estA_frtΔ digested with *Hind*III and *Not*I (3973 bp and 515 bp).

Following, the plasmid pK470_mob_estA_frtΔ was restriction digested with *Spe*I to incorporate the first homologous region *phaC1_1* previously digested with the same restriction enzyme (as described in material & methods 2.12.1). This homologous region was ranging from the start codon of the *phaC1* gene into approximately the middle of the gene with a size of 880 bp. After cloning the *phaC1_1* region into the vector backbone, 16 colonies were streaked out for plasmid isolation. Then, a restriction digest was conducted. The plasmid was digested with the restriction enzyme *Not*I to be able to verify the orientation of the cloned fragment *phaC1_1*. The *Not*I restriction site was only present in *estA* and the first homologous region thus, the orientation could be determined due to the restriction pattern. The orientation was essential for the following homologous integration. The plasmids in lane 5, 14 and 15 had incorporated the fragment in the desired orientation and showed a restriction pattern of 3909 bp and 1459 bp (Figure 26). All the other plasmids incorporated the homologous region in the unwished orientation (4501 bp and 867 bp) or the cloning of *phaC1_1* was not successful (lane 6, 10 and 13) due to vector religation (Figure 26).

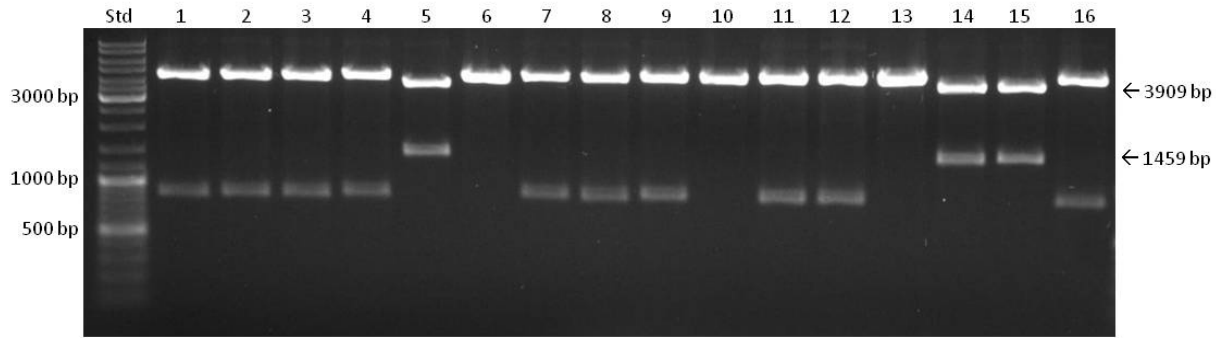

Figure 26. Agarose gel of restriction digest of pK470_mob_estA_frtΔ_phac1_1 with *Not*I to determine the orientation of the homologous region.
Std.: Gene Ruler^{TM} DNA Ladder Mix (500 ng); (1-16) pK470_mob_estA_frtΔ_phaC1_1 digested with *Not*I (3909 bp and 1459 bp).

Subsequently, the second homologous region *phaC1_2* comprised of 902 bp was cloned into the vector backbone pK470_mob_estA_frtΔ_phaC1_1 (5368 bp) after both fragments were digested with the restriction enzyme *Xho*I and purified. After ligation and transformation, a colony PCR on the transformants was carried out (see Table 13 for exact PCR conditions) to verify which transformant had the complete plasmid pK470_mob_estA_frtΔ_phaC1 after successful cloning of *phaC1_2* in the desired orientation. The forward primer (phaC1 Fwd XhoI) was binding at the beginning of the second homologous region *phaC1_2* whereas the reverse primer (colE1 rev) in the *ColE1* origin amplifying a fragment of 1573 bp. The transformants in lane 2-4, 7 and 12 had incorporated *phaC1_2* in the desired orientation (Figure 27A). Following, these transformants were streaked out for plasmid isolation and digested with the restriction enzyme *Asc*I. The successful constructed plasmid pK470_mob_estA_frtΔ_phaC1 showed a restriction pattern of 4977 bp and 1293 bp (Figure 27B). The results of the colony PCR could be confirmed by using the restriction enzyme *Asc*I, as the second homologous region *phaC1_2* has an *Asc*I restriction site and only after successful cloning in the correct orientation this restriction pattern could be gained.

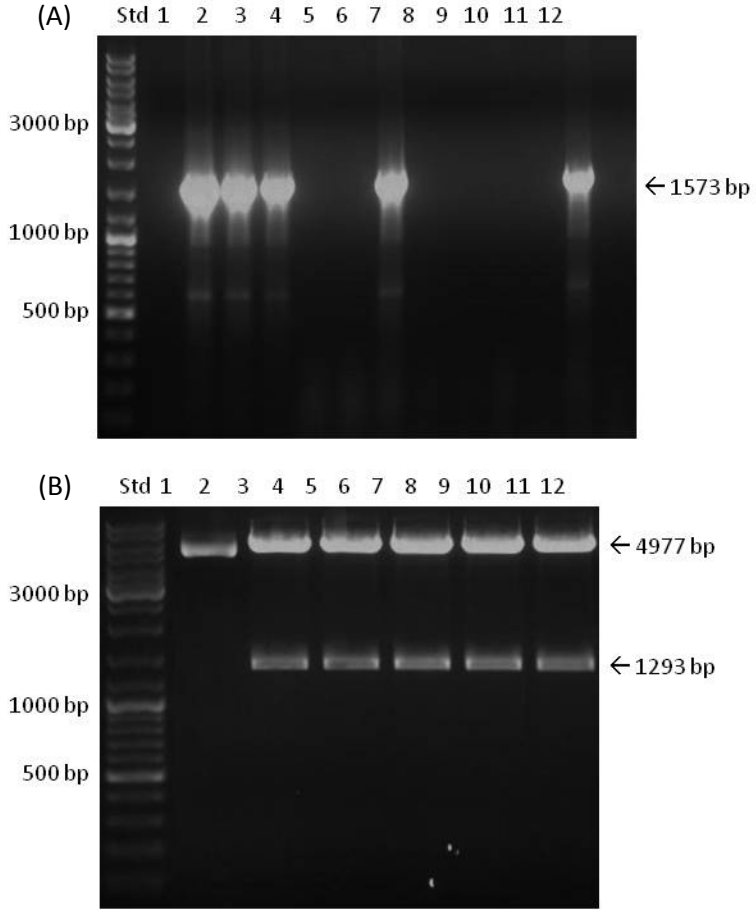

Figure 27. Agarose gel of (A) colony PCR of pK470_mob_estA_frtΔ_phaC1 of *phaC1_2* orientation and (B) restriction digest of pK470_mob_estA_frtΔ_phaC1 with *Asc*I.
Std.: Gene Ruler^{TM} DNA Ladder Mix (500 ng); (**A**) (1-13) amplification of a fragment of the *phaC1_2* region into the *ColE1 ori* of pK470_mob_estA_frtΔ_phaC1 transformants after cloning the second homologous region *phaC1_2* (phaC1 Fwd XhoI, colE1 rev; 1573 bp); (**B**) (1) pK470_mob_estA_frtΔ_phaC1 uncut, (2-6) pK470_mob_estA_frtΔ_phaC1 digested with *Asc*I (4977 bp and 1293 bp).

Finally, the *mob* region of pBBR1-MCS5 of the plasmid pK470_mob_estA_frtΔ_phaC1 was replaced by the *mob* region of the RK2 plasmid. The plasmid backbone was amplified via PCR (see Table 11 for exact PCR conditions) and *mobRK2* cloned via blunt-end ligation as described in the material and method section 2.12.1. Then, transformants were streaked out for plasmid isolation and a restriction digest with *Pst*I was carried out. The restriction pattern showed fragments of 2351 bp, 1563 bp, 1200 bp and 940 bp confirming the successful construction of the plasmid pK470_mobRK2_estA_frtΔ_phaC1 (Figure 28). Only the plasmid in lane 4 did not correlate with the expected restriction pattern, most likely due to the fact, that one *Pst*I restriction site was missing.

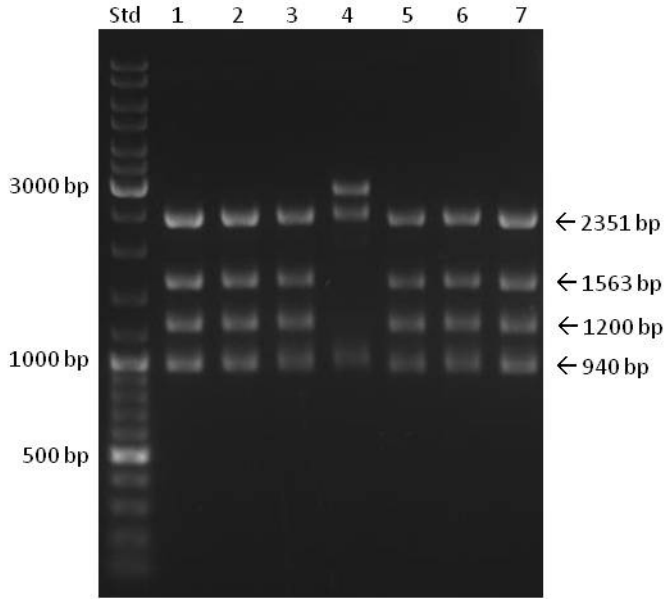

Figure 28. Agarose gel of restriction digest of pK470_mobRK2_estA_frtΔ_phaC1 with *Pst*I.
Std.: Gene Ruler™ DNA Ladder Mix (500 ng); (1-7) pK470_mobRK2_estA_frtΔ_phaC1 digested with *Pst*I (2351 bp, 1563 bp, 1200 bp and 940 bp).

After the successful construction of pK470_mobRK2_estA_frtΔ_phaC1 the plasmid was sent for sequencing to determine the correct sequence of the different fragments. The sequencing results revealed that the frt sites introduced via PCR were not complete although the sequence of the other fragments was correct. The frt site up was missing 5 base pairs whereas the frt site down was missing 2 base pairs. In the following, the frt sites were repaired, see therefore 3.3.3. Correction of frt sites and construction of pK470_mobRK2_estA_frt_phaC1.

Before the constructed plasmid was transferred into *R. eutropha* H16 via conjugation to promote a recombination event, a further PCR was performed to introduce a *Sph*I restriction site upstream of the promoter. This restriction site was of importance to be able to replace the expression cassette. After the successful amplification of the vector, the fragment was phosphorylated prior ligation and transformation and the isolated plasmid digested with *Sph*I. As only one *Sph*I restriction site should be present on the plasmid, the vector was linearized showing a fragment of 6054 bp after successful incorporation of the *Sph*I restriction site (Figure 29).

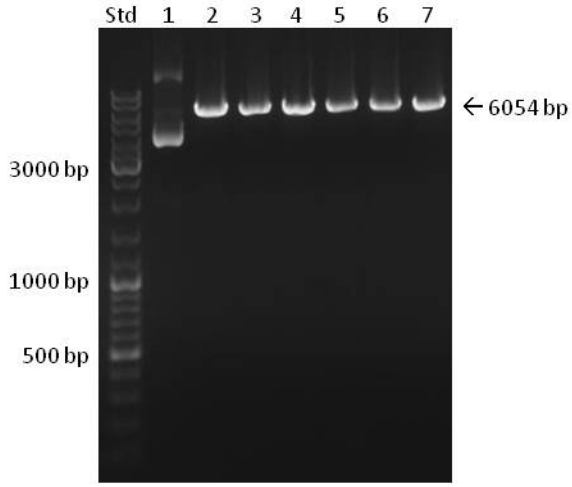

Figure 29. Agarose gel of *Sph*I restriction digest of pK470_mobRK2_estA_frtΔ_phaC1.
Std.: Gene Ruler^{TM} DNA Ladder Mix (500 ng); (1) pK470_mobRK2_estA_frtΔ_phaC1 uncut, (2-7) pK470_mobRK2_estA_frtΔ_phaC1 digested with *Sph*I (6054 bp).

3.3.2. Integration of pK470_mobRK2_estA_frtΔ_phaC1

Even though, the frt sites of the plasmid pK470_mobRK2_estA_frtΔ_phaC1 were not complete, the plasmid was used for conjugation. After the plasmid was transformed into *E. coli* S17-1 cells, a single colony was used to inoculate the overnight culture, following, conjugation was carried out. The *R. eutropha* H16 transconjugants already grew after two days of incubation at 28 °C indicating a successful recombination event. The previously obtained transconjugants always needed at least four to five days at 28 °C until cell growth was visible. Consequently, a colony PCR on a possible recombination event was performed with single colonies of the *R. eutropha* H16 transconjugants. The first primer pair (5' Int phaC1 Fwd, Int Est Rev) was used to confirm a possible integration event in the 5' region binding upstream of the *phaC1* gene on chromosome 1 and in the esterase. The second primer pair (Int KanR Fwd, 3' Int phaC1 Rev) was binding in kan^{r} and the 3' region downstream of the *phaC1* gene to confirm a possible integration event in the 3' region. Both PCRs were performed as integration could occur in both regions simultaneously as well as only over one region. Then, the PCR samples were loaded onto an agarose gel and finally, an integration event could be determined. After successful integration in the 5' region the amplified fragment had a size of 1499 bp whereas the fragment after integration in the 3' region was 1137 bp (Figure 30A). Moreover, both PCRs on the *R. eutropha* H16 wildtype (negative control) did not show any fragment (Figure 30A).

Subsequently, an additional colony PCR was performed with the outer primers 5' Int phaC1 Fwd and 3' Int phaC1 Rev, binding only on chromosome 1 of *R. eutropha* H16 up- and downstream of the *phaC1* gene. This PCR was conducted to show the difference between the *R. eutropha* H16 wildtype and *R. eutropha* H16 Δ*phaC*ΩKm*estA*$_{Rr}$ after integration of the expression cassette and kan^{r}. The amplified fragment of *R. eutropha* H16 Δ*phaC*ΩKm*estA*$_{Rr}$ had a size of 4685 bp after integration whereas only the *phaC1* gene of the *R. eutropha* H16 wildtype with a size of 1961 bp was amplified (Figure 30B). These results confirmed the integration via both homologous regions.

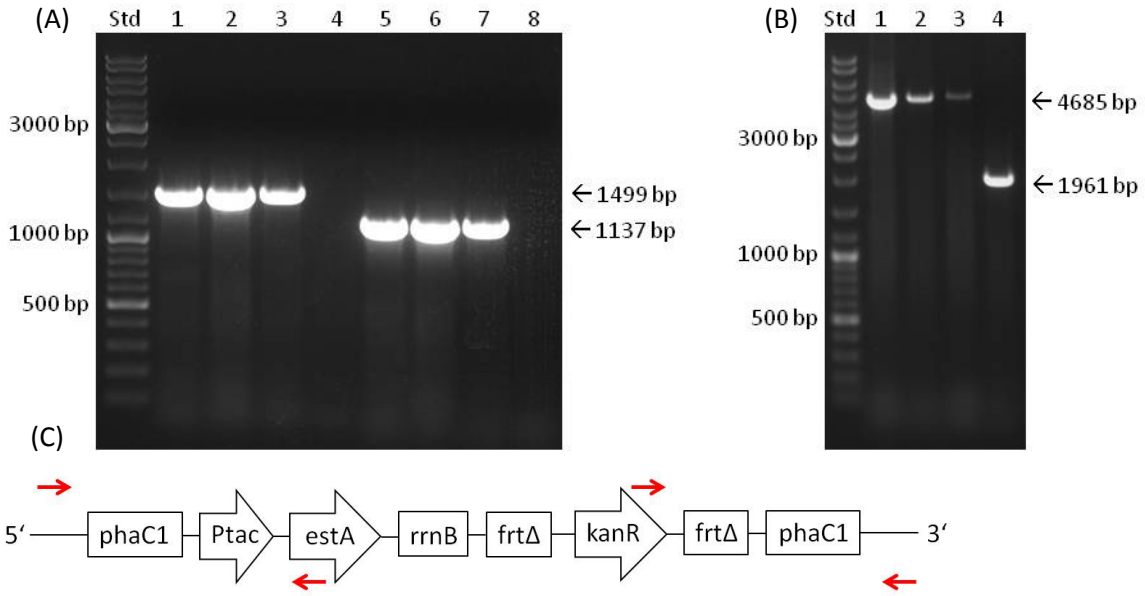

Figure 30. Agarose gel of colony PCR of *R. eutropha* H16 Δ*phaC*ΩKm*estA*$_{Rr}$ of (A) an integration event in the 5' and 3' region of *phaC1* and (B) the whole integrated fragment. (C) Location of primer binding site. Std.: Gene Ruler^{TM} DNA Ladder Mix (500 ng); (**A**) (1-3), *R. eutropha* H16 Δ*phaC*ΩKm*estA*$_{Rr}$, (4) *R. eutropha* H16 wildtype, amplified fragment of the 5' genomic region upstream of *phaC1* into the esterase (5' Int phaC1 Fwd, Int Est Rev; 1499 bp); (5-7) *R. eutropha* H16 Δ*phaC*ΩKm*estA*$_{Rr}$, (8) *R. eutropha* H16 wildtype, amplified fragment of kan^{r} into the 3' genomic region downstream of *phaC1* (Int KanR Fwd, 3' Int phaC1 Rev; 1137 bp); (**B**) amplified fragment ranging from the genomic region upstream of *phaC1* into the region downstream of *phaC1* (5' Int phaC1 Fwd, 3' Int phaC1 Rev); (**C**) The location of the primer binding site to verify an integration event up- and downstream of *phaC1* as well as to amplify the whole integrated fragment (outer primer) is indicated with red arrows.

Additionally, an esterase filter activity assay was conducted to determine the expression of the esterase in *R. eutropha* H16 after integration (material and method section 2.7). This assay is based on the catalytic activity of esterases to hydrolyze α-naphthyl acetate to α-naphthol and acetic acid. Following, α-naphthol and FastBlueB form a complex resulting in a discolouration to violet which can be used to determine esterase activity [98]. The discolouration of the positive control *E. coli* S17-1 [pK470_mobRK2_estA_frtΔ_phaC1] and of

R. eutropha H16 Δ*phaC*ΩKm*estA*$_{Rr}$ after integration is clearly visible in Figure 31. The esterase activity was already spotted on the filter after a few seconds. Furthermore, a single colony of the *R. eutropha* H16 wildtype was transferred on the Whatmann-filter as well as a negative control and as expected, no esterase activity could be determined (Figure 31).

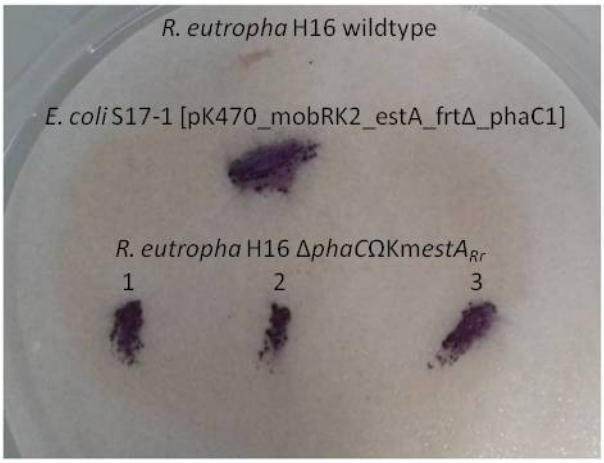

Figure 31. Esterase filter activity assay of *R. eutropha* H16 Δ*phaC*ΩKm*estA*$_{Rr}$ after the integration of *estA* of *R. ruber*.
R. eutropha H16 Δ*phaC*ΩKm*estA*$_{Rr}$ can be seen in the lower part of the figure whereupon the numbers 1-3 indicate three different transconjugants. The *R. eutropha* H16 wildtype (negative control) and the *E. coli* S17-1 [pK470_mobRK2_estA_frtΔ_phaC1] (positive control) are shown in the top of the figure. A discolouration to violet indicates EstA activity based on α-naphthyl acetate and FastBlueB.

Due to the results of the esterase filter activity assay, in the following, a SDS-PAGE (sodium dodecyl sulfate polyacrylamide gel electrophoresis) was carried out to show the esterase protein band. Prior staining of the protein bands, an activity stain was performed. Thereby, the proteins which were denaturated and then, separated during the SDS-PAGE were renaturated again before the esterase activity could be determined. The denaturation step was essential as the migration of the denaturated protein is more accurate than the native one and depends primarily on the molecular weight of the denatured protein. The esterase activity was determined similar to the filter assay based on α-naphthyl acetate and FastBlueB (see material and methods 2.5). The discolouration to violet of the esterase band of *R. eutropha* H16 Δ*phaC*ΩKm*estA*$_{Rr}$ was shown in lane 4 to 6 (Figure 32). Even though only one copy of the esterase of *R. ruber* was integrated into the genome of *R. eutropha* H16 the signal was quite strong and clearly visible. Moreover, the *R. eutropha* H16 wildtype did not show any esterase activity (lane 3). The esterase band of *R. eutropha* H16 Δ*phaC*ΩKm*estA*$_{Rr}$ corresponded to the one of *E. coli* S17-1 [pK470_mobRK2_estA_frtΔ_phaC1] (positive control, lane 2) with a size of 37 kDa as expected (Figure 32).

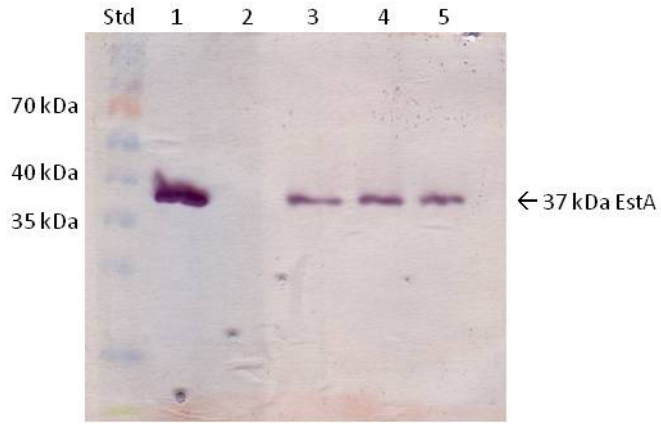

Figure 32. Esterase activity stain of SDS-PAGE of *R. eutropha* H16 Δ*phaC*ΩKm*estA*$_{Rr}$.
Std.: PageRuler Prestained Protein Ladder; (1) *E. coli* S17-1 [pK470_mobRK2_estA_frtΔ_phaC1], (2) *R. eutropha* H16 wildtype, (3-5) *R. eutropha* H16 Δ*phaC*ΩKm*estA*$_{Rr}$. The stained EstA bands based on α-naphthyl acetate and FastBlueB are shown at a size of 37 kDa.

After the activity stain was carried out, the gel was stained with Coomassie Brilliant Blue followed by discolouration of the proteins. Coomassie Brilliant Blue accumulates at the alkaline side chains of amino acids and thereby staining the previously separated proteins [102]. The protein band of the esterase at 37 kDa was visible on the stained gel in violet due to the previously conducted activity stain. After the Coomassie staining the difference of the protein pattern of *E. coli* S17-1 and *R. eutropha* H16 was observable (Figure 33). Moreover, it can be stated that the signal of the protein bands of the *R. eutropha* H16 wildtype was much weaker than the one of the other samples due to a lower sample concentration. However, no band at 37 kDa was detectable in the wildtype as expected (Figure 33).

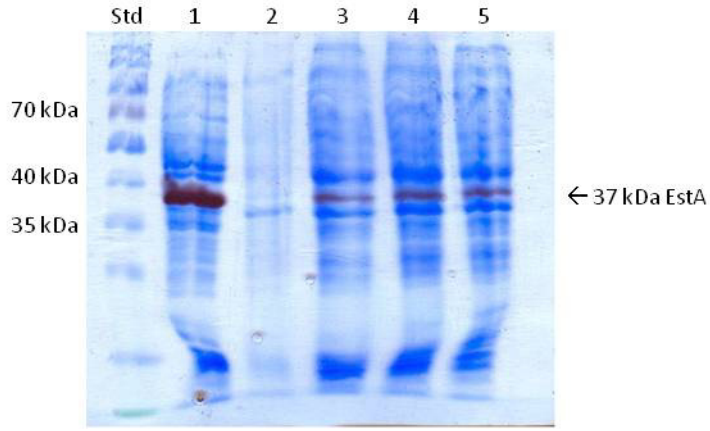

Figure 33. Coomassie Brilliant Blue stained SDS-PAGE of *R. eutropha* H16 Δ*phaC*ΩKm*estA*$_{Rr}$.
Std.: PageRuler Prestained Protein Ladder; (1) *E. coli* S17-1 [pK470_mobRK2_estA_frtΔ_phaC1], (2) *R. eutropha* H16 wildtype, (3-5) *R. eutropha* H16 Δ*phaC*ΩKm*estA*$_{Rr}$. The EstA band is indicated at a size of 37 kDA.

The results of the esterase filter activity assay were confirmed by the activity stain and the following Coomassie staining subsequent to the SDS-PAGE. The expression and activity of EstA of *R. ruber* in *R. eutropha* H16 was proved. Additionally, the phenotype of *R. eutropha* H16 Δ*phaC*ΩKm*estA*$_{Rr}$ was compared with the one of the wildtype related to PHB production. *R. eutropha* H16 produces large amounts of PHB under unbalanced growth conditions (high C/N ratio) [103]. *R. eutropha* H16 Δ*phaC*ΩKm*estA*$_{Rr}$ should not be able to produce PHB anymore due to the integration of the esterase in the *phaC1* gene as after the integration the *phaC* gene coding for the PHB synthase was knocked out. Even though, the full sequence of the *phaC1* gene was still present on the genome, it was interrupted by the integrated fragments and thus, it is not functional anymore as the original gene could not be transcribed and translated respectively.

The *R. eutropha* H16 wildtype as well as the transconjugants were streaked out on NB media plates supplemented with 5 g/L fructose and incubated at 28 °C. *R. eutropha* H16 Δ*phaC*ΩKm*estA*$_{Rr}$ did not show to produce PHB anymore as expected and appeared more transparent compared to the *R. eutropha* H16 wildtype (Figure 34).

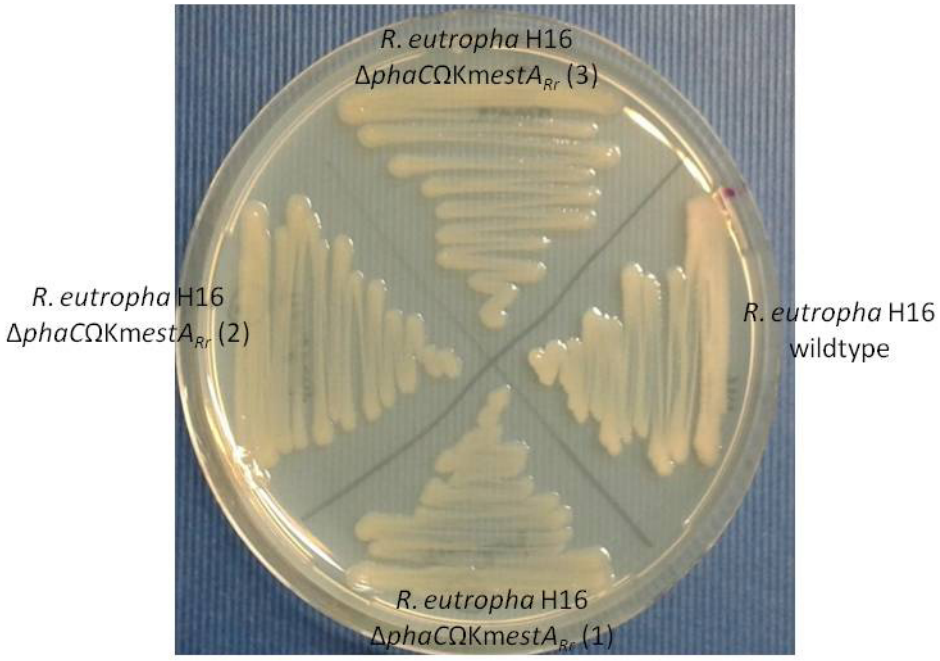

Figure 34. Growth of *R. eutropha* H16 Δ*phaC*ΩKm*estA*$_{Rr}$ compared to the wildtype on NB media supplemented with 5 g/L fructose. *R. eutropha* H16 Δ*phaC*ΩKm*estA*$_{Rr}$ appeared more transparent due the knockout of the polyhydroxybutyrate synthase.

3.3.3. Correction of frt sites and construction of pK470_mobRK2_estA_frt_phaC1

After the successful integration of the plasmid pK470_mobRK2_estA_frtΔ_phaC1 into the genome of *R. eutropha* H16, the incomplete frt sites of the plasmid had to be repaired before the flippase system could be tested. Following, the fragment NdeI_estA-rrnB-frt-kanR-frt_XhoI had to be generated via overlap extension PCR (see therefor material and methods 2.12.2 for details). First, the fragments to perform the overlap extension PCR were amplified and purified (fragment1 1389 bp, fragment2 865 bp; Figure 35A) prior the overlap extension PCR was performed. Then, the PCR mixture was loaded onto a preparative agarose gel and the appropriate band at 2254 bp excised and purified. Subsequently, the accurate size of the overlap fragment of 2254 bp was determined via control gel (Figure 35B) and the fragment cloned into the pJET1.2 cloning vector.

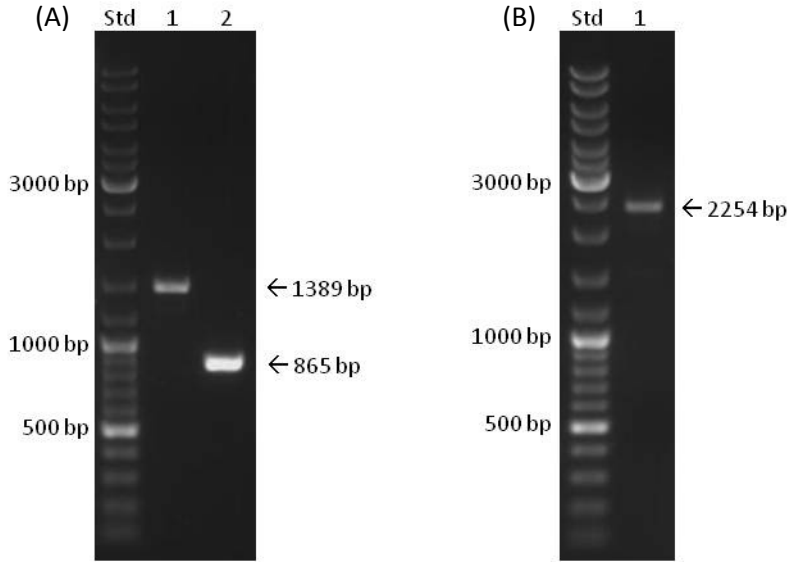

Figure 35. Agarose gel of (A) purified fragments for overlap extension PCR and (B) purified overlap fragment.
Std.: Gene Ruler™ DNA Ladder Mix (500 ng); (**A**) (1) fragment1 for overlap extension PCR (1389 bp), (2) fragment2 for overlap extension PCR (865 bp); (**B**) (1) overlap fragment (2254 bp).

Via sequencing, the correct sequence of the frt sites was confirmed. However, the template (pK470_mob_ca1_estA) used to generate the fragments for the overlap PCR had a *Xho*I restriction site between *estA* and the terminator region. Thus, the cloning of the fragment estA-rrnB-frt-kanR-frt with the restriction enzymes *Nde*I and *Xho*I was not possible. To overcome this problem, another overlap extension PCR was conducted whereas fragment1 was amplified of pK470_mobRK2_estA_frtΔ_phaC1 and fragment2 of the just generated pJET_estA_rrnB_frt_kanR_frt with the correct frt sites. For this overlap extension PCR a

region in the terminator sequence was used as homologous sequence. After fragment1 (1327 bp) and fragment2 (949 bp) were amplified, both fragments were purified and used as template for the overlap extension PCR (see Figure 8). The amplified fragment after the overlap extension PCR of 2254 bp was again cloned into the pJET1.2 cloning vector. Then, the generated plasmid pJET_estA_rrnB_frt_kanR_frt was digested with the restriction enzyme *Nde*I as well as double digested with *Nde*I and *Xho*I prior sequencing. After the double digest the restriction pattern of 2963 bp, 2247 bp and 28 bp confirmed the successful construction of the overlap fragment (Figure 36) and thus, the *Xho*I restriction site within the fragment could be removed. However, since the fragment at 28 bp was not visible on the gel, a restriction digest with only the *Nde*I restriction enzyme was carried out as well to assure that the *Nde*I restriction site was still present upstream of the esterase. The linearized fragment was 5238 bp of size (Figure 36).

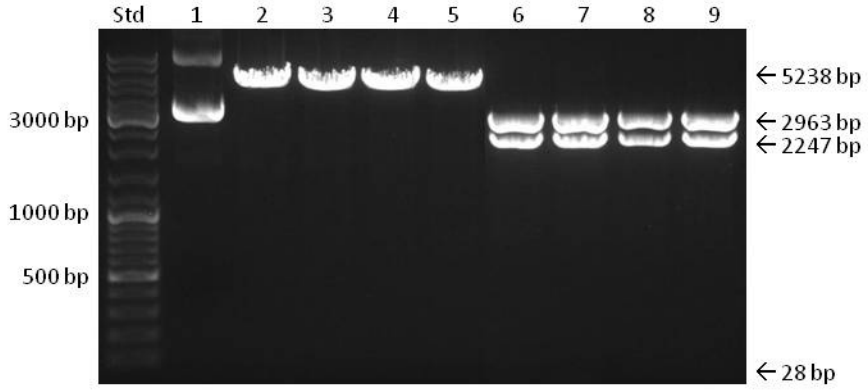

Figure 36. Agarose gel of restriction digest with *Nde*I and *Nde*I/*Xho*I of pJET_estA_rrnB_frt_kanR_frt. Std.: Gene Ruler™ DNA Ladder Mix (500 ng); (1) pJET_estA_rrnB_frt_kanR_frt uncut, (2-5) pJET_estA_rrnB_frt_kanR_frt digested with *Nde*I (5238 bp), (6-9) pJET_estA_rrnB_frt_kanR_frt double digested with *Nde*I and *Xho*I (2963 bp, 2247 bp and 28 bp).

The correct sequence of the plasmid pJET_estA_rrnB_frt_kanR_frt was confirmed by sequencing, the fragment estA_rrnB_frt_kanR_frt could be cloned into the plasmid pK470_mobRK2_estA_frtΔ_phaC1 via restriction digest with *Nde*I and *Xho*I, replacing the expression cassette as well as the incomplete frt sites as described in the material and method section 2.12.2; Figure 9. Following, plasmids of six transformants were isolated and digested with the restriction enzyme *Xba*I. Three *Xba*I restriction sites, of which two were in the frt sites respectively, were present on the plasmid pK470_mobRK2_estA_frt_phaC1_1. The successful plasmid construction could be confirmed as the restriction pattern of 2711 bp, 1417 bp and 851 bp was shown (Figure 37).

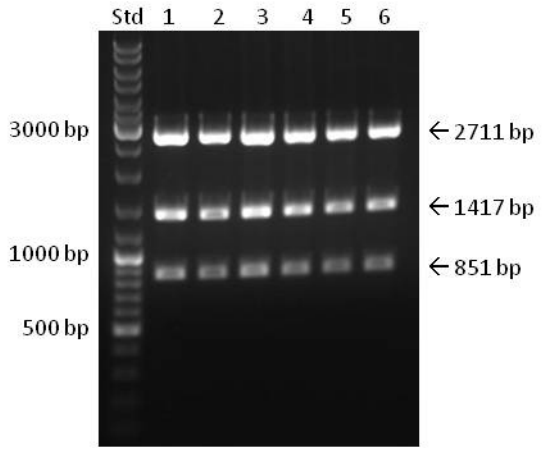

Figure 37. Agarose gel of restriction digest with *Xba*I of pK470_mobRK2_estA_frt_phaC1_1.
Std.: Gene Ruler^{TM} DNA Ladder Mix (500 ng); (1-6) pK470_mobRK2_estA_frt_phaC1_1 digested with *Xba*I (2711 bp, 1417 bp and 851 bp).

Subsequently, the second homologous region *phaC1_2* had to be cloned again into the plasmid pK470_mobRK2_estA_frt_phaC1_1 backbone as this region was excised during the previous *Xho*I digest. Transformants were selected and analyzed for the incorporation of *phaC1_2* in the desired orientation in pK470_mobRK2_estA_frt_phaC1 via colony PCR. The transformants 1-3 showed to have incorporated *phaC1_2* in the correct orientation as a fragment of 1658 bp could be amplified (Figure 38A). Following, the plasmids were isolated and the successful construction of pK470_mobRK2_estA_frt_phaC1 was verified via restriction digest with *Pst*I. Fragments of 2178 bp, 1567 bp, 1204 bp and 940 bp resulted of the restriction digest as expected (Figure 38B) and thereby conforming the successful construction of pK470_mobRK2_estA_frt_phaC1.

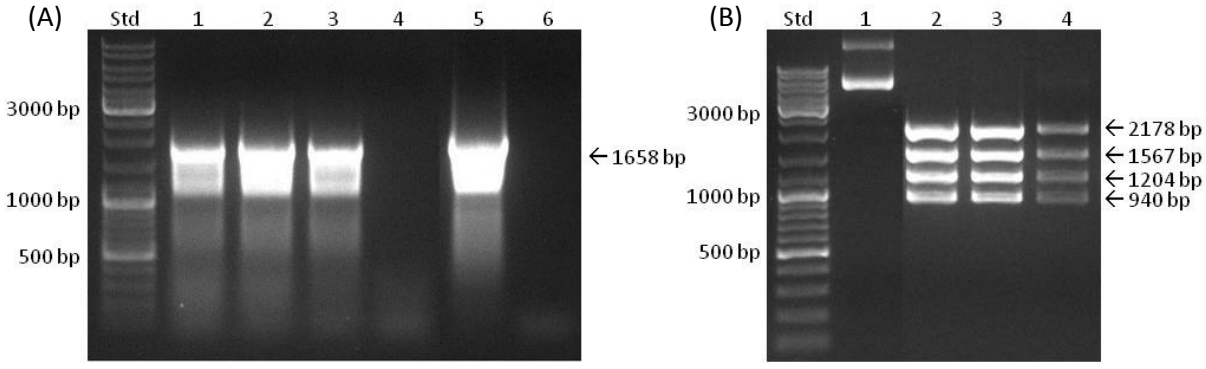

Figure 38. Agarose gel of (A) colony PCR of *phaC1_2* orientation and (B) restriction digest with *Pst*I of pK470_mobRK2_estA_frt_phaC1.
Std.: Gene Ruler^{TM} DNA Ladder Mix (500 ng); (**A**) amplification of a fragment of kan^{r} into the *phaC1_2* region of pK470_mobRK2_estA_frt_phaC1 (KanR Int Fwd, phaC1 Rev XhoI; 1658 bp), (1-4) *E. coli* Top10 [pK470_mobRK2_estA_frt_phaC1]; (5) *E. coli* Top10 [pK470_mobRK2_estA_frtΔ_phaC1] (positive control), (6) colony PCR Mastermix (negative control); (**B**) (1) pK470_mobRK2_estA_frt_phaC1 uncut, (2-4) pK470_mobRK2_estA_frt_phaC1 digested with *Pst*I (2178 bp, 1567 bp, 1204 bp and 940 bp).

3.3.4. Verification of the functionality of the Flp-frt system in *R. eutropha* H16

After the successful construction of pK470_mobRK2_estA_frt_phaC1, the flippase system could be tested in *R. eutropha* H16. Thus, on the one hand the suicide vector with the complete frt sites had to be integrated into the genome of *R. eutropha* H16 whereas on the other hand the plasmid pCM_mobRK2_flp comprised of the flippase had to be constructed. For the vector construction of pCM_mobRK2_flp see the material and method section 2.15 for details. After the cloning of the *flp* into the vector backbone, the plasmid was restriction digested with *Spe*I. Fragments of 2946 bp and 1781 bp confirmed the successful construction of pCM_mobRK2_flp (Figure 39).

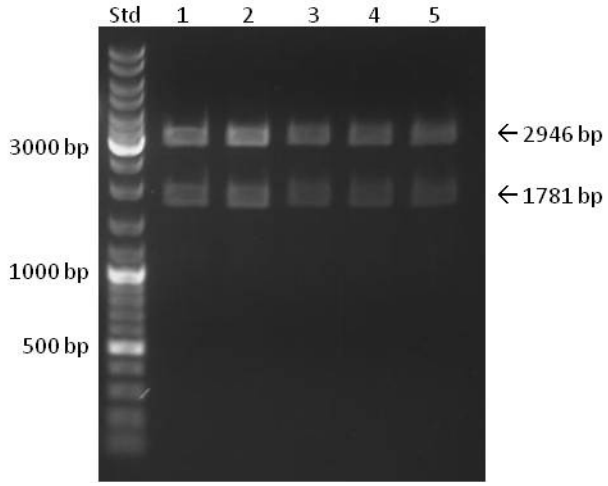

Figure 39. Agarose gel of restriction digest with *Spe*I of pCM_mobRK2_flp.
Std.: Gene Ruler^{TM} DNA Ladder Mix (500 ng); (1-5) pCM_mobRK2_flp digested with *Spe*I (2946 bp and 1781 bp).

In the following, the plasmid pK470_mobRK2_estA_frt_phaC1_1 was used for integration comprised of only one homologous region and the complete frt sites due to the problems cloning the second homologous region *phaC1_2*. After conjugation was carried out, two transconjugants were growing on the selective media (TSB media supplemented with 0.2 % fructose, gentamycin [20 µg/mL] and kanamycin [200 µg/mL]) and used for colony PCR to verify a recombination event ranging of the 5' region in front of *phaC1* on chromosome 1 of *R. eutropha* H16 into the esterase. The integration of the plasmid pK470_mobRK2_estA_frt_phaC1_1 could be confirmed in both *R. eutropha* transconjugants (*R. eutropha* H16 ΩKm*estA*$_{Rr}$) as a fragment of 1499 bp was amplified (Figure 40). Due to the fact that only one homologous region was present on the plasmid, the yield of transconjugants was much lower than observed during the integration of

pK470_mobRK2_estA_frtΔ_phaC1 comprised of two homologous regions. This confirmed the previous statement that the probability of a recombination event to happen is much higher using two homologous regions. Moreover, the whole plasmid pK470_mobRK2_estA_frt_phaC1_1 was integrated as only gene insertions and no gene knock-outs are possible using one homologous region. Thus, the *phaC1* gene of *R. eutropha* H16 was still expressed and functional.

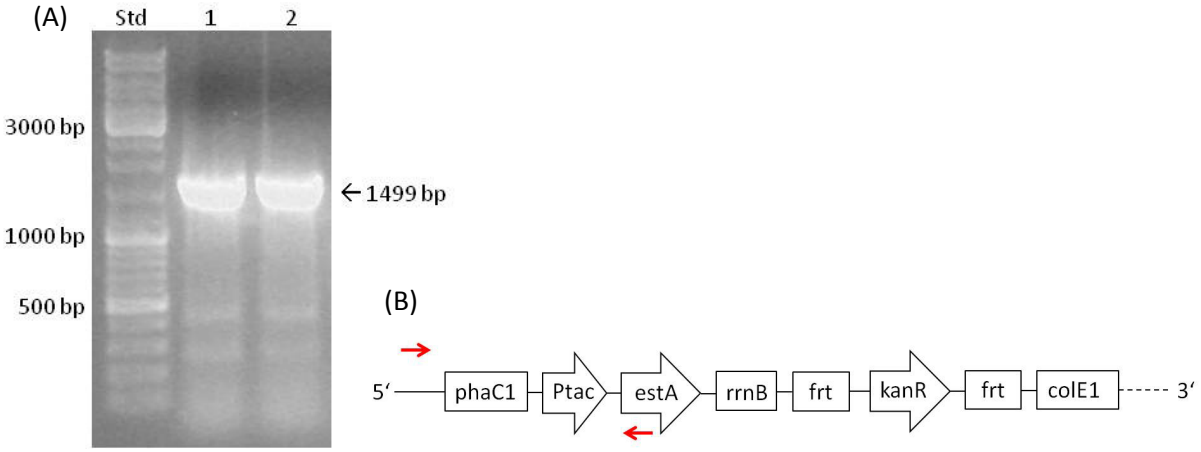

Figure 40. (A) Agarose gel of colony PCR of *R. eutropha* H16 ΩKm*estA*$_{Rr}$ of a 5' integration event. (B) Location of primer binding site.
(**A**) Std.: Gene Ruler^{TM} DNA Ladder Mix (500 ng); (1-2) *R. eutropha* H16 ΩKm*estA*$_{Rr}$; amplified fragment of the 5' genomic region upstream of *phaC1* into the esterase (5' Int phaC1 Fwd, Int Est Rev; 1499 bp). (**B**) The primer binding site is indicated with red arrows.

Afterwards, the plasmid pCM_mobRK2_flp was transferred from *E. coli* S17-1 into the previously obtained *R. eutropha* H16 ΩKm*estA*$_{Rr}$ which had integrated the plasmid pK470_mobRK2_estA_frt_phaC1_1. After conjugation was conducted, *R. eutropha* H16 ΩKm*estA*$_{Rr}$ was plated on TSB media only supplemented with gentamycin [20 µg/mL] and 0.2% fructose as the desired transconjugant should not imply any other resistance. The kanamycin resistance should have been excised by the flippase whereas the plasmid pCM_mobRK2_flp comprised of the chloramphenicol resistance is not stable in *R. eutropha* H16 due to the *ColE1* origin of replication and hence did not imply this resistance. A dilution of 10^{-7} was necessary to gain single colonies. Subsequently, 104 of these single colonies were streaked out on TSB media supplemented with gentamycin [20 µg/mL] and 0.2% fructose as well as TSB media with kanamycin [200 µg/mL], gentamycin [20 µg/mL] and 0.2% fructose. Only the *R. eutropha* transconjugants (*R. eutropha* H16 e*stA*$_{Rr}$) which did not grow on the media supplemented with kanamycin were analyzed for a successful excision of the

selection marker by the Flp-frt system. 26 colonies of 104 were not able to grow on the TSB media supplemented with kanamycin. Thus, the cell material of these identical colonies was taken of the TSB plate only supplemented with gentamycin, resuspended in ddH_2O and an aliquot used for the colony PCR. The primers Int KanR Fwd and colE1 Rev were used to amplify a fragment from the kanamycin resistance gene into the origin of replication using the *R. eutropha* H16 *estA*$_{Rr}$ as template. An amplification of this fragment would indicate that kan^r was still present on the genome of *R. eutropha* H16 e*stA*$_{Rr}$ and the excision of the selection marker did not work out. However, the fragment could not be amplified of the transconjugants 1, 17, 18 and 26 (Figure 41A) showing that these transconjugants had their selection marker excised by the flippase (Figure 41B). The other transconjugants showed to still have the antibiotic resistance integrated as a fragment of 741 bp could be amplified. *E. coli* S17-1 carrying the plasmid pK470_mobRK2_estA_frt_phaC1_1 as well as the originating *R. eutropha* H16 ΩKm*estA*$_{Rr}$ having integrated this plasmid were used as a positive control (lane 28 and 29) whereas the *R. eutropha* H16 wildtype was used as negative control (lane 27, Figure 41A). All controls showed the expected fragment sizes.

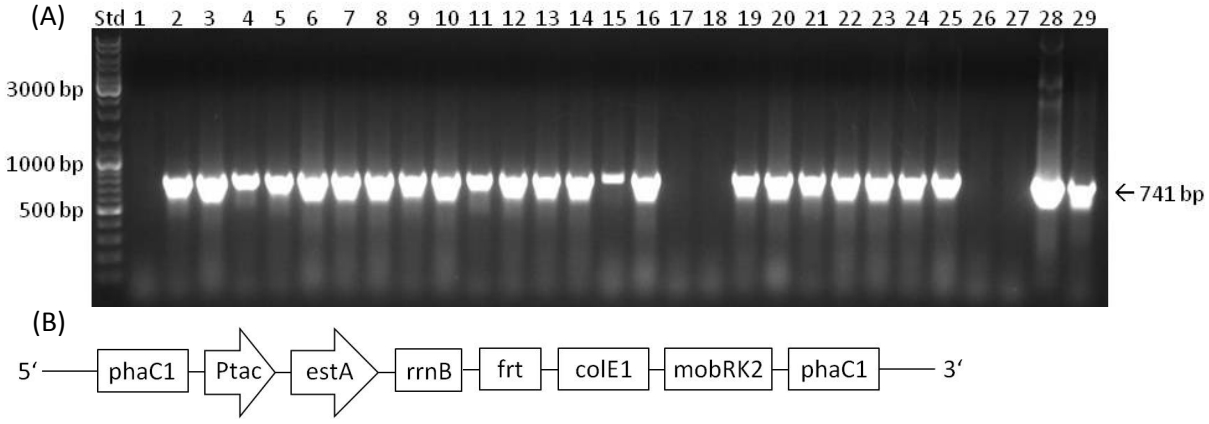

Figure 41. (A) Agarose gel of colony PCR of *R. eutropha* H16 *estA*$_{Rr}$ after kan^r excision by flippase; (B) *R. eutropha* H16 *estA*$_{Rr}$ genome sequence after kan^r excision.
Std.: Gene Ruler^{TM} DNA Ladder Mix (500 ng); (**A**) amplification of a fragment (741 bp) ranging from kan^r into the *ColE1* origin of replication of *R. eutropha* H16 *estA*$_{Rr}$ after excision of the selection marker by Flp (Int KanR Fwd, colE1 Rev), (1-26) *R. eutropha* H16 *estA*$_{Rr}$, (27) *R. eutropha* H16 wildtype (negative control), (28) *E. coli* S17-1 [pK470_mobRK2_estA_frt_phaC1_1] (positive control), (29) *R. eutropha* H16 ΩKm*estA*$_{Rr}$. (**B**) The integrated fragment is shown after the excision of kan^r by Flp-frt system.

It can be stated that the Flp-frt system is working in *R. eutropha* H16. The selection marker could be successfully excised by the flippase. Hence, the integration of different plasmids based on the same selection marker is possible on the basis of the Flp-frt system allowing the reuse of the same antibiotic resistance.

3.4. Expression of the T7 RNA polymerase in *R. eutropha* H16

3.4.1. Construction of pK470_mobRK2_T7_frtΔ_phaC1

The plasmid pK470_mobRK2_estA_frtΔ_phaC1 was used as a starting vector to construct pK470_mobRK2_T7_frtΔ_phaC1. Thereby, the plasmid was digested with *BamH*I and *Hind*III to gain the appropriate vector backbone of 5103 bp (Figure 42A). Simultaneously, the plasmid pKRtac_Par_T7pol_lacI was digested with the same restriction enzymes to gain the T7 RNA polymerase of a size of 2678 bp (Figure 42A). Then, the excised fragments were purified, the vector backbone dephosphorylated and a control gel run to determine the DNA concentration (Figure 42B).

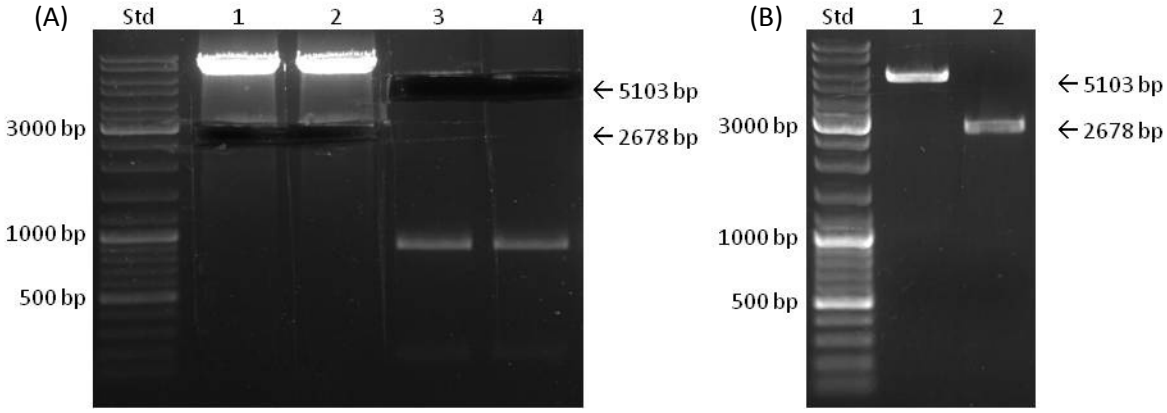

Figure 42. (A) Preparative agarose gel of restriction digest of pK470_mobRK2_estA_frtΔ_phaC1 and pKRtac_Par_T7pol_lacI with *BamH*I and *Hind*III and (B) agarose gel of the excised and purified fragments. Std.: Gene Ruler™ DNA Ladder Mix (500 ng); (**A**) (1-2) pKRtac_Par_T7pol_lacI digested with *BamH*I and *Hind*III (7511bp and 2678bp), (3-4) pK470_mobRK2_estA_frtΔ_phaC1 digested with *BamH*I and *Hind*III (5103 bp, 850 bp and 143 bp); (**B**) (1) pK470_mobRK2_frtΔ_phaC1 backbone (5103 bp), (2) T7 RNA polymerase (2678 bp).

After ligation and transformation, single colonies were streaked out for plasmid isolation. The isolated plasmids were then restriction digested with *Not*I and *Nde*I. However, none of the analyzed transformants showed to have the correct restriction pattern of 4270 bp and 3511 bp (Figure 43A). Only the transformant in lane 7 showed two DNA fragments, although, these fragments appeared to be higher than the expected size. Thus, a colony PCR was carried out to verify whether one of the transformants had incorporated the T7 RNA polymerase. No more than one transformant (transformant in lane 7) showed an amplified fragment of the T7 RNA polymerase of 759 bp due to the colony PCR results (data not shown). A further restriction digest with the restriction enzyme *Nde*I revealed that this transformant was approximately 3000 bp bigger than it should be as the linearized plasmid

pK470_mobRK2_T7_frtΔ_phaC1 after successful cloning should be comprised of 7781 bp (Figure 43B).

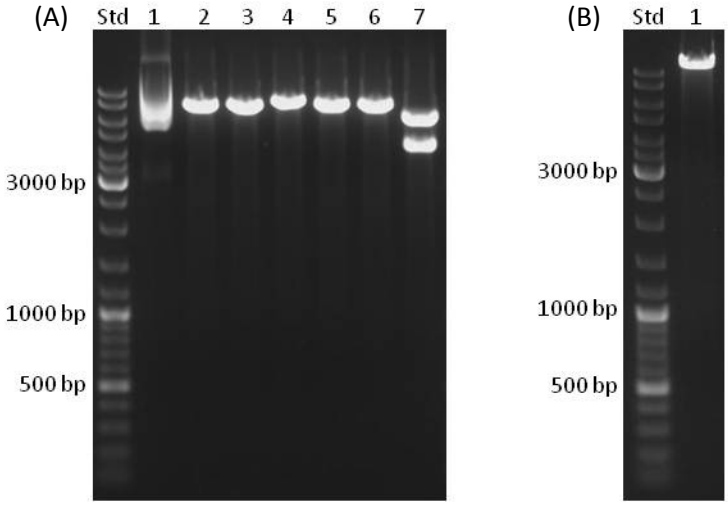

Figure 43. Agarose gel of restriction digest of pK470_mobRK2_T7_frtΔ_phaC1 with (A) *Not*I and *Nde*I and (B) *Nde*I.
Std.: Gene Ruler™ DNA Ladder Mix (500 ng); (**A**) (1) pK470_mobRK2_T7_frtΔ_phaC1 uncut, (2-7) pK470_mobRK2_T7_frtΔ_phaC1 digested with *Nde*I and *Not*I (4270 bp and 3511 bp); (**B**) pK470_mobRK2_T7_frtΔ_phaC1 digested with *Nde*I (7781 bp).

Even though the plasmid pK470_mobRK2_T7_frtΔ_phaC1 had successfully incorporated the T7 RNA polymerase, an unknown sequence of approximately 3000 bp was present on the plasmid.

Thus, the cloning of the T7 RNA polymerase into the pK470_mobRK2_frtΔ_phaC1 backbone was repeated. However, although a fragment of the T7 RNA polymerase could be amplified several times after transformation with the primer pair both seqT7pol_2 and seqT7pol_3 (759 bp) and seqT7pol_4 and seqT7pol_5 (849 bp), no restriction digest showed the expected restriction pattern. An example of such an agarose gel of the amplified T7 RNA polymerase fragment is shown in Figure 44. The positive control of the plasmid pKRtac_Par_T7pol_lacI is shown in lane 1 as well as 11 selected transformants after cloning the T7 RNA polymerase into the vector backbone. A fragment of 849 bp could be amplified in seven out of eleven clones indicating successful cloning (Figure 44).

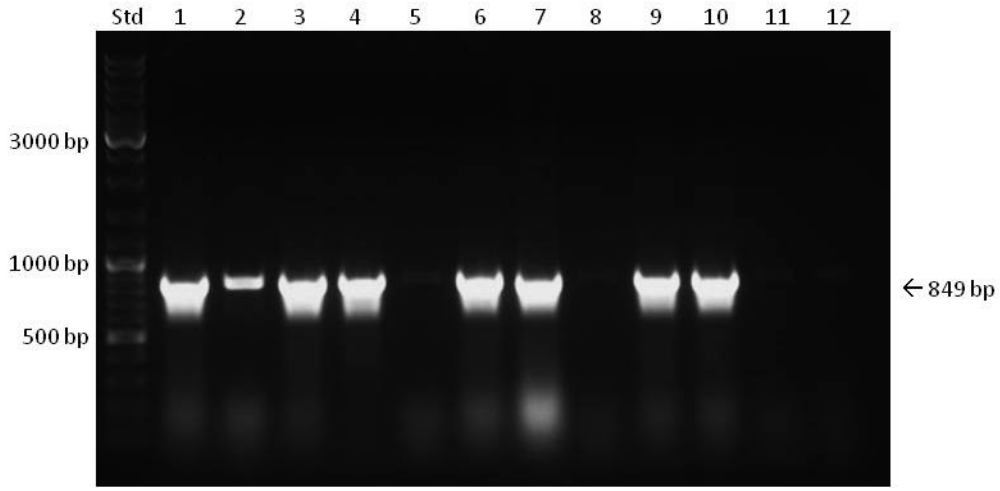

Figure 44. Agarose gel of colony PCR of a fragment of the T7 RNA polymerase of transformants of pK470_mobRK2_T7_frtΔ_phaC1.
Std.: Gene Ruler^{TM} DNA Ladder Mix (500 ng); amplification of a fragment of the T7 RNA polymerase after the cloning of pK470_mobRK2_T7_frtΔ_phaC1 (seqT7pol_4, seqT7pol_5; 849 bp); (1) pKRtac_Par_T7poly_lacI (positive control), (2-12) pK470_mobRK2_T7_frtΔ_phaC1.

However, as mentioned earlier, no subsequent restriction digest confirmed the successful construction of pK470_mobRK2_T7_frtΔ_phaC1. The restriction digest always resulted in an unexplainable restriction pattern (data not shown).

Hence, the originating plasmids (pK470_mobRK2_estA_frtΔ_phaC1, pKRtac_Par_T7pol_lacI) were digested with the restriction enzymes *EcoR*I and *Cla*I to gain the appropriate DNA fragments. This combination of restriction enzymes was used as *Cla*I cuts in the kanamycin resistance. Thereby, only positive transformants after cloning and transformation of the T7 RNA polymerase were expected as the unsuccessful construction would result in plasmids with no resistance to kanamycin. However, the same result of unexplainable restriction patterns after a restriction digest with *Pst*I or *Nde*I and *Not*I was obtained (data not shown).

Thus, in a further approach the Gibson cloning strategy was applied to construct pK470_mobRK2_T7_frtΔ_phaC1. See therefor 2.3.7 Gibson cloning and 2.13 Construction of pK470_mobRK2_T7_frtΔ_phaC1. 37 of the obtained transformants after Gibson cloning were then again analyzed via colony PCR. A fragment of the T7 RNA polymerase of 849 bp could be amplified of only 2 out of these 37 transformants. However, the restriction digest revealed again an unexplainable restriction pattern (data not shown).

3.4.2. Integration of theT7 RNA polymerase and determination of its functionality in *R. eutropha* H16

Even though no restriction digest of the plasmid pK470_mobRK2_T7_frtΔ_phaC1 was successful, it was possible to clone at least the T7 RNA polymerase into the vector backbone. Nevertheless, the plasmid pK470_mobRK2_T7_frtΔ_phaC1 was used to try to determine the functionality of the T7 RNA polymerase in *R. eutropha* H16. Thereby, the plasmid pK470_mobRK2_T7_frtΔ_phaC1 having an additional 3000 bp incorporated between the tac promoter and the T7 RNA polymerase (Figure 43B) was used for integration. After conjugation, single colonies of *R. eutropha* H16 transconjugants were used for colony PCR. A fragment of the T7 RNA polymerase as well as a possible integration event in the 3' region of the *phaC1* gene of *R. eutropha* H16 was determined. All selected *R. eutropha* H16 ΩKm*T7pol* transconjugants showed to have integrated the plasmid as a fragment of the T7 RNA polymerase of 759 bp could be amplified (Figure 45). Moreover, eight of eleven *R. eutropha* H16 ΩKm*T7pol* transconjugants had integrated the plasmid over the second homologous region as a fragment ranging from kan^r into the downstream region of *phaC1* of 1137 bp was successfully amplified (Figure 45). *R. eutropha* H16 ΩKm*T7pol* which did not show an integration event in the 5' region were most probably integrated over the first homologous region. However, due to the fact that the plasmid used for integration had an additional ~ 3000 bp upstream of the T7 RNA polymerase, this integration event could not be verified.

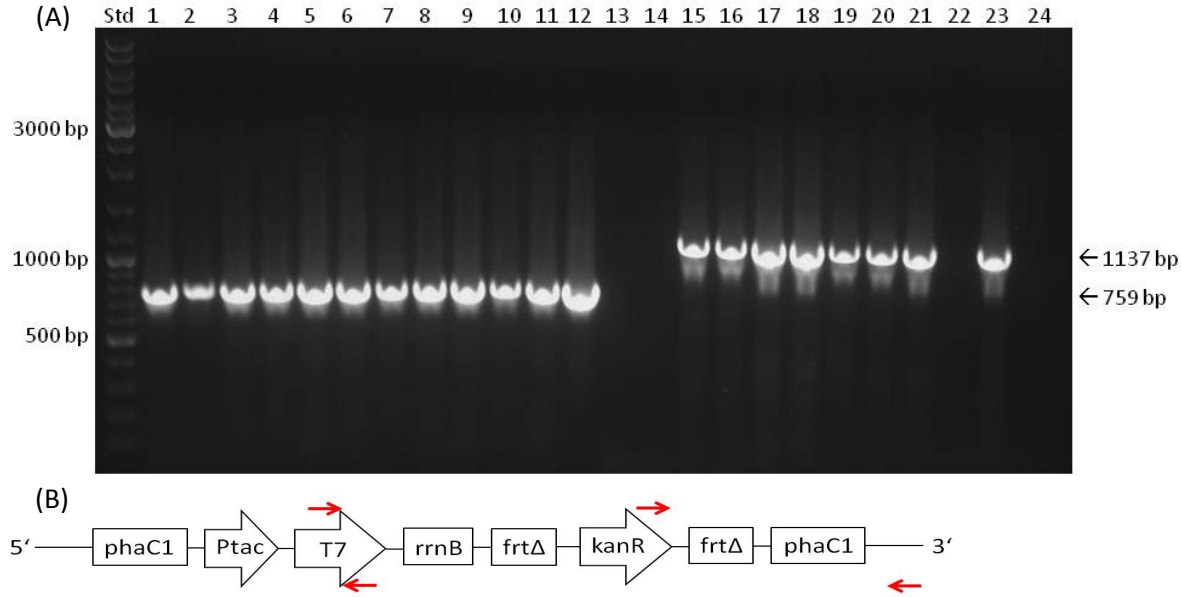

Figure 45. (A) Agarose gel of colony PCR of *R. eutropha* H16 ΩKm*T7pol* of a fragment of the T7 RNA polymerase and a 3' integration event; (B) Location of primer binding site.

Std.: Gene Ruler^{TM} DNA Ladder Mix (500 ng); (**A**) amplification of a fragment of the T7 RNA polymerase (seqT7pol_2, seqT7pol_3; 759 bp), (1-11) *R. eutropha* H16 ΩKm*T7pol*, (12) pKRtac_Par_T7poly_lacI (positive control); amplification of fragment of kan^{r} into the 3' genomic region downstream of *phaC1* (Int KanR Fwd, 3' Int phaC1 Rev; 1137 bp), (13-23) *R. eutropha* H16 ΩKm*T7pol*, (24) *R. eutropha* H16 wildtype (negative control). (**B**) The location of the primer binding site to verify an integration event downstream of *phaC1* (3' region) as well as to amplify a fragment of the T7 RNA polymerase is indicated with red arrows.

After the successful integration of pK470_mobRK2_T7_frtΔ_phaC1 into the genome of *R. eutropha* H16, the functionality of the T7 RNA polymerase had to be determined. This was done by expressing the reporter gene *egfp* under the regulation of the *T7* promoter, as only a functional T7 RNA polymerase would lead to a fluorescing signal of *R. eutropha* H16 ΩKm*T7pol*. Therefore, the plasmid pCM_PT7_RSF1010_eGFP_Pemlk_ΔlacI had to be generated. Originating from the plasmid pCM_PT7_RSF1010_eGFP_Pemlk_lacI, the *lacI* was deleted via a *Xho*I restriction digest as described in the material and method section 2.17. After the successful construction of pCM_PT7_RSF1010_eGFP_Pemlk_ΔlacI, the plasmid was transferred into *R. eutropha* H16 ΩKm*T7pol* via conjugation. A clear fluorescing signal of the growing transconjugants could be detected already on the selective media agar plate. The transconjugants appeared green confirming the functionality of the T7 RNA polymerase in *R. eutropha* H16 ΩKm*T7pol* [pCM_PT7_RSF1010_eGFP_Pemlk_ ΔlacI] Thus, the functional expression of the T7 RNA polymerase in *R. eutropha* H16 could be determined.

Moreover, the relative fluorescing units of *R. eutropha* H16 ΩKm*T7pol* [pCM_PT7_RSF1010_eGFP_Pemlk_ΔlacI] were determined; see therefor material and method section 2.9. The measurement was performed in triplicate and *R. eutropha* H16 ΩKm*T7pol* [pCM_PT7_RSF1010_eGFP_Pemlk_ΔlacI] with P_{T7} compared to *R. eutropha* H16 [pKRSF1010_Ptac_eGFP] having the reporter gene under the regulation of P_{tac}. *R. eutropha* H16 ΩKm*T7pol* [pCM_PT7_RSF1010_eGFP_Pemlk_ΔlacI] grew to an OD_{600} of 2.4 whereas *R. eutropha* H16 [pKRSF1010_Ptac_eGFP] reached an OD_{600} of 3.2. The differences in the cell density already indicated that the T7 system causes more stress to the cell leading to slower cell growth. Following, the measurement was conducted and the RFU of 10836 (*R. eutropha* H16 ΩKm*T7pol* [pCM_PT7_RSF1010_eGFP_Pemlk_ΔlacI]) and 5028 (*R. eutropha* H16 [pKRSF1010_Ptac_eGFP]) were calculated (Figure 46). The fluorescing signal of *R. eutropha* H16 ΩKm*T7pol* [pCM_PT7_RSF1010_eGFP_Pemlk_ΔlacI] was approximately twice as strong (10836 RFU) as of the one with the tac promoter (5028 RFU). However, these results have to be considered with caution as the integrated T7 RNA polymerase had an unknown sequence

of approximately 3000 bp between the promoter and the T7 RNA polymerase sequence. Thus, this sequence may have had an influence concerning the expression of the T7 RNA polymerase respectively.

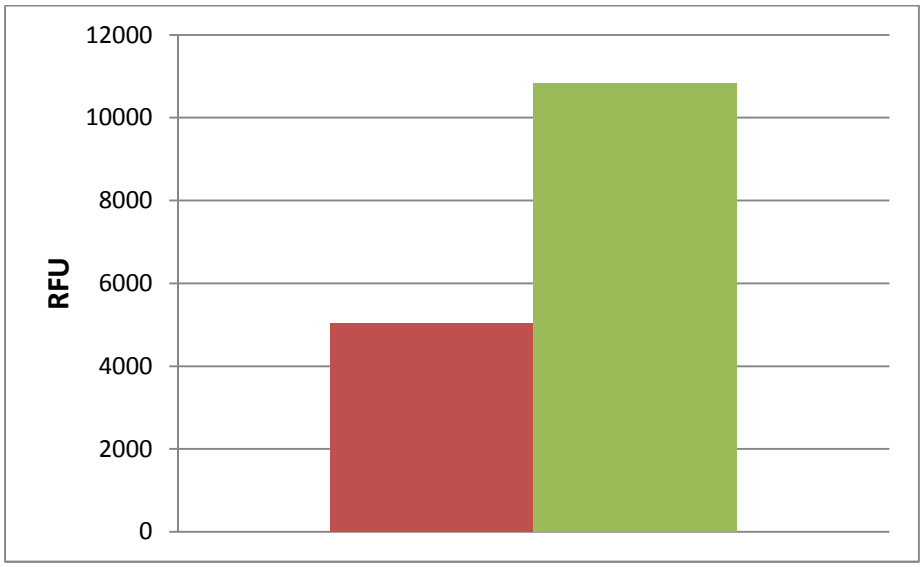

Figure 46. Relative fluorescing unit measurement of *R. eutropha* H16 [pKRSF1010_Ptac_eGFP] (red) and *R. eutropha* H16 ΩKm*T7pol* [pCM_PT7_RSF1010_eGFP_Pemlk_ΔlacI] (green). The difference of the eGFP expression under the regulation of P_{tac} and P_{T7} could be emphasized with the relative fluorescing unit measurement.

3.5. Construction of an inducible expression system for genomic integration in *R. eutropha* H16 based on the lactose permease

3.5.1. Construction of pK470_mobRK2_PCIV1bM_lacY_frtΔ_phaC1

The plasmid pK470_mobRK2_estA_frtΔ_phaC1 was used as a starting vector to construct pK470_mobRK2_PCIV1bM_lacY_frtΔ_phaC1. First, the fragment of the weak constitutive promoter CIV1bM and the *lacY* gene was amplified to introduce a *Sph*I and *Hind*III restriction site and cloned into the pJET1.2 cloning vector as described in the material and method section 2.14. After the correct sequence was confirmed the plasmids pJET_PCIV1bM_lacY and pK470_mobRK2_estA_frtΔ_phaC1 were digested at the *Sph*I and *Hind*III restriction sites. Following, the appropriate bands were excised of the preparative agarose gel, the fragments were purified and a control gel was performed to determine the accurate size and DNA concentration. The pK470_mobRK2_frtΔ_phaC1 backbone had a size of 4825 bp and the insert PCIV1bM_lacY of 1365 bp (Figure 47A). After ligation and transformation, single colonies of the transformants were streaked out for plasmid isolation. Then, the isolated plasmids were digested with the restriction enzymes *Not*I and *Nde*I. The restriction pattern of 4369 bp and 1821 bp confirmed the successful construction of pK470_mobRK2_PCIV1bM_lacY_frtΔ_phaC1 (Figure 47B).

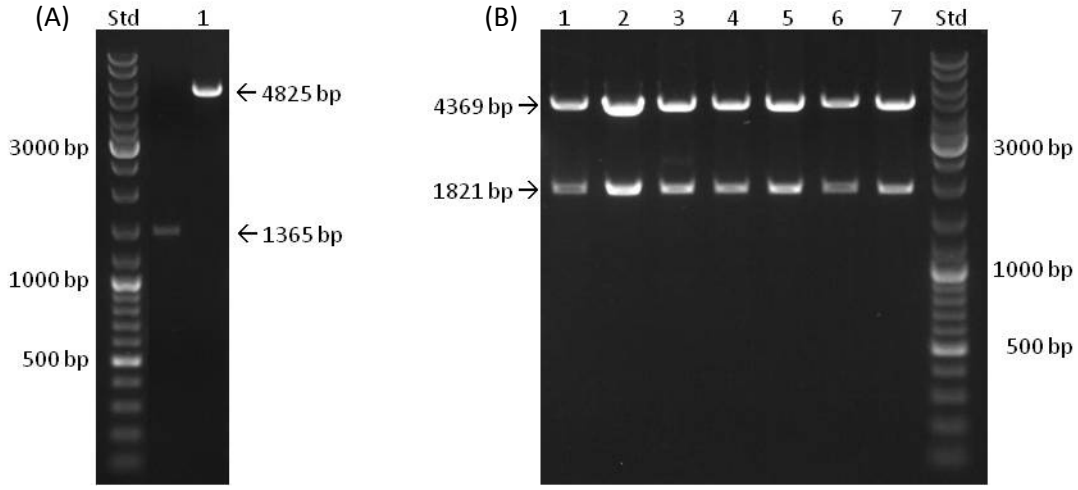

Figure 47. Agarose gel of (A) purified PCIV1bM_lacY and pK470_mobRK2_frtΔ_phaC1 fragments digested with *Sph*I and *Hind*III and (B) pK470_mobRK2_PCIV1bM_lacY_frtΔ_phaC1 restriction digest with *Nde*I and *Not*I.
Std.: Gene Ruler™ DNA Ladder Mix (500 ng); (**A**) (1) purified PCIV1bM_lacY fragment after *Sph*I and *Hind*III digest (1365 bp), (2) purified pK470_mobRK2_frtΔ_phaC1 backbone after *Sph*I and *Hind*III digest (4825 bp); (**B**) (1-7) pK470_mobRK2_PCIV1bM_lacY_frtΔ_phaC1 digested with *Nde*I and *Not*I (4369 bp and 1821 bp).

3.5.2. Integration of the lactose permease and determination of its functionality in *R. eutropha* H16

Following the successful construction of pK470_mobRK2_PCIV1bM_lacY_frtΔ_phaC1, the plasmid was transformed into *E. coli* S17-1 prior conjugation. After conjugation was carried out, single colonies of *R. eutropha* H16 Δ*phaC*ΩKm*lacY* were used to perform a colony PCR to determine a possible recombination event. Three out of twenty *R. eutropha* H16 Δ*phaC*ΩKm*lacY* transconjugants showed to have integrated the lactose permease via both homologous regions (data not shown). Thus, it can be assumed that every seventh *R. eutropha* H16 transconjugant will have integrated the fragment of the plasmid flanked by the homologous regions into the genome via gene replacement by knocking out the particular gene used as homologous region.

Two of these *R. eutropha* H16 Δ*phaC*ΩKm*lacY* clones were used to perform a further colony PCR to show again the integration upstream and downstream of the *phaC1* gene as well as to amplify the fragment of the genome after gene replacement in comparison to the *R. eutropha* H16 wildtype (Figure 48A). Afterwards an agarose gel was run showing a distinct band for an integration event in the upstream (1062 bp) and downstream (1137 bp) region of the *phaC1* gene. The performed PCRs on the *R. eutropha* H16 wildtype did not show any amplified fragment as expected. Moreover, the sequence difference of *R. eutropha* H16 Δ*phaC*ΩKm*lacY* after the integration event and the *R. eutropha* H16 wildtype could be clearly shown. A fragment of 1961 bp only comprised of the *phaC1* gene was amplified of the *R. eutropha* H16 wildtype whereas after the recombination event a fragment of 4853 bp could be amplified (Figure 48A). This PCR was only conducted with the outer primers shown in Figure 48B. Even though only a weak signal of *R. eutropha* H16 Δ*phaC*ΩKm*lacY* could be obtained after the PCR, the difference of the amplified fragment to the one of the *R. eutropha* H16 wildtype was demonstrated. The weak signal could be explained most likely due to the fact that long fragments to be amplified always come along with difficulties using the DreamTaq polymerase.

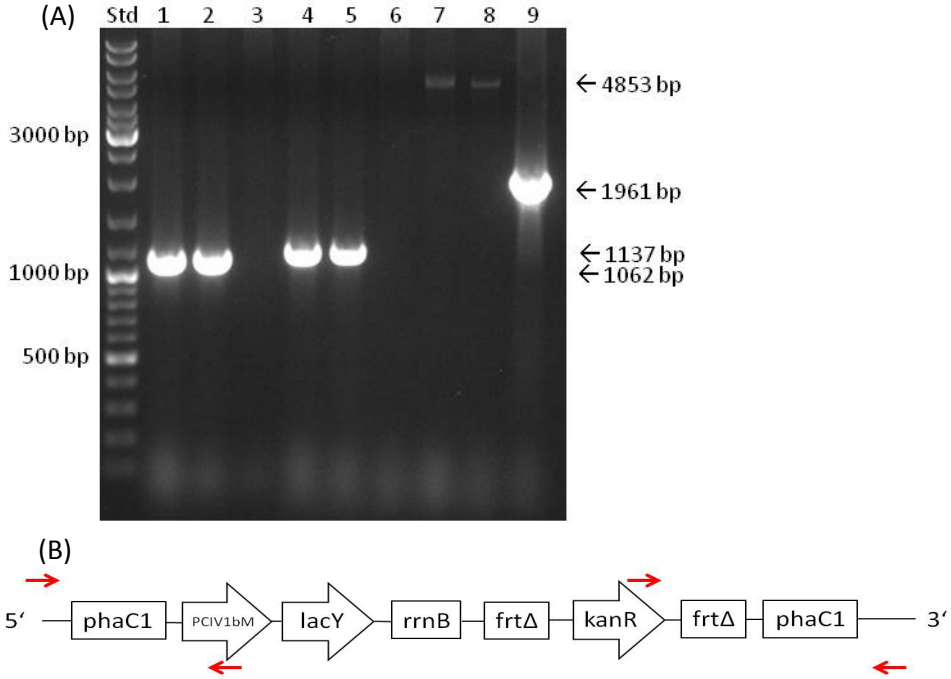

Figure 48. (A) Agarose gel of the colony PCR to verify integration of the lactose permease into the genome of *R. eutropha* H16; (B) Location of primer binding site.
Std.: Gene Ruler^{TM} DNA Ladder Mix (500 ng); (**A**) amplified fragment of the 5' genomic region upstream of *phaC1* into the promoter CIV1bM (5' Int phaC1 Fwd, PCIV1bMrev; 1062 bp), (1-2) *R. eutropha* H16 Δ*phaC*ΩKm*lacY*, (3) *R. eutropha* H16 wildtype; amplified fragment of kan^{r} into the 3' genomic region downstream of *phaC1* (Int KanR Fwd, 3' Int phaC1 Rev; 1137 bp), (4-5) *R. eutropha* H16 Δ*phaC*ΩKm*lacY*, (6) *R. eutropha* H16 wildtype; amplified fragment ranging from the genomic region upstream of *phaC1* into the region downstream of *phaC1* (5' Int phaC1 Fwd, 3' Int phaC1 Rev), (7-8) *R. eutropha* H16 Δ*phaC*ΩKm*lacY* (4853 bp), (9) *R. eutropha* H16 wildtype (1961 bp).
(**B**) Location of primer binding site to verify an integration event up- and downstream of *phaC1* as well as to amplify the whole integrated fragment is indicated with red arrows.

After the successful integration of the lactose permease into the genome of *R. eutropha* H16, its expression and functionality had to be determined. Therefore, the plasmid pCM_Ptac_Par_eGFP_RSF1010_lacI was constructed as described in the material and method section 2.16. After the cloning of the *RSF1010* origin and the *lacI* gene, the plasmid pCM_Ptac_Par_eGFP_RSF1010_lacI was digested with the restriction enzyme *Spe*I. The successful plasmid construction was confirmed as a restriction pattern of 10575 bp and 1504 bp was shown (Figure 49). Again, the band of ~3500 bp was due to the *RSF1010* origin in particular its conformational behaviour and could be considered as uncut plasmid.

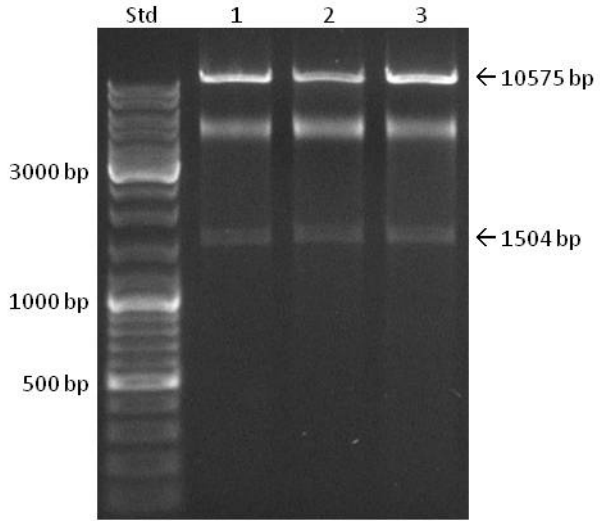

Figure 49. Agarose gel of restriction digest of pCM_Ptac_Par_eGFP_RSF1010_lacI with *Spe*I.
Std.: Gene Ruler^{TM} DNA Ladder Mix (500 ng); (1-3) pCM_Ptac_Par_eGFP_RSF1010_lacI digested with *Spe*I (10575 bp and 1504 bp).

In the following, the plasmid was transformed into *E. coli* S17-1 and transferred into *R. eutropha* H16 Δ*phaC*ΩKm*lacY* via conjugation to determine the functionality of *lacY*. However, no *R. eutropha* H16 Δ*phaC*ΩKm*lacY* [pCM_Ptac_Par_eGFP_RSF1010_lacI] transconjugants were obtained after conjugation. Thus, the plasmid pCM_Ptac_Par_eGFP_RSF1010_lacI was sent for sequencing to determine the correct sequence of the origin of replication *RSF1010*. The sequencing result revealed a mutation in the replication gene *repA*. This mutation did not affect the replication behaviour in *E. coli*, however the plasmid could not replicate in *R. eutropha* H16 resulting in no growth of *R. eutropha* H16 Δ*phaC*ΩKm*lacY* [pCM_Ptac_Par_eGFP_RSF1010_lacI]. Thus, the expression and functionality of *lacY* could not be determined using this plasmid due to time reasons. In further steps the origin of replication should be replaced by one without any mutation to be able to determine the functionality of the lactose permease in *R. eutropha* H16.

4. Discussion

The Gram-negative facultative lithoautotrophic soil bacterium *Ralstonia eutropha* H16 has attracted significant interest in recent years towards biotechnological applications. Several different publications show the expression of heterologous genes based on complex inducible systems in *R. eutropha* H16 either with the *E. coli* promoter P_{BAD} inducible with L-arabinose [79] or with the promoters P_{phaP} or P_{phaC} derived from *R. eutropha* H16 itself [16], [77]. The successful heterologous gene expression under the control of P_{lac} or P_{tac} was demonstrated as well, even though only under constitutive conditions as an active transport system for the inducer lactose and IPTG respectively is missing in *R. eutropha* H16 [21], [77]. Hence, a simple and tightly regulated inducible expression system for *R. eutropha* H16 was yet required. Thus, the main focus of this work was to construct and establish a system for the integration into the genome of *R. eutropha* H16 and in the following to thereby provide the basis for inducible expression systems by integrating the T7 RNA polymerase and the lactose permease respectively as well as to establish the Flp-frt system to enable selection marker recycling in *R. eutropha* H16.

Construction of the different integration vectors for *R. eutropha* H16 and the following homologous integration based on one homologous region

At the beginning the plasmid pK470_mob_ca1_estA (Figure 15) consisting of the *ColE1* origin of replication, kanamycin resistance, the mobilization region of the pBBR1-MCS5 plasmid, the carbonic anhydrase 1 (*ca1*) as homologous region and *estA* as reporter gene was tried to be integrated into the genome of *R. eutropha* H16. The *ColE1* origin of replication was used in all suicide vectors as this origin was not able to replicate in *R. eutropha* H16 (unpublished data). Although, cell growth of *R. eutropha* H16 transconjugants was visible after 4-5 days, none of the analyzed transconjugants showed to have integrated the plasmid according to the colony PCR results (Figure 16). These results were unexpected as the *R. eutropha* H16 cells were able to grow on TSB media containing 0.2 % fructose, kanamycin [200 µg/mL] and gentamycin [20 µg/mL] even though the strain did not confer any kanamycin resistance (Figure 17). The growth of the donor strain *E. coli* S17-1 [pK470_mob_ca1_estA] could be suppressed by gentamycin which does not affect *R. eutropha* H16 due to a natural resistance against this antibiotic [76]. The phenomenon of the growth of *R. eutropha* H16 on TSB media

conferring kanamycin resistance was already observed on the control plate (*R. eutropha* H16 empty strain). It was assumed that the sudden resistance to kanamycin could be a response of the bacterium to the exposed stress. This stress can be argued by the occurrence of shear forces while pipetting, an adaptation of the bacterium to the antibiotic due to an exposure for a longer period of time (several days) or by the conjugation event itself reasoned by the forced plasmid transfer and uptake. The argument of the adaptation of *R. eutropha* H16 is probably the most reasonable one as it was already published that this bacterium is very versatile and showed various metabolic adaptations [104]. Thus, it could be possible that some *R. eutropha* H16 cells were able to adapt to the environmental impact, in this case the antibiotic kanamycin, leading for example to a more robust cell wall not being able to be passed by the antibiotic or at least not the same amount.

In order to overcome the problem of the false-positive *R. eutropha* H16 transconjugants on the selective media, the plasmid pCM_mob_ca1 was constructed, consisting of the chloramphenicol resistance instead of the kanamycin resistance gene. Chloramphenicol itself is smaller than kanamycin; hence, the probability of chloramphenicol to pass the cell wall of *R. eutropha* H16 should be increased. After the successful cloning of cm^r into the plasmid backbone of pK470_mob_ca1 to generate pCM_mob_ca1, the plasmid was transferred into *R. eutropha* H16 via conjugation. A clear decrease in *R. eutropha* H16 transconjugants on the selective media supplemented with 0.2 % fructose, gentamycin [20 µg/mL] and chloramphenicol [100 µg/mL] could be observed after 5-6 days of growth. However, almost the same amount of *R. eutropha* H16 wildtype cells was able to grow on the selective media (control plate). The following colony PCR on several selected transconjugants revealed that none of the *R. eutropha* H16 transconjugants integrated the plasmid pCM_mob_ca1 into the genome. Possible reasons are again the adaptation behaviour of *R. eutropha* H16 or an antibiotic concentration which was already too little to inhibit growth due to the low stability of chloramphenicol after several days at 28 °C [100].

Hence, no recombination event could be accomplished the plasmid pCM_mob_ca1 was further modified. In the following, the previous homologous region *ca1* of 672 bp was replaced by the reductase A9 (*redA9*) and a part of the reductase B2 (*redB2*). These two fragments were selected because the size of 1061 bp (*redA9*) and of 458 bp (*redB2*) was

considered to be optimal to verify whether the length of the homologous sequence is essential for a recombination event. Moreover, the choice of using these homologous sequences was supported by different publications. Voss and Steinbüchel [20] already demonstrated an successful integration event by using an homologous region of ~500 bp in *R. eutropha* H16 whereas Simpson et al. [62] reported that with increasing length of the homologous sequence the frequency of an integration event increases.

In addition, the mobilization region of the pBBR1-MCS5 plasmid in pCM_mob_ca1 was replaced by the mobilization region of the RK2 plasmid (*mobRK2*) and the RSF1010 plasmid (*mobRSF1010*). Taking into account the number of grown transconjugants after conjugation on selective media a low mobilization efficiency of 20 to 30 transconjugants could be determined. Especially by comparing these numbers to the obtained colonies on the *R. eutropha* H16 control plates which were quite similar. R. Meyer [99] compared two different mobilization regions of the pSC101 and R1162 plasmid and thereby highlighting big differences in the mobilization efficiency of the examined regions. Moreover, he introduced different mutations in the *mob* regions to further determine the importance of the genes of which the *mob* region is comprised (*mobA*, *mobB* and *mobC*) and could verify a dramatic decline of the mobilization frequency when harbouring any mutation [99]. Thus, the usage of another mobilization sequence could boost the obtained number of transconjugants and in that way increase the probability of an integration event to happen. Voss and Steinbüchel [20], Srinivasan et al. [16], [17] and Barnard et al. [18] already published different integration strategies in *R. eutropha* H16 thereby using the mobilization region of the RK2 plasmid to enable the conjugational plasmid transfer. Moreover, Meyer [99] used the mobilization region of the RSF1010 plasmid (virtually the same as R1162 plasmid) and could demonstrate a good mobilization efficiency. Thus, the use of these mobilization regions (*mobRK2* and *mobRSF1010*) most probably would enhance the mobilization efficiency.

After several cloning steps, the homologous region and the mobilization region of pCM_mob_ca1 were replaced and the plasmids pCM_mobRK2_redA9 and pCM_mobRK2_redB2 as well as pCM_mobRSF1010_redA9 and pCM_mobRSF1010_redB2 successfully constructed. In the following, only the plasmids harbouring the mobilization sequence of the RK2 plasmid (pCM_mobRK2_redA9/redB2) were used for the conjugational plasmid transfer to *R. eutropha* H16 due to the best results concerning the mobilization

efficiency (discussed below). Again, the *R. eutropha* H16 transconjugants had to be incubated on the selection plates for 4-5 days until cell growth was visible. This incubation time of several days until the first cells were visible on the plate was assumed to be too long for a transconjugant harbouring the appropriate antibiotic resistance gene and thus, only promotes the growth of false-positive clones. Nevertheless, several *R. eutropha* H16 transconjugants were selected and used as template for the colony PCR. The colony PCR was performed on a possible integration event (Figure 23) as well as the chloramphenicol gene was tried to be amplified (Figure 24). However, none of the selected *R. eutropha* H16 transconjugants showed to have integrated one of the transferred plasmids. Hence, no difference in the integration frequency concerning the length of the homologous region could be observed. These results were surprising, as a mobilization region with a higher mobilization efficiency than the one of the mobilization sequence of the pBBR1-MCS5 plasmid was used for this approach. We supposed that *R. eutropha* H16 transconjugants which grew after 4-5 days can be considered as false-positive ones and that transconjugants which successfully integrated the plasmid should be able to grow within 1-2 days.

Even though the requirements for a successful recombination event should have been given by this approach no integration event could be verified. This was most likely due to the fact that a recombination event involving only one homologous region is not as frequent as a single-crossover event of a plasmid carrying two homologous regions flanking the gene to be integrated. Thus, far more of the cell suspension resuspended from the NB agar after conjugation would have had to be plated on the selective agar to gain an appropriate *R. eutropha* H16 transconjugant having integrated the plasmid. Several different publications demonstrated the usage of two homologous regions flanking the gene to be integrated [16], [17], [20]. Thereby, not only the fragment to be integrated can be reduced to the gene of interest and not the whole transferred plasmid but also gene knock-outs can be achieved instead of only homologous integrations. Thus, a new approach was developed using a plasmid with two homologous regions to finally promote a homologous recombination event (discussed later).

Mobilization efficiency of the mobilization sequences of pBBR1-MCS5, RK2 and RSF1010

Subsequently, the mobilization regions of the broad-host range plasmids pBBR1-MCS5, RK2 and RSF1010 were cloned into the plasmid pKR_Ptac_Par_eGFP_pSa constructing pKR_Ptac_Par_eGFP_mobRK2_pSa, pKR_Ptac_Par_eGFP_mobRSF1010_pSa and pKR_Ptac_Par_eGFP_mob_pSa to be able to determine the according mobilization efficiency. The mobilization efficiency is defined as the ability of the mobilization region to enable the conjugative plasmid transfer from *E. coli* S17-1 to *R. eutropha* H16. A significant increase in the mobilization efficiency by the mobilization sequences of the RK2 and the RSF1010 plasmid could be demonstrated. The mobilization region of the RK2 plasmid showed to have the best mobilization efficiency based on the obtained results (Table 21). The mobilization efficiency of *mobRK2* was approximately 50.000 times and the one of *mobRSF1010* at least 5.000 times better than the one of the mobilization sequence of the plasmid pBBR1-MCS5 (published in [101]). The excellent mobilization efficiency of the mobilization sequence of the RK2 plasmid compared to the one of the RSF1010 can be argued by the fact that the *tra* genes integrated into the genome of *E. coli* S17-1 are as well of the RK2 plasmid. Hence, the interplay of these regions for the successful mobilization of the plasmid is obviously better than the one of more distantly related regions as the mobilization sequence of the RSF1010 plasmid. However, the plasmid RSF1010 is not self-transmissible and thus has to rely on trans-acting components of other plasmids like the *tra* genes of the RK2 plasmid [34]. In addition, a really low mobilization efficiency can be due to a weak interaction of the *oriT* binding proteins (*mobA-C*) with the origin of transfer. Even closely related plasmids like RK2 (IncPα) and R751 (IncPβ) encode for enzymes not being able to nick within the origin of transfer of the other plasmid according to Thomas and Smith [40]. Thus, the poor mobilization efficiency of the mobilization sequence of the plasmid pBBR1-MCS5 could be due to a weak recognition, binding and nicking of the *oriT* by the encoded proteins. Due to the obtained results of the comparison of the mobilization efficiency of the different mobilization sequences, the mobilization region of the RK2 plasmid was used for all further conjugative plasmid transfers as mentioned earlier.

Integration of the reporter gene *estA* and the establishment of the Flp-frt system in *R. eutropha* H16

In the following, based on the obtained results for integration and mobilization, an integration vector consisting of two homologous regions flanking the reporter gene *estA* and the kanamycin resistance gene was constructed. The vector pK470_mob_ca1 was chosen as starting vector and the homologous region *phaC1*, as well as the reporter gene *estA* and the mobilization region of the RK2 plasmid successfully cloned into the vector backbone. The *phaC1* gene encoding for the PHB synthase was chosen as locus for homologous recombination. The PHB synthase is the essential enzyme in PHB production in *R. eutropha* H16. The establishment of a heterologous gene expression system in *R. eutropha* H16 does not require PHB production, which would even be a disadvantage. Thus, *phaC1* will be knocked out after a successful recombination event over both homologous regions (gene replacement) and thereby bringing the benefit that no nutrient flux will go into PHB production limiting the nutrients for the expression of the integrated heterologous gene.
Moreover, the frt sites flanking the kanamycin resistance were introduced in the plasmid via PCR. However, sequencing of the frt sites revealed that 5 bp were missing in the frt site upstream and 2 bp in the frt site downstream of kan^r. These missing base pairs were in both cases in the core region of the frt site leading to the deletion of the *Xba*I restriction site. Such deletions in the core region of two or more base pairs of the frt site would have severe effects on the binding ability of the flippase which would not be able to recognize and cleave the corresponding sequence anymore [65]. However, although the frt sites were incomplete the plasmid was still used for conjugation as all necessary fragments for a successful plasmid mobilization from *E. coli* S17-1 to *R. eutropha* H16 and the subsequent homologous recombination event were present on the plasmid. After the plasmid pK470_mobRK2_estA_frtΔ_phaC1 was transformed into *E. coli* S17-1 it was conjugationally transferred into *R. eutropha* H16. The *R. eutropha* H16 transconjugants already grew after 2 days of incubation at 28 °C indicating a successful homologous recombination event. The subsequent colony PCR confirmed that the *R. eutropha* H16 transconjugants successfully integrated a part of pK470_mobRK2_estA_frtΔ_phaC1. A recombination event over both homologous regions in the three examined *R. eutropha* H16 Δ*phaC*ΩKm$estA_{Rr}$ colonies could be determined leading to the integration of the reporter gene *estA* and the kanamycin

resistance (Figure 30). Thus, the problem of false-positive *R. eutropha* H16 transconjugants could be overcome by a shortened incubation time on the selective media. As assumed earlier, *R. eutropha* H16 transconjugants conferring the antibiotic resistance were able to grow within two days allowing the statement, that all *R. eutropha* H16 transconjugants which need 4-5 days to grow are false-positive ones. However, as we were now able to integrate into the genome of *R. eutropha* H16, we did not look further into the mechanisms enabling *R. eutropha* H16 to grow on TSB media supplemented among others with kanamycin [200 µg/mL] after 4-5 days.

In the following, an esterase filter activity assay was carried out to demonstrate the expression and correct folding of EstA in *R. eutropha* H16 Δ*phaC*ΩKm*estA*$_{Rr}$. The esterase was nicely expressed and showed a high activity on the model substrate α-naphthyl acetate even though only one copy of the gene was integrated into the genome of *R. eutropha* H16 Δ*phaC*ΩKm*estA*$_{Rr}$ (Figure 31). Subsequently, a SDS-PAGE was prepared to demonstrate the accurate size of the protein band of EstA on the gel. Prior the Coomassie Blue staining, an activity stain was carried out to show off once more the catalytic activity of EstA. The results of the esterase filter activity assay could be confirmed by the activity stain as the substrate α-naphthyl acetate could be successfully hydrolyzed again. The according protein band of EstA of 37 kDa correlated with the one of *E. coli* S17-1 [pK470_mobRK2_estA_frtΔ_phaC1] (positive control; Figure 32). The signal of *R. eutropha* H16 Δ*phaC*ΩKm*estA*$_{Rr}$ among each other was similar whereas the one of the positive control was considerably stronger. This was not surprising as several copies of *estA* were present in *E. coli* S17-1 whereupon only one copy was integrated into the genome of *R. eutropha* H16. Moreover, the signal of *R. eutropha* H16 Δ*phaC*ΩKm*estA*$_{Rr}$ was quite considerable and clearly visible for one copy of *estA*. If a higher expression of the integrated gene would be desirable, multiple-copy gene integrations could be carried out to raise the copy-number of the integrated heterologous gene. This was already shown by Srinivasan et al. [17] who integrated one, two and three copies of the organophosphohydrolase (OPH) into the genome of *R. eutropha* H16. Thereby, a linear increase in active OPH related to the gene copy-number could be demonstrated [17].

After the activity stain, the gel was stained with Coomassie Brilliant Blue. The various protein bands which were separated during SDS-PAGE were stained. Thereby, a clear difference

between the protein pattern of *E. coli* S17-1 and *R. eutropha* H16 was visible (Figure 33). Furthermore, the protein band of EstA of 37 kDa was only present in the positive control as well as *R. eutropha* H16 Δ*phaC*ΩKm*estA*$_{Rr}$ and not in its wildtype as expected.

In addition, the phenotype of *R. eutropha* H16 Δ*phaC*ΩKm*estA*$_{Rr}$ was compared with the one of the wildtype. *R. eutropha* H16 accumulates large amounts of PHB under unbalanced growth conditions [103]. However, *R. eutropha* H16 Δ*phaC*ΩKm*estA*$_{Rr}$ should not be able to produce PHB anymore as the essential gene for PHB production (PHB synthase) was knocked out due to the integration event. This could be confirmed during growth on NB media supplemented with 5 g/L fructose by showing off the difference of the phenotype of *R. eutropha* H16 wildtype in contrast to the *R. eutropha* H16 strain with the *phaC1* knockout. *R. eutropha* H16 Δ*phaC*ΩKm*estA*$_{Rr}$ appeared to be more transparent than the wildtype strain due to the knockout of the PHB synthase (Figure 34). This was already reported by Schwab [105].

The integration strategy based on two homologous regions was successful. Thus, in the following, the incomplete frt sites of the plasmid pK470_mobRK2_estA_frtΔ_phaC1 were repaired to be able to establish the Flp-frt system in *R. eutropha* H16. Thereby, the incomplete frt sites could be successfully replaced by frt sites consisting of the complete 34 bp flanking kan^r and the plasmid pK470_mobRK2_estA_frt_phaC1 constructed. However, due to problems cloning the second homologous region (*phaC1_2*) into the backbone, the plasmid pK470_mobRK2_estA_frt_phaC1_1 consisting of only one homologous region was used for the integration and the subsequent marker excision. The successful integration of the plasmid pK470_mobRK2_estA_frt_phaC1_1 was again verified via colony PCR (Figure 40). The whole plasmid backbone was integrated into the genome of *R. eutropha* H16 as only one homologous region was present on the plasmid. Only two *R. eutropha* H16 transconjugants could be selected from six agar plates on which the cell suspension was plated after conjugation to select for a homologous recombination event whereas these two transconjugants showed to have integrated the plasmid. By comparing this yield of a homologous recombination event with the one using a plasmid based on two homologous regions (40-70 *R. eutropha* H16 transconjugants per plate), the big difference of the probability of a recombination event to happen concerning the homologous region could be demonstrated. Following the successful integration of the plasmid having kan^r flanked by the

frt sites, the plasmid pCM_mobRK2_flp was conjugationally transferred to *R. eutropha* H16 ΩKm*estA*$_{Rr}$. This plasmid encoded for the flippase under the regulation of the strong promoter P_{tac}. Moreover, the origin of replication *ColE1* not able to replicate in *R. eutropha* H16 was encoded on this plasmid. Thus, the flippase was only expressed for a short period of time. However, this short expression should suffice for the marker excision of the genome of *R. eutropha* H16 ΩKm*estA*$_{Rr}$. The successful excision of kan^r was confirmed via colony PCR (Figure 41). 26 *R. eutropha* H16 transconjugants were not able to grow on TSB media supplemented with 0.2 % fructose, gentamycin [20 µg/mL] and kanamycin [200 µg/mL] indicating the successful excision of kan^r. However, only 4 out of these 26 examined *R. eutropha* H16 *estA*$_{Rr}$ did not confer the kanamycin resistance anymore due to the colony PCR results. This can may be argued by the recombination event itself whereupon the site-specific recombinase Flp could not successfully excise the selection marker but somehow led to an inactivation of the kanamycin resistance gene. Nevertheless, it could be demonstrated that the Flp-frt system is functional in *R. eutropha* H16 as kan^r could be successfully excised of the genome of *R. eutropha* H16 ΩKm*estA*$_{Rr}$. This site-specific recombination system was already demonstrated to be functional in a variety of prokaryotes and eukaryotes but never before in *R. eutropha* H16 [67]–[71]. However, the frequency of the marker excision was quite low according to the results, especially when compared to the data of Hoang et al. [68] who proposed a high frequency of up to 100 % of the Flp-frt system in *Pseudomonas aeruginosa*. This low frequency was maybe due to the fact that a plasmid which was not stable in *R. eutropha* H16 was used to express the flippase resulting in little enzyme being able to excise the selection marker. In comparison, Hoang et al. [68] expressed the flippase on a plasmid which could be maintained in *P. aeruginosa* until cured by counter selection on sucrose. Hence, the flippase should be expressed on a plasmid able to replicate in *R. eutropha* H16 to determine its frequency of the marker excision. Another strategy to enhance the selection marker recycling system could be to express the flippase under the control of a stronger promoter such as P_{T5} *to* increase the concentration of the recombinase in the cell. Nevertheless, the application of the Flp-frt system in *R. eutropha* H16 enables the successful selection marker recycling.

Integration of the bacteriophage T7 RNA polymerase in *R. eutropha* H16

By the successful integration of the reporter gene *estA* into the *R. eutropha* H16 genome, the used integration strategy, conducted with the newly created vector pK470_mobR2_estA_frt_phaC1 was proven to be successful. In the following the bacteriophage T7 RNA polymerase was cloned into the vector backbone to create pK470_mobRK2_T7_frtΔ_phaC1. This plasmid still consisted of the incomplete frt sites; however, this does not affect the integration behaviour. The cloning of the T7 RNA polymerase came along with big difficulties. Different restriction enzyme combinations were used to clone the T7 RNA polymerase into the vector backbone as well as the Gibson cloning approach. Although, several of the obtained transformants had incorporated the T7 RNA polymerase due to the colony PCR results (Figure 44), no expected plasmid restriction pattern was obtained. Nevertheless, one plasmid which had incorporated an additional 3000 bp upstream of the T7 RNA polymerase was chosen to be transferred into *R. eutropha* H16. This plasmid was chosen as it showed to have the *Nde*I restriction site only present in the T7 RNA polymerase and a fragment of the T7 RNA polymerase could be amplified via colony PCR. Following the construction of pK470_mobRK2_T7_frtΔ_phaC1, the plasmid was transferred from *E. coli* S17-1 to *R. eutropha* H16 via conjugation. All selected *R. eutropha* H16 transconjugants had integrated the T7 RNA polymerase into the genome whereupon several integrated the plasmid over the 3' region (Figure 45). A possible recombination event in the 5' region could not be determined due to the unknown DNA sequence in between. Following the successful integration of the T7 RNA polymerase into the genome of *R. eutropha* H16, the plasmid pCM_PT7_RSF1010_eGFP_Pemlk_ΔlacI was conjugationally transferred into *R. eutropha* H16 ΩKm*T7pol*. This plasmid was comprised among others of the *RSF1010* origin of replication which can be stably maintained in *R. eutropha* H16 and the reporter gene *egfp* under the regulation of the strong T7 promoter. The T7 RNA polymerase is very specific for its own promoters and thus, only an expressed and correctly folded T7 RNA polymerase is able to bind to the promoter region expressing the reporter gene *egfp*. The expression of *egfp* could already be observed on the selection plate as the growing *R. eutropha* H16 ΩKm*T7pol* [pCM_PT7_RSF1010_eGFP_Pemlk_ΔlacI] colonies appeared green. These results were expected as Barnard et al. [18] already demonstrated the functionality of the bacteriophage T7 RNA polymerase in *R. eutropha* H16. Moreover, the

relative fluorescing units of *R. eutropha* H16 carrying the plasmid pKRSF1010_Ptac_eGFP having the reporter gene *egfp* under the regulation of P_{tac} were determined and compared with the relative fluorescing units of *R. eutropha* H16 ΩKm*T7pol* [pCM_PT7_RSF1010_eGFP_Pemlk_ΔlacI]. The *egfp* expression of the T7 expression system was approximately twice as strong as the one under the regulation of P_{tac} according to the relative fluorescing units (Figure 46). However, these results must be taken with caution as the effect if any of the additional 3000 bp downstream of the tac promoter region but upstream of the T7 RNA polymerase may have an influence on the expression of the T7 RNA polymerase and the subsequent gene expression. Hence, the T7 RNA polymerase should be successfully cloned into the vector backbone without any additional sequences to be able to determine the exact expression levels under the control of the strong constitutive tac promoter.

The use of the strong T7 RNA polymerase expression system in *E. coli* was demonstrated in various studies and led to very high heterologous gene expression levels [91]. In addition, the T7 expression system was already applied in *R. eutropha* H16 to boost heterologous gene expression as demonstrated by Barnard et al. [18]. Thereby, the T7 RNA polymerase was integrated into the genome of *R. eutropha* H16 under the regulation of the strong inducible phaP promoter. Following, the OPH gene under the regulation of P_{T7} was randomly integrated into the chromosome and high expression levels of OPH (10 g/L) could be achieved [18]. The concentration of 10 g/L of OPH using the T7 based expression system was approximately 10 times greater than previously reported expressing OPH under the regulation of the phaP promoter with a host encoded polymerase [16]. The study of Barnard et al. [18] indicates that an inducible expression of the T7 RNA polymerase would further boost the expression of heterologous genes in *R. eutropha* H16. In contrast, Bi et al. [87] published data which does not correlate neither with the findings of this work nor the ones of Barnard et al. [18] suggesting that the T7 expression system had very little expression in *R. eutropha* H16 after induction with L-arabinose of P_{BAD} regulating the expression of T7 RNA polymerase. This was surprising as small amounts of T7 RNA polymerase would already suffice for high level gene expression according to Studier and Moffat [91].

Integration of the *E. coli* lactose permease in *R. eutropha* H16

Furthermore, the *E. coli* lactose permease gene was cloned into the backbone of the suicide vector pK470_mobRK2_estA_frtΔ_phaC1. Thereby, P_{tac} as well as the reporter gene *estA* were replaced by P_{CIV1bM} and *lacY* successfully constructing pK470_mobRK2_PCIV1bM_lacY_frtΔ_phaC1. In doing so, *lacY* was under the control of the weak constitutive promoter CIV1bM. Following the successful plasmid transformation into *E. coli* S17-1, the plasmid was transferred via conjugation into *R. eutropha* H16. A possible homologous recombination event was again determined via colony PCR (Figure 48). 20 *R. eutropha* H16 transconjugants were selected of which three integrated a part of the plasmid over both homologous regions whereas all the other examined *R. eutropha* H16 transconjugants showed to have integrated the plasmid only over one homologous region. Thus, approximately every seventh *R. eutropha* H16 transconjugant integrated the plasmid via gene replacement due to these results. This indicates that no further round of recombination with an additional selection pressure is essential to promote the second homologous recombination event. Nevertheless, different publications demonstrated the use of the second counterselection marker *sacB* in addition to an antibiotic resistance marker also encoded on the plasmid to be integrated [16], [18], [20]. *SacB* encodes for the levansucrase of *Bacillus subtilis* enabling the counterselection for a double recombination event. SacB is lethal to various Gram-negative bacteria in the presence of sucrose, thereby promoting the second cross-over event [106]–[108]. However, as could be shown in this work, the necessity of such a second counterselection marker is not given even though it would simplify the screening of *R. eutropha* H16 transconjugants. Moreover, the expression of *sacB* when encoded on the plasmid would represent a different approach for the selection marker recycling in contrast to the Flp-frt system when the gene to be integrated is flanked by the homologous regions [109].

Following, the lactose permease was successfully integrated into the *phaC1* locus of *R. eutropha* H16 a further plasmid was transferred into *R. eutropha* H16 Δ*phaC*ΩKm*lacY* via conjugation to determine the functionality of the lactose transport system. The plasmid pCM_Ptac_Par_eGFP_RSF1010_lacI was comprised among others of the *RSF1010* origin of replication as well as the *lac* repressor *lacI* and P_{tac} enabling inducible gene expression of the reporter gene *egfp*. Surprisingly, no *R. eutropha* H16 transconjugants were obtained after

the conjugational plasmid transfer of pCM_Ptac_Par_eGFP_RSF1010_lacI into *R. eutropha* H16 Δ*phaC*ΩKm*lacY.* Thus, the plasmid was sent for sequencing which revealed a mutation in the *repA* gene of the *RSF1010* origin essential for plasmid replication. Although, this mutation did not affect the replication behaviour in *E. coli*, the plasmid was not able to replicate in *R. eutropha* H16 resulting in no growth of *R. eutropha* H16 transconjugants. Hence, the determination of the functionality of the lactose permease and the subsequent establishment of an inducible expression system based on the *lac* operon in *R. eutropha* H16 was not possible. Further cloning steps would have been necessary to replace the *RSF1010* origin with one not harbouring any mutation to be able to determine the functionality and correct membrane incorporation of *lacY* in *R. eutropha* H16. However, these additional steps could not be carried out during this work due to time reasons.

The successful lactose transport into *R. eutropha* H16 could not be confirmed during this work. However, a previous study by Pries et al. [86] already demonstrated the functionality of the lactose permease and the subsequent lactose uptake and utilization. Thereby, the genes *lacY* and *lacZ* were under the regulation of the promoter of the *R. eutropha* H16 PHB genes. The uptake of lactose and the successive complete utilization of its derivatives glucose and galactose could be demonstrated in *R. eutropha* H16 showing the successful application of the lactose permease in *R. eutropha* H16 [86]. Moreover, Bi et al. [87] recently published data demonstrating the expression of a codon-optimized *lacY* gene under the regulation of a constitutive promoter in *R. eutropha* H16. Thereby, the red fluorescent protein (RFP) could be successfully expressed after IPTG-induction. However, the expression levels were surprisingly low compared to the promoter system P_{BAD} [87]. This can be argued by a low number of permeases resulting in a low inducer concentration inside the cell to bind the *lac* repressor and thereby enabling only weak heterologous gene expression [81].

In contrast, in this work the original *lacY* gene was used and genomically integrated into the genome of *R. eutropha* H16. Furthermore, the *lacY* expression was under the regulation of the weak constitutive promoter CIV1bM after its integration into the genome of *R. eutropha* H16. This promoter was used, as it was expected to facilitate the successful membrane integration when the expression levels were low. Unfortunately the correct membrane integration and the subsequent IPTG uptake could not be verified during this work. Nevertheless, the successful IPTG uptake based on *lacY* and in doing so the establishment of

an inducible expression system in *R. eutropha* H16 should work out due to the previously published data.

5. Conclusion and Outlook

During this work different strategies for the integration into the genome of *R. eutropha* H16 were established varying in the antibiotic resistance marker, the length of the homologous region as well as the mobilization sequence. A successful recombination event could finally be determined with the plasmid pK470_mobRK2_estA_frtΔ_phaC1 based on the mobilization region of the RK2 plasmid, the *ColE1* origin of replication, and two homologous regions of approximately 900 bp flanking the reporter gene *estA* and kan^r. The mobilization sequence of the RK2 plasmid was used due to the best results in the mobilization efficiency compared to the mobilization region of pBBR1-MCS5 and RSF1010 plasmid. Moreover, the Flp-frt site-specific recombination system could be successfully established in *R. eutropha* H16 enabling the selection marker recycling.

Following, the bacteriophage T7 RNA polymerase was successfully integrated into the genome of *R. eutropha* H16 and the functionality of the T7 expression system confirmed by fluorescent unit measurement. However, an additional unknown DNA sequence was cloned into the plasmid upstream of the T7 RNA polymerase which may influence the binding and the subsequent heterologous gene expression. Thus, this experiment should be repeated to determine the exact activity of the T7 RNA polymerase in *R. eutropha* H16.

Moreover, the *E. coli* lactose permease was successfully integrated into the genome of *R. eutropha* H16 as well. However, the correct membrane incorporation of *lacY* and the subsequent active lactose uptake could not be determined. The plasmid to be used to verify the efficient lactose uptake showed to have a mutation in the replication gene *repA* not allowing the plasmid to replicate in *R. eutropha* H16. Hence, further cloning steps are necessary to be carried out before the *lacY* functionality can be proved.

After the functionality of the lactose permease was verified in *R. eutropha* H16, the establishment of a simple inducible expression system would be achieved. Further steps would include the generation of a *R. eutropha* H16 strain which has integrated both the bacteriophage T7 RNA polymerase under the regulation of P_{tac}/P_{lac} as well as the lactose permease gene. Hence, a simple inducible and strong gene expression system could be established in *R. eutropha* H16 for homologous and heterologous gene expression based on the T7 expression system.

6. References

[1] H. G. Aragno and M. Schlegel, “The mesophilic hydrogen-oxidizing (knallgas) bacterium,” in *The prokaryotes: a handbook on the biology of bacteria: ecophysiology, isolation, identification, applications*, 1st ed., K. H. Balows, A. Truper, H. G. Dworkin, M. Harder, and W. Schleifer, Eds. New York: Springer, 1992, pp. 344–384.

[2] A. Pohlmann, W. F. Fricke, F. Reinecke, B. Kusian, H. Liesegang, R. Cramm, T. Eitinger, C. Ewering, M. Pötter, E. Schwartz, A. Strittmatter, I. Voss, G. Gottschalk, A. Steinbüchel, B. Friedrich, and B. Bowien, “Genome sequence of the bioplastic-producing ‘Knallgas’ bacterium *Ralstonia eutropha* H16,” *Nat. Biotechnol.*, vol. 24, no. 10, pp. 1257–1262, Oct. 2006.

[3] E. Schwartz, A. Henne, R. Cramm, T. Eitinger, B. Friedrich, and G. Gottschalk, “Complete nucleotide sequence of pHG1: A *Ralstonia eutropha* H16 megaplasmid encoding key enzymes of H2-based lithoautotrophy and anaerobiosis,” *J. Mol. Biol.*, vol. 332, no. 2, pp. 369–383, Sep. 2003.

[4] C. König, I. Sammler, E. Wilde, and H. G. Schlegel, “Konstitutive Glucose-6-phosphat-Dehydrogenase bei Glucose verwertenden Mutanten von einem kryptischen Wildstamm,” *Arch. Mikrobiol.*, vol. 67, no. 1, pp. 51–57, 1969.

[5] K. Peplinski, A. Ehrenreich, C. Döring, M. Bömeke, F. Reinecke, C. Hutmacher, and A. Steinbüchel, “Genome-wide transcriptome analyses of the ‘Knallgas’ bacterium *Ralstonia eutropha* H16 with regard to polyhydroxyalkanoate metabolism,” *Microbiology*, vol. 156, pp. 2136–2152, Jul. 2010.

[6] B. Bowien and B. Kusian, “Genetics and control of CO2 assimilation in the chemoautotroph *Ralstonia eutropha*,” *Arch. Microbiol.*, vol. 178, no. 2, pp. 85–93, Aug. 2002.

[7] A. Tran-Betcke, U. Warnecke, C. Bocker, C. Zaborosch, and B. Friedrich, “Cloning and nucleotide sequences of the genes for the subunits of NAD-reducing hydrogenase of *Alcaligenes eutrophus* H16,” *J. Bacteriol.*, vol. 172, no. 6, pp. 2920–2929, Jun. 1990.

[8] C. Kortluke, K. Horstmann, E. Schwartz, M. Rohde, R. Binsack, and B. Friedrich, “A gene complex coding for the membrane-bound hydrogenase of *Alcaligenes eutrophus* H16,” *J. Bacteriol.*, vol. 174, no. 19, pp. 6277–6289, Oct. 1992.

[9] J. Pfitzner and H. G. Schlegel, “Denitrifikation bei *Hydrogenomonas eutropha* Stamm H16,” *Arch. Mikrobiol.*, vol. 90, no. 3, pp. 199–211, 1973.

[10] A. Schenzle, H. Lenke, P. Fischer, P. Williams, and H. Knackmuss, “Catabolism of 3-Nitrophenol by *Ralstonia eutropha* JMP 134,” *Appl. Envir. Microbiol.*, vol. 63, no. 4, pp. 1421–1427, Apr. 1997.

[11] A. Y. Dursun and O. Tepe, “Internal mass transfer effect on biodegradation of phenol by Ca-alginate immobilized *Ralstonia eutropha*,” *J. Hazard. Mater.*, vol. 126, no. 1–3, pp. 105–11, Nov. 2005.

[12] S. J. Lee and S. Y. Park, “Fermentative production of short-chain-length PHAs,” in *Biotechnology of biopolymers: from synthesis to patents*, A. Steinbüchel and Y. Dio, Eds. Weinheim, Germany: Wiley-VCH, 2005, pp. 207–234.

[13] A. Steinbüchel and B. Füchtenbusch, “Bacterial and other biological systems for polyester production,” *Trends Biotechnol.*, vol. 16, no. 10, pp. 419–427, Oct. 1998.

[14] H. G. Schlegel, G. Gottschalk, and R. von Bartha, “Formation and utilization of poly-β-hydroxybutyric acid by Knallgas bacteria (*Hydrogenomonas*),” *Nature*, vol. 191, pp. 463–465, 1961.

[15] J. Asrar and K. J. Gruys, “Biodegradable polymer (Biopol®),” in *Biopolymers Vol.4*, Y. Doi and A. Steinbüchel, Eds. Weinheim, Germany: Wiley-VCH, 2002, pp. 53–90.

[16] S. Srinivasan, G. C. Barnard, and T. U. Gerngross, “A novel high-cell-density protein expression system based on *Ralstonia eutropha*,” *Appl. Environ. Microbiol.*, vol. 68, no. 12, pp. 5925–5932, 2002.

[17] S. Srinivasan, G. C. Barnard, and T. U. Gerngross, “Production of recombinant proteins using multiple-copy gene integration in high-cell-density fermentations of *Ralstonia eutropha*,” *Biotechnol. Bioeng.*, vol. 84, no. 1, pp. 114–120, Oct. 2003.

[18] G. C. Barnard, G. E. Henderson, S. Srinivasan, and T. U. Gerngross, “High level recombinant protein expression in *Ralstonia eutropha* using T7 RNA polymerase based amplification,” *Protein Expr. Purif.*, vol. 38, no. 2, pp. 264–71, Dec. 2004.

[19] G. C. Barnard, J. D. McCool, D. W. Wood, and T. U. Gerngross, “Integrated recombinant protein expression and purification platform based on *Ralstonia eutropha*,” *Appl. Environ. Microbiol.*, vol. 71, no. 10, pp. 5735–5742, 2005.

[20] I. Voss and A. Steinbüchel, “Application of a KDPG-aldolase gene-dependent addiction system for enhanced production of cyanophycin in *Ralstonia eutropha* strain H16,” *Metab. Eng.*, vol. 8, no. 1, pp. 66–78, Jan. 2006.

[21] S. Sichwart, S. Hetzler, D. Bröker, and A. Steinbüchel, “Extension of the substrate utilization range of *Ralstonia eutropha* strain H16 by metabolic engineering to include mannose and glucose,” *Appl. Environ. Microbiol.*, vol. 77, no. 4, pp. 1325–34, Feb. 2011.

[22] B. Friedrich, C. Hogrefe, and H. G. Schlegel, “Naturally occurring genetic transfer of hydrogen-oxidizing ability between strains of *Alcaligenes eutrophus*,” *J. Bacteriol.*, vol. 147, no. 1, pp. 198–205, 1981.

[23] F. Reinecke and A. Steinbüchel, "*Ralstonia eutropha* strain H16 as model organism for PHA metabolism and for biotechnological production of technically interesting biopolymers," *J. Mol. Microbiol. Biotechnol.*, vol. 16, pp. 91–108, 2009.

[24] A. Steinbüchel, F. B. Oppermann-Sanio, C. Ewering, and M. Pötter, *Mikrobiologisches Praktikum: Versuche und Theorie*. Springer Berlin Heidelberg, 2013, pp. 237–239.

[25] M. F. Alexeyev, "The pKNOCK series of broad-host-range mobilizable suicide vectors for gene knockout and targeted DNA insertion into the chromosome of Gram-negative bacteria," *Biotechniques*, vol. 26, no. 5, pp. 824–828, 1999.

[26] P. Mazodier, R. Petter, and C. Thompson, "Intergeneric conjugation between *Escherichia coli* and *Streptomyces species*," *J. Bacteriol.*, vol. 171, no. 6, pp. 3583–3585, Jun. 1989.

[27] P. Trieu-Cuot, C. Carlier, P. Martin, and P. Courvalin, "Plasmid transfer by conjugation from *Escherichia coli* to Gram-positive bacteria," *FEMS Microbiol. Lett.*, vol. 48, no. 1, pp. 289–294, 1987.

[28] J. A. Heinemann and G. F. Sprague Jr, "Bacterial conjugative plasmids mobilize DNA transfer between bacteria and yeast," *Nature*, vol. 340, pp. 205–209, 1989.

[29] R. Simon, U. Priefer, and A. Pühler, "A broad host range mobilization system for in vivo genetic engineering: transposon mutagenesis in Gram negative bacteria," *Nat. Biotechnol.*, vol. 1, pp. 784–791, 1983.

[30] N. Willetts, "Sites and systems for conjugal DNA transfer in bacteria," in *Molecular biology, pathogenicity, and ecology of bacterial plasmids*, S. B. Levy, R. C. Clowes, and E. L. Koenig, Eds. Springer US, 1981, pp. 207–215.

[31] R. Daugelavicius, J. Bamford, A. Grahn, E. Lanka, and D. Bamford, "The IncP plasmid-encoded cell envelope-associated DNA transfer complex increases cell permeability," *J. Bacteriol.*, vol. 179, no. 16, pp. 5195–5202, Aug. 1997.

[32] M. Lessl, D. Balzer, K. Weyrauch, and E. Lanka, "The mating pair formation system of plasmid RP4 defined by RSF1010 mobilization and donor-specific phage propagation," *J. Bacteriol.*, vol. 175, no. 20, pp. 6415–6425, Oct. 1993.

[33] N. Willetts and B. Wilkins, "Processing of plasmid DNA during bacterial conjugation," *Microbiol. Rev.*, vol. 48, no. 1, pp. 24–41, Mar. 1984.

[34] V. L. Waters, "Conjugative transfer in the dissemination of beta-lactam and aminoglycoside resistance," *Front. Biosci.*, vol. 4, pp. 433–456, May 1999.

[35] B. Wilkins and E. Lanka, "DNA processing and replication during plasmid transfer between Gram-negative Bacteria," in *Bacterial conjugation*, D. B. Clewell, Ed. Springer US, 1993, pp. 105–136.

[36] D. Balzer, W. Pansegrau, and E. Lanka, “Essential motifs of relaxase (TraI) and TraG proteins involved in conjugative transfer of plasmid RP4,” *J. Bacteriol.*, vol. 176, no. 14, pp. 4285–4295, Jul. 1994.

[37] J. Haase, R. Lurz, A. Grahn, D. Bamford, and E. Lanka, “Bacterial conjugation mediated by plasmid RP4: RSF1010 mobilization, donor-specific phage propagation, and pilus production require the same Tra2 core components of a proposed DNA transport complex,” *J. Bacteriol.*, vol. 177, no. 16, pp. 4779–4791, Aug. 1995.

[38] W. Pansegrau, E. Lanka, P. T. Barth, D. H. Figurski, D. G. Guiney, D. Haas, D. R. Helinski, H. Schwab, V. A. Stanisich, and C. M. Thomas, “Complete nucleotide sequence of Birmingham IncP alpha plasmids: Compilation and comparative analysis,” *J. Mol. Biol.*, vol. 239, no. 5, pp. 623–663, Jun. 1994.

[39] E. Scherzinger, R. Lurz, S. Otto, and B. Dobrinski, “In vitro cleavage of double- and single-stranded DNA by plasmid RSF1010-encoded mobilization proteins,” *Nucleic Acids Res.*, vol. 20, no. 1, pp. 41–48, Jan. 1992.

[40] C. M. Thomas and C. A. Smith, “Incompatibility group P plasmids: genetics, evolution, and use in genetic manipulation,” *Annu. Rev. Microbiol.*, vol. 41, pp. 77–101, Jan. 1987.

[41] A. Toukdarian, “Plasmid strategies for broad-host-range replication in Gram-negatve bacteria,” in *Plasmid Biology*, G. J. Funnell and B. E. Phillips, Eds. Washington, DC, USA: ASM Press, 2004, pp. 259–270.

[42] P. Scholz, V. Haring, B. Wittmann-Liebold, K. Ashman, M. Bagdasarian, and E. Scherzinger, “Complete nucleotide sequence and gene organization of the broad-host-range plasmid RSF1010,” *Gene*, vol. 75, no. 2, pp. 271–288, Feb. 1989.

[43] W. Pansegrau and E. Lanka, “Enzymology of DNA transfer by conjugative mechanisms,” *Prog. Nucleic Acid Res. Mol. Biol.*, vol. 54, pp. 197–251, Jan. 1996.

[44] V. L. Waters, K. H. Hirata, W. Pansegrau, E. Lanka, and D. G. Guiney, “Sequence identity in the nick regions of IncP plasmid transfer origins and T-DNA borders of Agrobacterium Ti plasmids,” *Proc. Natl. Acad. Sci.*, vol. 88, no. 4, pp. 1456–1460, Feb. 1991.

[45] W. Pansegrau, W. Schroder, and E. Lanka, “Relaxase (TraI) of IncP alpha plasmid RP4 catalyzes a site-specific cleaving-joining reaction of single-stranded DNA,” *Proc. Natl. Acad. Sci.*, vol. 90, no. 7, pp. 2925–2929, Apr. 1993.

[46] M. Brigulla and W. Wackernagel, “Molecular aspects of gene transfer and foreign DNA acquisition in prokaryotes with regard to safety issues,” *Appl. Microbiol. Biotechnol.*, vol. 86, no. 4, pp. 1027–41, Apr. 2010.

[47] S. C. Kowalczykowski, D. A. Dixon, A. K. Eggleston, S. D. Lauder, and W. M. Rehrauer, “Biochemistry of homologous recombination in *Escherichia coli*,” *Microbiol. Rev.*, vol. 58, no. 3, pp. 401–65, Sep. 1994.

[48] P. Meier and W. Wackernagel, “Mechanisms of homology-facilitated illegitimate recombination for foreign DNA acquisition in transformable *Pseudomonas stutzeri*,” *Mol. Microbiol.*, vol. 48, no. 4, pp. 1107–1118, May 2003.

[49] S. D. Ehrlich, H. Bierne, E. d’Alençon, D. Vilette, M. Petranovic, P. Noirot, and B. Michel, “Mechanisms of illegitimate recombination,” *Gene*, vol. 135, no. 1–2, pp. 161–166, Dec. 1993.

[50] N. D. F. Grindley, K. L. Whiteson, and P. A. Rice, “Mechanisms of site-specific recombination,” *Annu. Rev. Biochem.*, vol. 75, pp. 567–605, Jan. 2006.

[51] D. Dixon and S. C. Kowalczykowski, “The recombination hotspot χ is a regulatory sequence that acts by attenuating the nuclease activity of the E. coli RecBCD enzyme,” *Cell*, vol. 73, no. 1, pp. 87–96, Apr. 1993.

[52] R. Holliday, “A mechanism for gene conversion in fungi,” *Genet. Res.*, vol. 5, no. 02, pp. 282–304, Apr. 2009.

[53] R. P. Cunningham, A. M. Wu, T. Shibata, C. Dasgupta, and C. M. Radding, “Homologous pairing and topological linkage of DNA molecules by combined action of *E. coli* recA protein and topoisomerase I,” *Cell*, vol. 24, no. 1, pp. 213–223, Apr. 1981.

[54] S. D. Ehrlich, “Illegitimate recombination in bacteria,” in *Mobile DNA*, D. E. Berg and M. M. Howe, Eds. Washington, DC: American Society for Microbiology, 1989, pp. 799–824.

[55] N. Hülter and W. Wackernagel, “Double illegitimate recombination events integrate DNA segments through two different mechanisms during natural transformation of *Acinetobacter baylyi*,” *Mol. Microbiol.*, vol. 67, no. 5, pp. 984–995, Mar. 2008.

[56] R. Meima, G.-J. Haan, G. Venema, S. Bron, and S. de Jong, “Sequence specificity of illegitimate plasmid recombination in *Bacillus subtilis*: Possible recognition sites for DNA topoisomerase I,” *Nucleic Acids Res.*, vol. 26, no. 10, pp. 2366–2373, May 1998.

[57] H. Bierne, S. D. Ehrlich, and B. Michel, “Deletions at stalled replication forks occur by two different pathways,” *EMBO J.*, vol. 16, no. 11, pp. 3332–40, Jun. 1997.

[58] J. de Vries and W. Wackernagel, “Integration of foreign DNA during natural transformation of *Acinetobacter sp.* by homology-facilitated illegitimate recombination,” *Proc. Natl. Acad. Sci. U. S. A.*, vol. 99, no. 4, pp. 2094–9, Feb. 2002.

[59] M. Prudhomme, V. Libante, and J.-P. Claverys, “Homologous recombination at the border: insertion-deletions and the trapping of foreign DNA in *Streptococcus pneumoniae*,” *Proc. Natl. Acad. Sci. U. S. A.*, vol. 99, no. 4, pp. 2100–2105, Feb. 2002.

[60] K. Harms, V. Schön, E. Kickstein, and W. Wackernagel, “The RecJ DNase strongly suppresses genomic integration of short but not long foreign DNA fragments by homology-facilitated illegitimate recombination during transformation of *Acinetobacter baylyi*,” *Mol. Microbiol.*, vol. 64, no. 3, pp. 691–702, May 2007.

[61] S. T. Lovett, R. L. Hurley, V. A. J. Sutera, R. H. Aubuchon, and M. A. Lebedeva, “Crossing over between regions of limited homology in *Escherichia coli*: RecA-dependent and RecA-independent pathways,” *Genetics*, vol. 160, no. 3, pp. 851–859, Mar. 2002.

[62] D. J. Simpson, L. F. Dawson, J. C. Fry, H. J. Rogers, and M. J. Day, “Influence of flanking homology and insert size on the transformation frequency of *Acinetobacter baylyi* BD413,” *Environ. Biosafety Res.*, vol. 6, no. 1–2, pp. 55–69, Jan. 2007.

[63] C. J. Brigham, C. F. Budde, J. W. Holder, Q. Zeng, A. E. Mahan, C. Rha, and A. J. Sinskey, “Elucidation of beta-oxidation pathways in *Ralstonia eutropha* H16 by examination of global gene expression,” *J. Bacteriol.*, vol. 192, no. 20, pp. 5454–64, Oct. 2010.

[64] C. S. Kristensen, L. Eberl, J. M. Sanchez-Romero, M. Givskov, S. Molin, and V. De Lorenzo, “Site-specific deletions of chromosomally located DNA segments with the multimer resolution system of broad-host-range plasmid RP4,” *J. Bacteriol.*, vol. 177, no. 1, pp. 52–58, Jan. 1995.

[65] M. McLeod, S. Craft, and J. R. Broach, “Identification of the crossover site during FLP-mediated recombination in the *Saccharomyces cerevisiae* plasmid 2 microns circle,” *Mol. Cell. Biol.*, vol. 6, no. 10, pp. 3357–3367, Oct. 1986.

[66] N. Sternberg, D. Hamilton, and R. Hoess, “Bacteriophage P1 site-specific recombination,” *J. Mol. Biol.*, vol. 150, no. 4, pp. 487–507, Aug. 1981.

[67] P. P. Cherepanov and W. Wackernagel, “Gene disruption in *Escherichia coli*: TcR and KmR cassettes with the option of Flp-catalyzed excision of the antibiotic-resistance determinant,” *Gene*, vol. 158, no. 1, pp. 9–14, Jan. 1995.

[68] T. T. Hoang, R. R. Karkhoff-Schweizer, a J. Kutchma, and H. P. Schweizer, “A broad-host-range Flp-FRT recombination system for site-specific excision of chromosomally-located DNA sequences: application for isolation of unmarked *Pseudomonas aeruginosa* mutants,” *Gene*, vol. 212, no. 1, pp. 77–86, May 1998.

[69] K. a Datsenko and B. L. Wanner, “One-step inactivation of chromosomal genes in *Escherichia coli* K-12 using PCR products,” *Proc. Natl. Acad. Sci. U. S. A.*, vol. 97, no. 12, pp. 6640–6645, Jun. 2000.

[70] F. Storici, M. Coglievina, and C. V Bruschi, “A 2-micron DNA-based marker recycling system for multiple gene disruption in the yeast *Saccharomyces cerevisiae*,” *Yeast*, vol. 15, no. 4, pp. 271–283, Mar. 1999.

[71] K. G. Golic and S. Lindquist, “The FLP recombinase of yeast catalyzes site-specific recombination in the drosophila genome,” *Cell*, vol. 59, no. 3, pp. 499–509, Nov. 1989.

[72] X. H. Qian, R. B. Inman, and M. M. Cox, “Protein-based asymmetry and protein-protein interactions in FLP recombinase-mediated site-specific recombination,” *J. Biol. Chem.*, vol. 265, no. 35, pp. 21779–21788, Dec. 1990.

[73] P. Sadowski, “Site-specific recombinases: changing partners and doing the twist,” *J. Bacteriol.*, vol. 165, no. 2, pp. 341–347, Feb. 1986.

[74] R. M. Gronostajski and P. D. Sadowski, “The FLP recombinase of the *Saccharomyces cerevisiae* 2 microns plasmid attaches covalently to DNA via a phosphotyrosyl linkage,” *Mol. Cell. Biol.*, vol. 5, no. 11, pp. 3274–3279, Nov. 1985.

[75] D. Vetter, B. J. Andrews, L. Roberts-Beatty, and P. D. Sadowski, “Site-specific recombination of yeast 2-micron DNA in vitro,” *Proc. Natl. Acad. Sci.*, vol. 80, no. 23, pp. 7284–7288, Dec. 1983.

[76] E. Wilde, “Untersuchungen über Wachstum und Speicherstoffsynthese von *Hydrogenomas*,” *Arch. Mikrobiol.*, vol. 43, no. 2, pp. 109–137, 1962.

[77] T. Fukui, K. Ohsawa, J. Mifune, I. Orita, and S. Nakamura, “Evaluation of promoters for gene expression in polyhydroxyalkanoate-producing *Cupriavidus necator* H16,” *Appl. Microbiol. Biotechnol.*, vol. 89, no. 5, pp. 1527–36, Mar. 2011.

[78] L. Guzman, D. Belin, M. Carson, and J. Beckwith, “Tight regulation, modulation, and high-level expression by vectors containing the arabinose PBAD promoter,” *J. Bacteriol.*, vol. 177, no. 14, pp. 4121–4130, Jul. 1995.

[79] T. Fukui, H. Abe, and Y. Doi, “Engineering of *Ralstonia eutropha* for Production of Poly(3-hydroxybutyrate- co -3-hydroxyhexanoate) from Fructose and Solid-State Properties of the Copolymer,” *Biomacromolecules*, vol. 3, no. 3, pp. 618–624, May 2002.

[80] T. D. Pollard, W. C. Earnshaw, and J. Lippincott-Schwartz, *Cell Biology: Das Original Mit Übersetzungshilfen*, 2nd ed. Spektrum Akademischer Verlag, 2007, pp. 253–278.

[81] J. M. G. Vilar, C. C. Guet, and S. Leibler, “Modeling network dynamics: the lac operon, a case study,” *J. Cell Biol.*, vol. 161, no. 3, pp. 471–476, May 2003.

[82] D. G. Yansura and D. J. Henner, “Use of the *Escherichia coli* lac repressor and operator to control gene expression in *Bacillus subtilis*,” *Proc. Natl. Acad. Sci.*, vol. 81, no. 2, pp. 439–443, Jan. 1984.

[83] J. P. Fürste, W. Pansegrau, R. Frank, H. Blöcker, P. Scholz, M. Bagdasarian, and E. Lanka, “Molecular cloning of the plasmid RP4 primase region in a multi-host-range tacP expression vector,” *Gene*, vol. 48, no. 1, pp. 119–131, Jan. 1986.

[84] E. Amann, B. Ochs, and K.-J. Abel, “Tightly regulated tac promoter vectors useful for the expression of unfused and fused proteins in *Escherichia coli*,” *Gene*, vol. 69, no. 2, pp. 301–315, Sep. 1988.

[85] K. Terpe, “Overview of bacterial expression systems for heterologous protein production: from molecular and biochemical fundamentals to commercial systems,” *Appl. Microbiol. Biotechnol.*, vol. 72, no. 2, pp. 211–222, Sep. 2006.

[86] A. Pries, A. Steinbüchel, and H. Schlegel, “Lactose- and galactose-utilizing strains of poly(hydroxyalkanoic acid)-accumulating *Alcaligenes eutrophus* and *Pseudomonas saccharophila* obtained by recombinant DNA technology,” *Appl. Microbiol. Biotechnol.*, vol. 33, no. 4, pp. 410–417, Jul. 1990.

[87] C. Bi, P. Su, J. Müller, Y.-C. Yeh, S. R. Chhabra, H. R. Beller, S. W. Singer, and N. J. Hillson, “Development of a broad-host synthetic biology toolbox for *Ralstonia eutropha* and its application to engineering hydrocarbon biofuel production,” *Microb. Cell Fact.*, vol. 12, no. 1, p. 107, 2013.

[88] D. Jeruzalmi and T. A. Steitz, “Structure of T7 RNA polymerase complexed to the transcriptional inhibitor T7 lysozyme,” *EMBO J.*, vol. 17, no. 14, pp. 4101–4113, Jul. 1998.

[89] V. L. Tunitskaya and S. N. Kochetkov, “Structural-functional analysis of bacteriophage T7 RNA polymerase,” *Biochemistry*, vol. 67, no. 10, pp. 1124–1135, Oct. 2002.

[90] P. Davanloo, A. H. Rosenberg, J. J. Dunn, and F. W. Studier, “Cloning and expression of the gene for bacteriophage T7 RNA polymerase,” *Proc. Natl. Acad. Sci.*, vol. 81, no. 7, pp. 2035–2039, Apr. 1984.

[91] F. W. Studier and B. A. Moffatt, “Use of bacteriophage T7 RNA polymerase to direct selective high-level expression of cloned genes,” *J. Mol. Biol.*, vol. 189, no. 1, pp. 113–130, May 1986.

[92] M. Chamberlin, J. McGratz, and L. Waskell, “New RNA Polymerase from *Escherichia coli* infected with Bacteriophage T7,” *Nature*, vol. 228, no. 5268, pp. 227–231, Oct. 1970.

[93] D. R. Wycuff and K. S. Matthews, “Generation of an AraC-araBAD promoter-regulated T7 expression system,” *Anal. Biochem.*, vol. 277, no. 1, pp. 67–73, Jan. 2000.

[94] S. Tabor and C. C. Richardson, “A bacteriophage T7 RNA polymerase/promoter system for controlled exclusive expression of specific genes,” *Proc. Natl. Acad. Sci.*, vol. 82, no. 4, pp. 1074–1078, Feb. 1985.

[95] F. W. Studier, “Use of bacteriophage T7 lysozyme to improve an inducible T7 expression system,” *J. Mol. Biol.*, vol. 219, no. 1, pp. 37–44, May 1991.

[96] X. Zhang and F. W. Studier, “Mechanism of inhibition of bacteriophage T7 RNA polymerase by T7 lysozyme,” *J. Mol. Biol.*, vol. 269, no. 1, pp. 10–27, May 1997.

[97] R. A. Ikeda and C. C. Richardson, “Interactions of the RNA polymerase of bacteriophage T7 with its promoter during binding and initiation of transcription,” *Proc. Natl. Acad. Sci.*, vol. 83, no. 11, pp. 3614–3618, Jun. 1986.

[98] A. Schlacher, T. Stanzer, I. Osprian, M. Mischitz, E. Klingsbichel, K. Faber, and H. Schwab, “Detection of a new enzyme for stereoselective hydrolysis of linalyl acetate using simple plate assays for the characterization of cloned esterases from *Burkholderia gladioli*,” *J. Biotechnol.*, vol. 62, no. 1, pp. 47–54, 1998.

[99] R. Meyer, “Identification of the mob genes of plasmid pSC101 and characterization of a hybrid pSC101-R1162 system for conjugal mobilization,” *J. Bacteriol.*, vol. 182, no. 17, pp. 4875–4881, Sep. 2000.

[100] Carl Roth GmbH, “Antibiotika,” 2009. [Online]. Available: http://www.carlroth.at/website/de-de/pdf/Antibiotika.pdf. [Accessed: 07-Apr-2014].

[101] S. Gruber, J. Hagen, H. Schwab, and P. Koefinger, “Versatile and stable vectors for efficient gene expression in *Ralstonia eutropha* H16,” *J. Biotechnol.*

[102] I. Syrovy and Z. Hodny, “Staining and quantification of proteins separated by polyacrylamide gel electrophoresis,” *J. Chromatogr.*, vol. 569, pp. 175–196, 1991.

[103] G. Du, J. Chen, J. Yu, and S. Lun, “Continuous production of poly-3-hydroxybutyrate by *Ralstonia eutropha* in a two-stage culture system,” *J. Biotechnol.*, vol. 88, no. 1, pp. 59–65, Jun. 2001.

[104] M. Raberg, J. Bechmann, U. Brandt, J. Schlüter, B. Uischner, B. Voigt, M. Hecker, and A. Steinbüchel, “Versatile metabolic adaptations of *Ralstonia eutropha* H16 to a loss of PdhL, the E3 component of the pyruvate dehydrogenase complex,” *Appl. Environ. Microbiol.*, vol. 77, no. 7, pp. 2254–2263, Apr. 2011.

[105] H. Schwab, “Transfer von Plasmid-DNS in das Bakterium *Alacaligenes eutrophus* H16,” Technische Universität Graz, 1980.

[106] M. Steinmetz, D. Le Coq, S. Aymerich, G. Gonzy-Tréboul, and P. Gay, “The DNA sequence of the gene for the secreted *Bacillus subtilis* enzyme levansucrase and its genetic control sites,” *Mol. Gen. Genet.*, vol. 200, no. 2, pp. 220–228, 1985.

[107] P. Gay, D. Le Coq, M. Steinmetz, T. Berkelman, and C. I. Kado, “Positive selection procedure for entrapment of insertion sequence elements in Gram-negative bacteria,” *J. Bacteriol.*, vol. 164, no. 2, pp. 918–921, Nov. 1985.

[108] J.-M. Reyrat, V. Pelicic, B. Gicquel, and R. Rappuoli, “Counterselectable markers: untapped tools for bacterial genetics and pathogenesis,” *Infect. Immun.*, vol. 66, no. 9, pp. 4011–4017, Sep. 1998.

[109] C. J. Marx, “Development of a broad-host-range sacB-based vector for unmarked allelic exchange,” *BMC Res. Notes*, vol. 1, no. 1, Jan. 2008.

7. List of Figures

8. List of Tables

9. Appendix

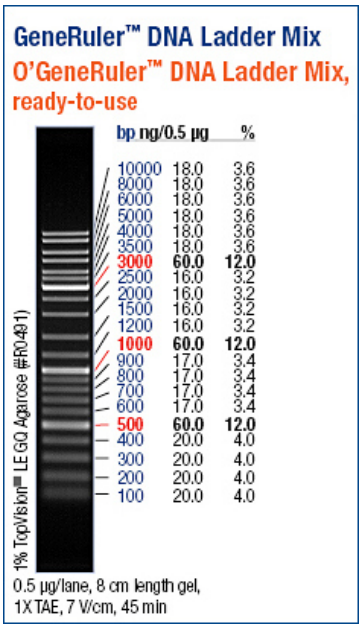

Figure 50. GeneRuler™ DNA Ladder Mix (Thermo Scientific).

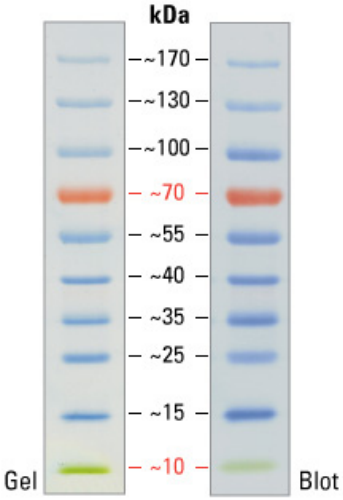

Figure 51. PageRuler™ Prestained Protein Ladder (Thermo Scientific, St. Leon-Rot, Germany).